WISSENSCHAFTLICHE MITTEILUNGEN

aus dem Institut für Meteorologie der Universität Leipzig

BAND 61

M. Wendisch (Hrsg.)

Meteorologische Arbeiten XXVIII

Jahresbericht 2022

UNIVERSITÄT LEIPZIG

Wissenschaftliche Mitteilungen

aus dem
Institut für Meteorologie der Universität Leipzig

ISBN **978-3-9823985-1-8**

Meteorologische Arbeiten (XXVIII) und Jahresbericht 2022 des Instituts für Meteorologie der Universität Leipzig

Hrsg.: Manfred Wendisch

Leipzig 2023

Band 61

Wissenschaftliche Mitteilungen aus dem Institut für Meteorologie der Universität Leipzig Bd. 61 (2023)

Airborne observations of Arctic air mass transformations during the HALO-(AC)^3 campaign

Klingebiel, M.[1], Schäfer, M.[1], Kirbus, B.[1], Maherndl, N.[1], Becker, S.[1], Brückner, M.[1], Jäkel, E.[1], Lonardi, M.[1], Luebke, A. E.[1], Maahn, M.[1], Müller, H.[1], Röttenbacher, J.[1], Schmidt, J.[1], Schwarz, A.[1], Sperzel, T. R.[1], Ehrlich, A.[1], Wendisch, M.[1]

[1] *Leipzig Institute for Meteorology, Leipzig University, Germany*
✉*e-mail: marcus.klingebiel@uni-leipzig.de*

Summary: The HALO-(AC)^3 campaign was conducted in March and April 2022 to investigate warm air intrusions into the Arctic and marine cold air outbreaks. In coordinated flights over the Arctic, the High Altitude and Long Range Research Aircraft (HALO), equipped with a remote sensing payload and dropsondes, investigated these air mass transformations together with the research aircraft Polar 5 and Polar 6. In this report, we give an overview about the research flights and preliminary results from projects, which are carried out by employees of the Leipzig Institute for Meteorology (LIM).

Zusammenfassung: Die HALO-(AC)^3 Kampagne wurde im März und April 2022 durchgeführt, um Warmlufteinbrüche in die Arktis und marine Kaltluftausbrüche zu untersuchen. Das "High Altitude and Long Range Research Aircraft" (HALO), ausgestattet mit Instrumenten zur Fernerkundung und Standardmeteorologiesonden, untersuchte zusammen mit den Forschungsflugzeugen Polar 5 und Polar 6, in koordinierten Flügen über der Arktis, diese Veränderungen der Luftmassen. In diesem Bericht wird eine Übersicht über die durchgeführten Forschungsflüge gegeben und Forschungsprojekte werden vorgestellt, welche von Mitarbeitern des Leipziger Instituts für Meteorologie (LIM) durchgeführt werden.

1 Introduction

Over the last decades, the Arctic experienced an enhanced warming up to four times stronger than the mid-latitudes, which is known as Arctic amplification (Serreze and Barry, 2011; Wendisch et al., 2023; Rantanen et al., 2022). The Transregional Collaborative Research Center (TR 172) called *Arctic Amplification: Climate Relevant Atmospheric and Surface Processes, and Feedback Mechanisms* ((AC)^3, www.ac3-tr.de), lead by the Leipzig Institute for Meteorology (LIM), investigates the processes and key factors to get a better understanding of the causes driving the Arctic amplification. One of the suspects are general circulation patterns related to the jet stream, which might get weaker because of Arctic amplification. This results in a higher amount of blocking situations, which promote Warm Air Intrusions (WAIs) and Cold Air Outbreaks (CAOs). Such WAIs, which are most prominent in the winter time Arctic, lead to a northward

transport of moisture and clouds and, thus, increase the downward terrestrial radiation and warms the near surface air.

To understand this positive feedback mechanism and investigate air mass transformations in more detail, the HALO-(AC)^3 campaign was conducted in March and April 2022 to study WAIs and CAOs. The general objectives of the HALO-(AC)^3 mission are:

- To perform quasi-Lagrange observations of air-mass transformation processes during meridional transports with a particular focus on pronounced WAIs and marine CAOs.
- To test the ability of numerical atmospheric models to reproduce the measurements, which then can be applied to investigate the linkages between Arctic amplification and mid-latitude weather.

Extended information on the HALO-(AC)^3 mission are provided at the campaign webpage (HALO-(AC)^3 Website, 2023). Three research aircraft were involved in the campaign with different instrumentation and flight patterns, aiming at the above mentioned objectives.

The High Altitude and LOng Range (HALO) research aircraft from German Aerospace Center (DLR) is the only German research aircraft, which is capable of covering distances to up to 10000 km (10 hours flight time). For this reason, HALO is the ideal tool to perform the planned quasi-Lagrange air-mass observations. HALO is equipped with meteorological and remote sensing instruments, as well as dropsondes, to observe the complete vertical tropospheric air mass column up to an altitude of 15 km. These observations contain meteorological quantities (temperature, pressure, humidity), turbulence parameters, water vapor, aerosol particles, and clouds (HALO-(AC)^3 Website, 2023). During the HALO-(AC)^3 campaign, HALO was stationed at Kiruna, where a large hangar was available for safe and convenient aircraft operations.

The two research aircraft from the Alfred-Wegener-Institut Helmholtz Centre for Polar and Marine Research (AWI), namely Polar 5 and Polar 6, were used to study the lower atmosphere, up to 3 km. While Polar 5 was equipped with remote sensing instruments and dropsondes, Polar 6 performed in-situ measurements of cloud and aerosol particles in the boundary layer. Polar 5 and Polar 6 were stationed in Longyearbyen, Svalbard and conducted measurements in the vicinity of Svalbard. Both aircraft are specially modified to fly under extreme polar conditions and into clouds (Wesche et al., 2016).

An overview of the flight tracks from HALO, Polar 5, and Polar 6 is given in Fig. 1. As presented in Fig. 1a, HALO covers a spatial range from Kiruna towards the North Pole. Polar 5 and Polar 6 sampled a target area west of Svalbard, including the marginal sea ice zone (Fig. 1b). The research aircraft HALO allowed to follow air masses over several consecutive days to study their development over a larger time range. In contrast, Polar 5 and Polar 6 have the ability to study cloud micro- and macrophysics in more detail due to their slower cruising speed and lower altitudes. Therefore, the combination of the measurements from HALO and the Polar aircraft gives the unique opportunity to study the development of air masses, i.e., WAIs and CAOs, on large and small scales. A more detailed overview about the conducted flights is given in Table 1, which shows for each flight the objective, flight time and the launched number of dropsondes. For

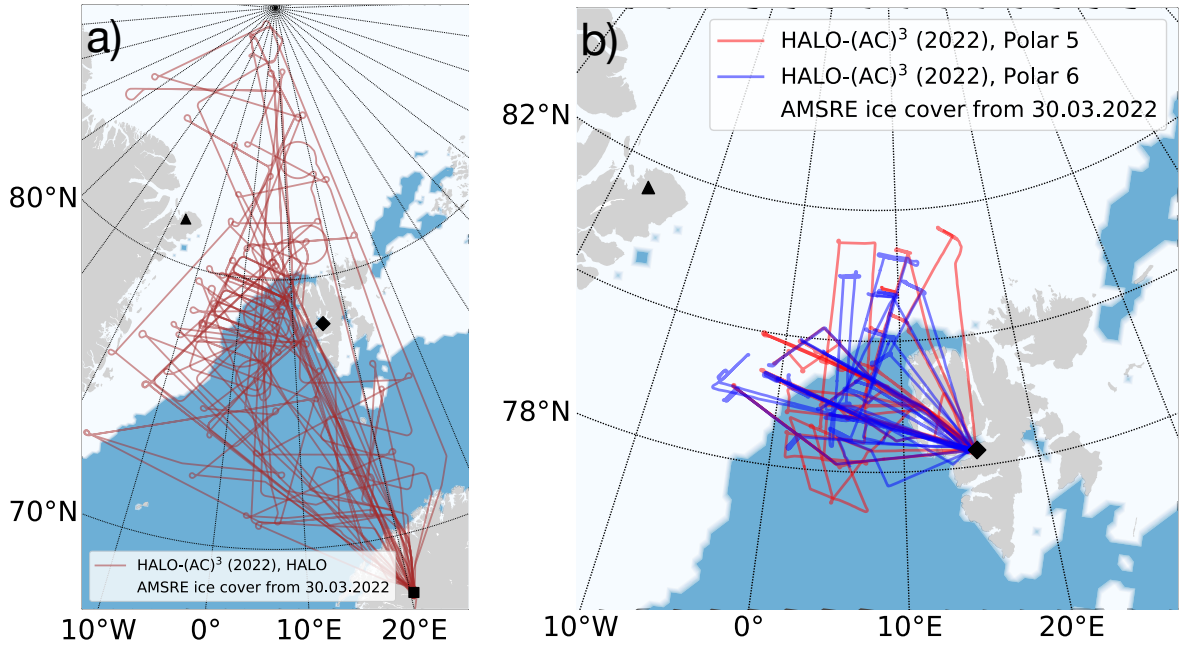

Figure 1: *Flight tracks of the HALO-(AC)^3 campaign from a) the research aircraft HALO and b) Polar 5 (red) and Polar 6 (blue). The black markers indicate the location of Station North (triangle), Longyearbyen (diamond) and Kiruna (square).*

the whole campaign we spend more than 264 hours in the air (HALO: 147 h, Polar 5: 54 h, Polar 6: 63 h). In total 492 dropsondes were launched, which provided valuable atmospheric profile data without technical issues in more than 95 % .

In the following we will give an overview of research projects at LIM, which are linked to HALO-(AC)^3 and make use of the airborne observations. Section 2 is focusing on atmospheric vertical profiles, which were observed by dropsondes launched over sea-ice and ice-free ocean. Section 3 shows an example of a collocated flight from Polar 5 and Polar 6. In Sect. 4 a Lagrangian trajectory analysis of a WAI is presented, followed by a summary of the results.

2 Vertical profiles of the atmosphere

During the HALO-(AC)^3 campaign, 350 dropsondes were launched from the HALO and 142 from the Polar 5 aircraft. This large amount of dropsondes is statistically applied to identify the typical differences of vertical profiles over the Arctic sea-ice and ice-free ocean. Therefore, we analysed all dropsondes launched from HALO poleward of 75°N. This threshold was chosen to only compare the atmosphere in the vicinity of the marginal sea ice zone.

The separated profiles over sea-ice and ice-free ocean are shown in Fig. 2. It is obvious that over sea-ice the atmosphere shows in general a lower temperature below 2000 m (Fig. 2a and b) and is also dryer (Fig. 2c). As shown in Fig. 2d, the wind speed throughout the whole vertical profile is lower over ice than over the ice-free ocean and is affected by the friction from the ground. Above sea ice, a temperature inversion is visible in an altitude below 1000 m (Fig. 2a), which is very typical over sea-ice. The

Date	Flight #	HALO Objective	Duration	Dropsondes	Flight #	Polar 5 Objective	Duration	Dropsondes	Flight #	Polar 6 Objective	Duration
25 February 2022	**0**	Scientific test flight	04:41	2							
10 March 2022					**0**	Scientific test flight	02:00				
11 March 2022	**1**	Transfer to Kiruna	03:03								
12 March 2022	**2**	Warm air intrusion #1, Day 1	08:22	20							
13 March 2022	**3**	Warm air intrusion #1, Day 2	08:48	23 (2 failed)							
14 March 2022	**4**	Warm air intrusion #1, Day 3	08:33	11 (1 failed)							
15 March 2022	**5**	Atmospheric river #1, Day 1	08:42	25							
16 March 2022	**6**	Atmospheric river #1, Day 2	09:29	25 (2 failed)							
20 March 2022	**7**	Day before cold air outbreak #1	09:08	18 (1 failed)	**1**	P5 & P6 collocation over sea ice and ocean	04:12	12	**1**	Low level clouds & aerosol	04:40
21 March 2022	**8**	Coordination with in-situ meas. by FAAM	07:47	13							
22 March 2022					**2**	CAO #1	01:35	2	**2**	In-situ cloud & aerosol	05:30
					3	CAO #1	04:15	10			
24 March 2022									**3**	In-situ cloud & aerosol	05:24
25 March 2022					**4**	Boundary layer flight over MIZ	04:56	4			
26 March 2022									**4**	Low level clouds of CAO	04:00
28 March 2022	**9**	CAO #2	07:27	22 (6 failed)	**5**	Cloud streets in Svalbard lee	04:35	15	**5**	Moderate CAO and cloud streets	04:50
29 March 2022	**10**	Coordination east of Svalbard with FAAM	08:24	18	**6**	Test of noseboom	01:01		**6**	Stack profile patterns	05:28
					7	Boundary layer flight over sea ice and open ocean	05:10	5			
30 March 2022	**11**	CAO #2, Divergence circles	08:24	32	**8**	Weak outflow of CAO	04:23	15	**7**	Racetrack pattern in vicinity of HALO track	05:00
01 April 2022	**12**	CAO #2, Rectangular divergence pattern	08:11	45 (5 failed)	**9**	Different stages of cloud streets with P6 and HALO	05:02	18	**8**	Coordinated flights with P5 and HALO	05:13
03 April 2022											
04 April 2022	**13**	CAO #2, collocated flights	08:52	13	**10**	CAO and convergence	04:16	14	**9**	Clouds over open water	04:20
05 April 2022					**11**	Wing-by-wing and collocation with P6	04:20	10	**10**	Wing-by-wing and collocation with P6	04:30
07 April 2022	**14**	Arctic cirrus #1, collocated flights	07:45	16	**12**	Upper cirrus over low level clouds	04:23	18			
08 April 2022	**15**	Polar low	07:19	21					**11**	Clouds in vicinity of polar low	05:15
09 April 2022									**12**	Boundary layer measurements	04:48
10 April 2022	**16**	Arctic cirrus #2, Day 1	06:30	22	**13**	Low level clouds over sea ice and open ocean	04:56	19 (1 failed)	**13**	Cloud measurements ove ice and open ocean	04:58
11 April 2022	**17**	Arctic cirrus #2, Day 2	07:55	7							
12 April 2022	**18**	Arctic cirrus #2, Day 3	08:06	17							
Total:			**147:26**	**350 (17 failed)**			**54:08**	**142 (1 failed)**			**63:56**

Table 1: *Overview of the research flights of the HALO, Polar 5, and Polar 6 during HALO-(AC)*^{3}.

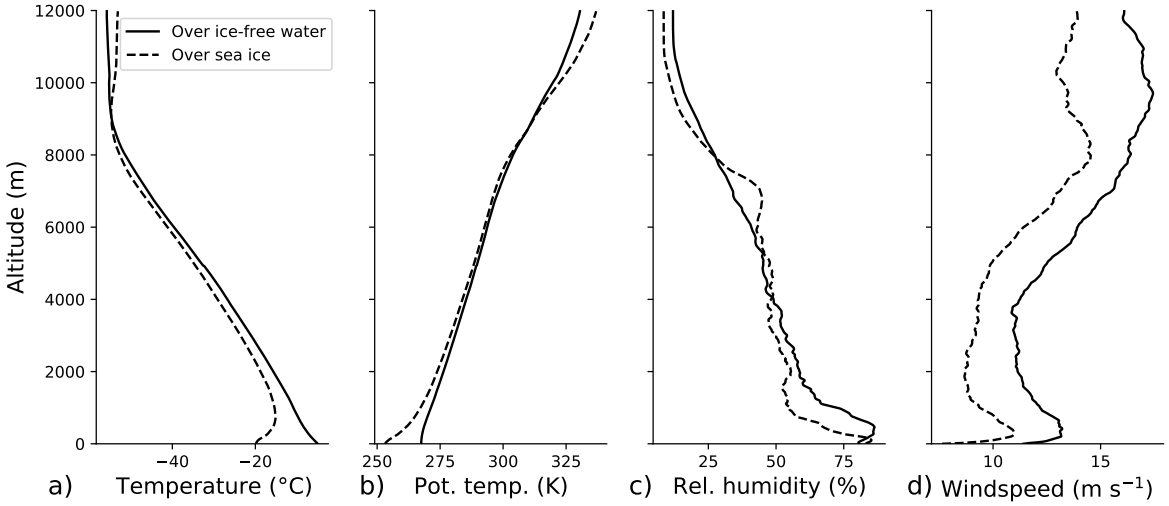

Figure 2: *Averaged dropsonde profiles, launched from HALO, over Arctic sea ice (dashed) and over ice-free ocean during HALO-(AC)*^{3}*. Only dropsondes launched poleward of 75°N are displayed here, which results in 122 dropsondes over ice-free ocean and 109 over sea-ice.*

relative humidity profiles indicate that less clouds were observed over sea ice (Fig. 2c).

2.1 Profiles along a cold air outbreak

Marine CAOs are very common in the Arctic winter time and can influence the weather in Europe. The CAOs can often be easily identified by their typical roll cloud structure, which is visible from satellite images. In the vicinity of Svalbard, in particular on the west side, CAOs are very typical with a north-south wind direction (Brümmer, 1996; Dahlke et al., 2022). Usually, the roll clouds develop over the marginal sea ice zone with an increasing cloud top height towards the south. The development process of the roll clouds is related to the increased temperature and moisture over the ice-free ocean. Towards the south, the surface temperature increases, which strengthens the convection and increases the cloud top height. The change in cloud top height also influences the horizontal size of the roll clouds, because the distance between the rolls depends on the cloud top height and the ratio is about 2:1 (Lemone, 1976). Roll clouds in connection with CAOs were extensively studied before (Kuettner, 1971; Lemone, 1976; Brümmer, 1996; Tornow et al., 2022; Dahlke et al., 2022), but covering a CAO event with different aircraft on a small (with Polar 5 and Polar 6) and large (with HALO) scale is new and gives a whole new insight of the development of these air masses.

The development of atmospheric vertical profiles along a CAO is presented in Fig. 3. This CAO case was observed on 01 April 2022. Illustrated by the flight track in Fig. 3a, the HALO aircraft covers a majority of the roll cloud structures starting from the beginning until almost the end of their development. Along that path, several dropsondes were launched. Here, we focus on the dropsonde profiles at the eastern leg of the flight track along the roll convection (marked by the dots in Fig. 3). Figures 3b and c show profiles of temperature and potential temperature, respectively, of the developing CAO and indicate the typical increase of temperature from north to south. The increase in cloud top height

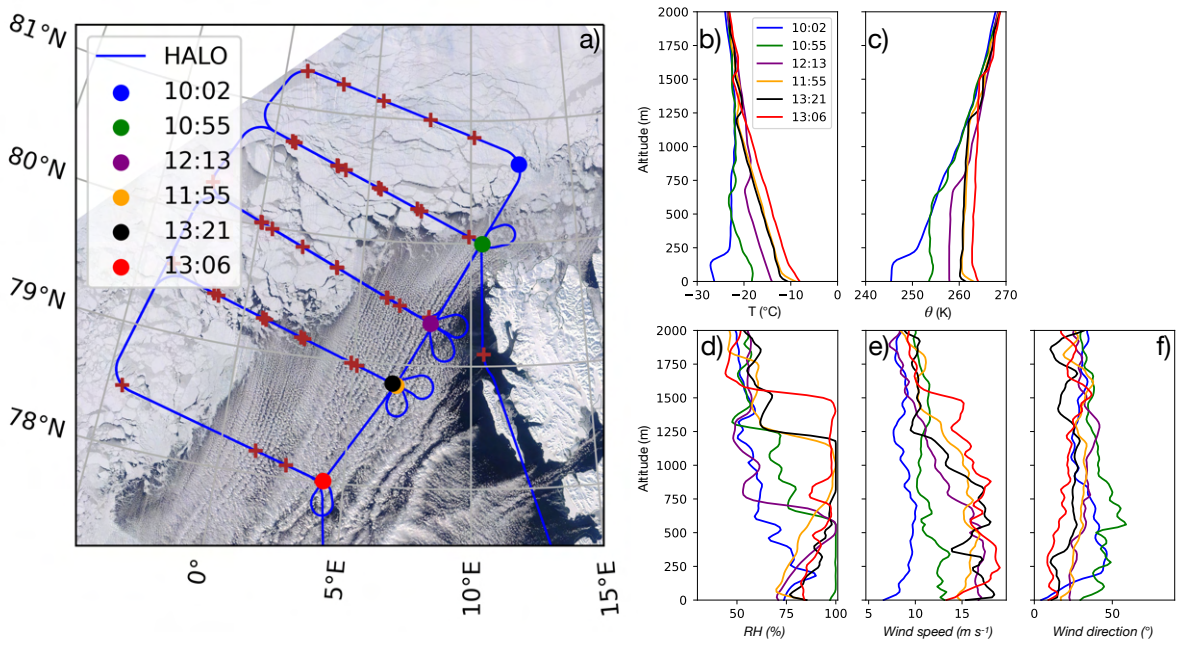

Figure 3: *a) HALO flight track from the 01 April 2022 in the vicinity of Svalbard. The crosses mark the positions of the launched dropsondes and the satellite picture is a snapshot from NASA worldview (MODIS). The dots indicate the dropsondes where the vertical profiles of different parameters are shown in panels b to f.*

is linked to the change of inversion height from about 100 m (blue point over ice) to about 1500 m (red point over water). That almost no clouds are present over the Arctic sea-ice is concluded from the relative humidity profiles in Fig. 3d. Here, a relative humidity of 100 %, which means the presence of clouds, is only reached over water and not for the profile over sea ice (blue). The wind speed (see Fig. 3e) shows an increase towards the south, which is contrarily to CAOs observed in earlier campaigns. Typically, the wind speed is highest above the ice where surface friction is low. Wind direction (see Fig. 3f) is in a narrow range for all profiles, which confirms a very steady air mass flow from the north. It might be noted that the dropsondes at 11:55 UTC and 13:21 UTC were launched at a very similar position. This was done to examine the temporal consistency of the dropsonde profiles. It turns out that the profiles are very consistent, in particular for the temperature, even though the measurements were taken 86 minutes apart.

This analysis shows that dropsonde measurements can be used to study the development of CAOs. This is a first step to obtain a better understanding of the development process of CAOs. Including radar reflectivity data from the Microwave Radar/radiometer for Acrtic Clouds (MiRAC) instrument (Mech et al., 2019) and radiance data from the Spectral Modular Airborne Radiation measurement sysTem (SMART) instrument (Wendisch et al., 2001) in the analysis, both on board of Polar 5, we will obtain more information about the distribution of ice and liquid water in the roll clouds.

3 Collocated research flights

A major goal of the HALO-(AC)^3 campaign was the collocation of measurements from different aircraft, in particular from Polar 5 and Polar 6. Performing remote-sensing

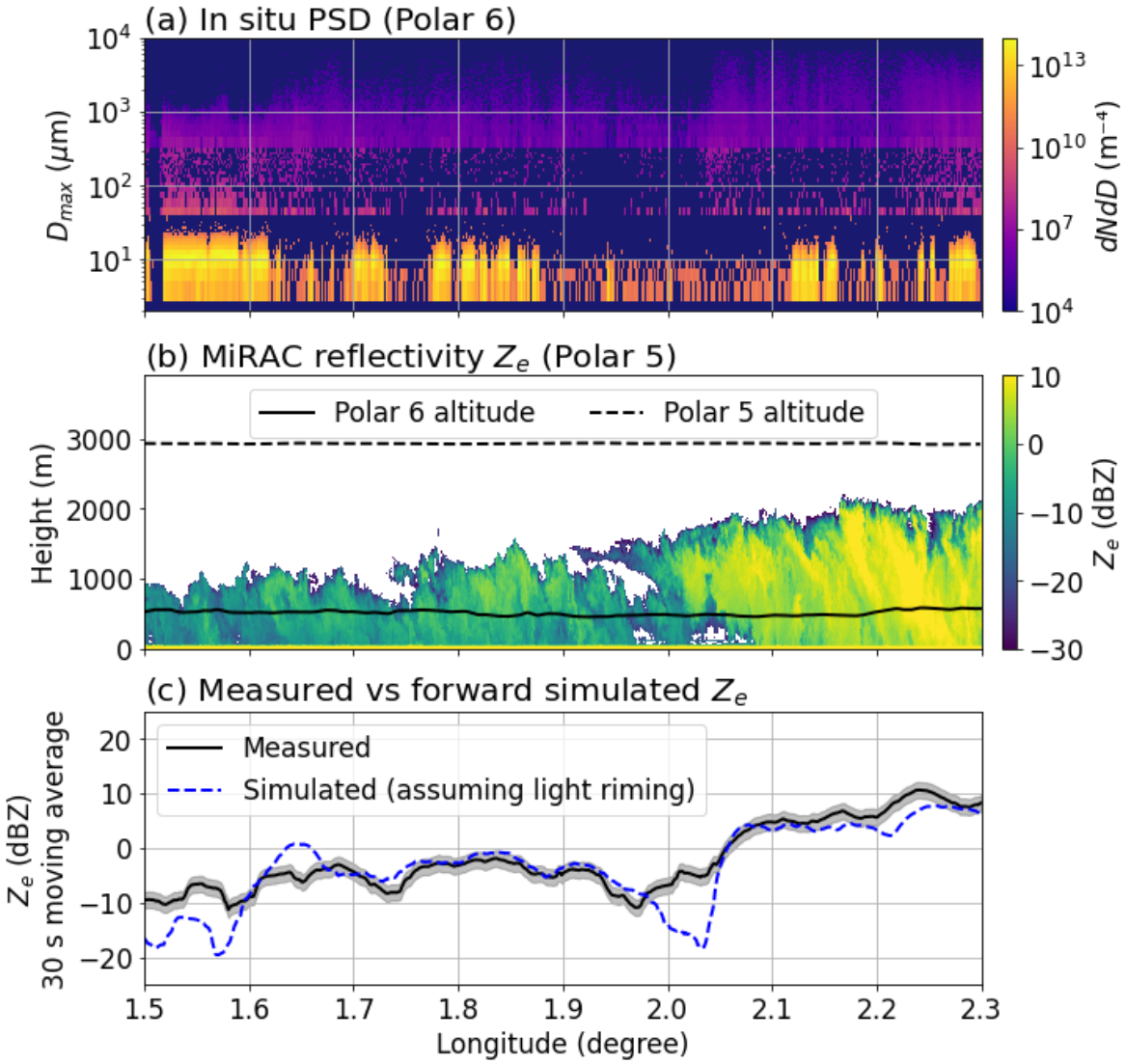

Figure 4: *Collocated flight between Polar 5 and Polar 6 for a flight segment of 12 minutes on 28 March 2022, between 14:12:30 and 14:14:20 UTC. a) in-situ particle size distributions (PSD), recorded with different instruments on the Polar 6 aircraft. b) MiRAC radar reflectivity measurements taken from the Polar 5 aircraft. The horizontal lines represent the altitude from the two Polar research aircraft. c) Measured (MiRAC) and simulated (PAMTRA) radar reflectivity for the flight altitude of the Polar 6.*

observations with Polar 5 and in-situ measurements with Polar 6 is used to characterize cloud micro- and macrophysical properties. These collocated data set is very valuable for the development of cloud retrieval algorithms. During the HALO-(AC)^3 campaign both Polar aircraft spent in total 13 hours and 17 minutes, in a spatial range of 10 km and a temporal range of 5 minutes, together. A section of these collocated measurements is displayed in Fig. 4. The measurements from 28 March 2022 show a size distribution of in-situ particle measurements, operated on Polar 6 (Fig. 4a) and radar reflectivity measurements from the MiRAC instrument (Mech et al., 2019) on Polar 5 (Fig. 4b). Based on the in-situ particle measurements, forward simulations were made with the Passive and Active Microwave TRAnsfer (PAMTRA) tool (Mech et al., 2020), assuming light riming. The result of the simulations is shown in Fig. 4c and compared to the

measured radar reflectivity. In general there is a good agreement, just below 1.6° and around 2.0° longitude the simulations are clearly below the measured radar reflectivity, which indicates a stronger riming of the particles at these locations. The analysis of this flight section demonstrates that it is possible to derive the radar reflectivity from in situ particle size distributions. In a future study we aim to invert the radar measurements and use similar tools to derive the cloud particle properties from remote sensing. This will be more challenging, because the PSD and the amount of riming is unknown.

4 Lagrangian trajectory analysis of a Warm Air Intrusion

The meteorological state in the Arctic was analyzed based on ERA5 reanalysis data (Hersbach et al., 2020). Many atmospheric observations collected during the campaign, such as most dropsonde thermodynamics profiles, were directly assimilated into ERA5. Furthermore, ERA5 has been shown to outperform several other reanalyses in Fram Strait (Graham et al., 2019a,b). For trajectory calculations, ERA5 wind fields were used in conjunction with the *Lagranto* analysis tool (Sprenger and Wernli, 2015). For the analysis presented here, trajectories were started:

- Temporally, every full hour between 9-15 March 2022
- Horizontally, along the 80°N latitude circle, in 1° steps between 15°W to 10°E (i.e., between Greenland and Svalbard)
- Vertically, at a pressure level of 850 hPa

Trajectories were calculated 60 hours (2.5 days) forward in time. Along the trajectories, a set of meteorological parameters were extracted from ERA5. In particular, the analysis aimed at:

- The normalized density of trajectories per 100 km^2 area
- The air mass properties at the start of the drift, i.e., in Fram Strait
- The total change in meteorological parameters, i.e., the end value (t = +60 hours) minus the start value (t = 0 hours)

4.1 Synoptic conditions and air mass pathways

Figure 5 shows the ERA5-derived synoptic conditions for two distinct periods in mid-March 2022. The period 9-11 March 2022 was defined as background period, as here no increased values for total column water vapor were detected in the central Arctic. On the contrary, 12-15 March 2022 was defined as WAI period. Driven by a dipole pattern in mean sea-level pressure (black isobars), large amounts of water vapor (upper row) and heat (lower row, air temperature at 850 hPa altitude) were advected towards the North Pole. In the following chapter, the differences between these two periods are characterized.

Figure 6 depicts the normalized density of air masses on their 2.5-day drift, starting in Fram Strait. As can be seen, two very separate pathways emerge for the two time

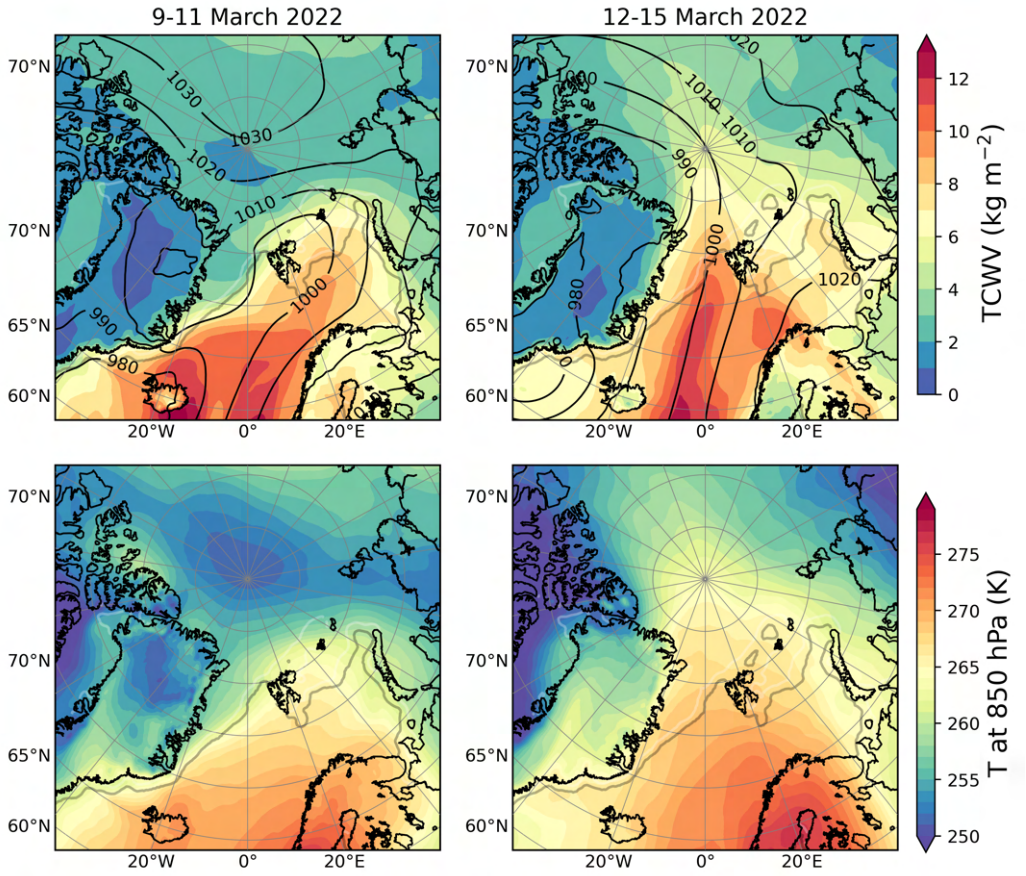

Figure 5: *Synoptic overview of the two periods, based on ERA5. Depicted are the mean values of (top panel) total column water vapor (filled contours), mean sea-level pressure (contours, in hPa), (bottom panel) air temperature at the 850 hPa pressure level. In all graphs, the gray lines denote the 15 % and 80 % sea-ice margins.*

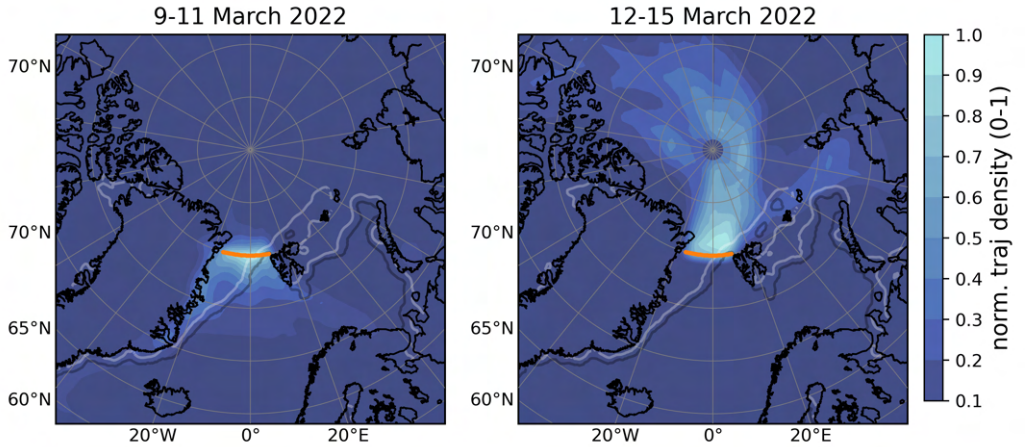

Figure 6: *Normalized density of air mass trajectories initiated at 850 hPa altitude in Fram Strait (orange line) along their 2.5-day drift. Two distinct periods are contrasted, 9-11 March 2022 versus 12-15 March 2022. The gray lines denote the 15 % and 80 % sea-ice margins. Data is based on ERA5 wind fields and Lagranto.*

periods. During 9-11 March 2022 air masses mostly drifted very slowly and generally southwards. On the contrary, 12-15 March 2022 air masses were strongly pushed northwards and traversed the North Pole.

These two pathways were not only geographically different, the properties of air masses at the start and along the flow were also different.

4.2 Properties along pathways

Figures 7a and b compare the frequency distribution of the potential temperature θ and specific humidity q of the two air masses at the start of the trajectories. The change of both parameters along the air mass trajectory is presented in Fig. 7c and d. At the starting location, the background period of 9-11 March 2022 was characterized by an air mass with a mean 850 hPa potential temperature of around 270 K, and on average very low specific humidities of about 1 g kg^{-1}. On their 2.5-day drift, the air mass generally underwent medium moistening by 0-2 g kg^{-1}. The distribution of potential temperature change was bimodal. One mode was centered around 0 K, i.e., air masses moved isentropically and did not undergo excessive heating. The slightly weaker second mode peaked at an average diabatic warming of about 7 K. Overall, the 9-11 March 2022 air parcels showed many properties, which hinted towards a weak CAO, i.e., slight moistening and diabatic heating, possibly reinforced by surface sensible and latent heat fluxes from the warm ocean. This is in line with the trajectories depicted in Fig. 6.

In contrast, the WAI during 12-15 March 2022 caused a different transition of the air mass. Already at the start location, potential temperatures were about 10 K higher, at around 280 K. Furthermore, most air masses had an initial specific humidity of more than 3 g kg^{-1}. On their path towards the North Pole, these air masses lost most of their

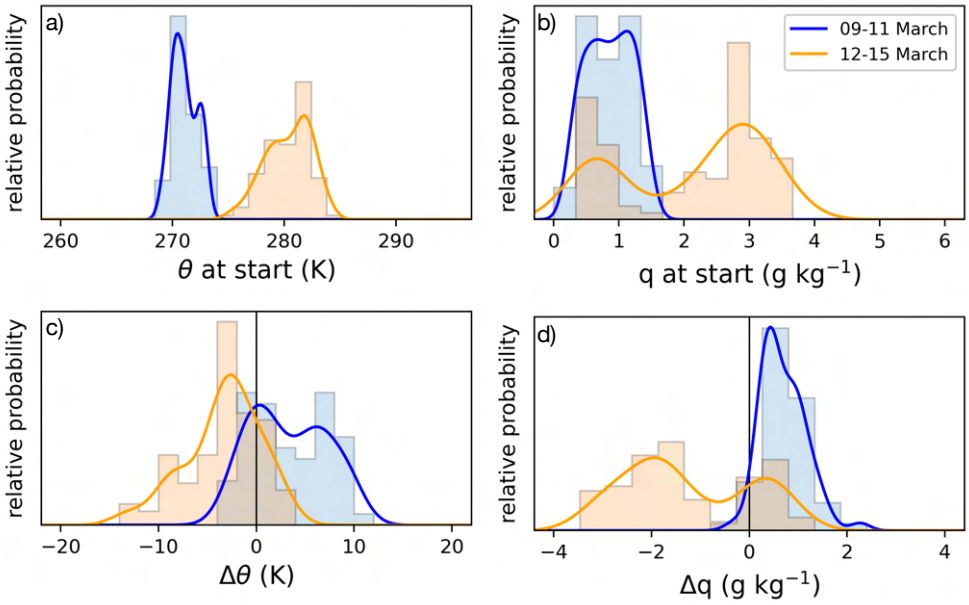

Figure 7: *Comparison of different air mass properties at the start and during their 2.5-day drift. Shown are the histograms and kernel density functions for 9-11 March 2022 in contrast to 12-15 March 2022. The parameters comprise a) potential temperature θ and b) specific humidity q at start, as well as their total change within 2.5 days (c and d).*

water vapor. Not least to their high initial air temperatures, they also cooled diabatically, with mean values of -3 K to -8 K in 2.5 days.

5 Summary and conclusions

In this report, we summarized the current activities of LIM with respect to the airborne observations of Arctic air mass transformations during the HALO-(AC)^3 mission. The campaign was conducted in March and April 2022 with the goal to perform quasi-Lagrange observations of air mass transformations and to test the ability of numerical atmospheric models to reproduce the measurements. Three aircraft, namely HALO, Polar 5 and Polar 6, were involved to study clouds and the Arctic atmosphere on large and small spatial scales. Three studies using HALO-(AC)^3 observations and reanalysis data that are lead by LIM are reported here.

Vertical profiles characterizing the Arctic atmosphere are analyzed. With 492 launched dropsondes, the Arctic atmosphere was extensively probed during HALO-(AC)^3. Vertical profiles of atmospheric properties were compared for locations over sea-ice and the ice-free ocean. The comparison shows that in general lower temperatures, lower relative humidities and lower wind speeds were present over ice than over ice-free ocean. In addition, dropsonde profiles were analyzed along a CAO and show how the warm ocean surface affects the air mass transformation.

Collocated observations from Polar 5 and Polar 6 were analyzed. In particular, radar reflectivities were simulated based on in-situ measurements of cloud particle properties measured with the Polar 6 aircraft. To evaluate how accurate these simulations are, the results were compared with the radar measurements from the Polar 5 aircraft. This comparison shows a good agreement between radar reflectivity measurements and simulations based on in-situ measurements indicating the potential of the collocated data set.

Lagrangian trajectory analysis were used to characterize the synoptic conditions during mid-March 2022, i.e., at the start of the HALO-(AC)^3 airborne campaign. The background period defined here as 9-11 March 2022 was compared to the WAI period of 12-15 March 2022. Two distinct pathways of air masses were found for these periods. While the background case showed a slow southward drift of Fram Strait air parcels, the WAI pushed large amounts of air towards the North Pole and beyond. The analysis of air mass properties along their trajectories showed that not only the air-mass properties at the start in Fram Strait differed, but also thermodynamic processes along the flow (diabatic heating/cooling, moisture changes). It can be concluded that air masses in the two periods underwent clearly distinct transformation processes.

These examples indicate the potential of the observations during the HALO-(AC)^3 mission. Future analyis of the data will aim at a better understanding of how the transport of air masses in the Arctic works and how it affects the large-scale environment.

Acknowledgements

We gratefully acknowledge the funding by the Deutsche Forschungsgemeinschaft (DFG, German Research Foundation) – Project Number 268020496 5 – TRR 172, within the

Transregional Collaborative Research Center "ArctiC Amplification: Climate Relevant Atmospheric and SurfaCe Processes, and Feedback Mechanisms $(AC)^3$.

References

Brümmer, B.: Boundary-layer modification in wintertime cold-air outbreaks from the Arctic sea ice, Boundary-Layer Meteorology, 80, 109–125, doi:10.1007/BF00119014, 1996.

Dahlke, S., Solbès, A., and Maturilli, M.: Cold Air Outbreaks in Fram Strait: Climatology, Trends, and Observations During an Extreme Season in 2020, Journal of Geophysical Research: Atmospheres, 127, doi:10.1029/2021JD035741, 2022.

Graham, R., Cohen, L., Ritzhaupt, N., et al.: Evaluation of six atmospheric reanalyses over Arctic sea ice from winter to early summer, J. Clim., 32, 4121–4143, doi:10.1175/JCLI-D-18-0643.1, 2019a.

Graham, R. M., Itkin, P., Meyer, A., et al.: Winter storms accelerate the demise of Arctic sea ice, Sci. Rep., 9, 9222, doi:10.1038/s41598-019-45574-5, 2019b.

HALO-$(AC)^3$ Website: HALO-$(AC)^3$ - Arctic Air Mass Transformations During Warm Air Intrusions and Marine Cold Air Outbreaks, URL `https://halo-ac3.de/halo-ac3/campaign/`, 2023.

Hersbach, H., Bell, B., Berrisford, P., et al.: The ERA5 global reanalysis, Quarterly Journal of the Royal Meteorological Society, 146, 1999–2049, doi:10.1002/qj.3803, 2020.

Kuettner, J. P.: Cloud bands in the earth's atmosphere: Observations and Theory, Tellus, 23, 404–426, doi:10.1111/j.2153-3490.1971.tb00585.x, 1971.

Lemone, M. A.: Modulation of turbulence energy by longitudinal rolls in an unstable planetary boundary layer, Journal of the Atmospheric Sciences, 33, 1308–1320, 1976.

Mech, M., Kliesch, L.-L., Anhäuser, A., et al.: Microwave Radar/radiometer for Arctic Clouds (MiRAC): first insights from the ACLOUD campaign, Atmospheric Measurement Techniques, 12, 5019–5037, doi:10.5194/amt-12-5019-2019, 2019.

Mech, M., Maahn, M., Kneifel, S., et al.: PAMTRA 1.0: the Passive and Active Microwave radiative TRAnsfer tool for simulating radiometer and radar measurements of the cloudy atmosphere, Geoscientific Model Development, 13, 4229–4251, doi:10.5194/gmd-13-4229-2020, 2020.

Rantanen, M., Karpechko, A. Y., Lipponen, A., et al.: The Arctic has warmed nearly four times faster than the globe since 1979, Communications Earth & Environment, 3, 168, doi:10.1038/s43247-022-00498-3, 2022.

Serreze, M. C. and Barry, R. G.: Processes and impacts of Arctic amplification: A research synthesis, Global and Planetary Change, 77, 85–96, doi:10.1016/j.gloplacha.2011.03.004, 2011.

Sprenger, M. and Wernli, H.: The Lagrangian analysis tool LAGRANTO – version 2.0, Geosci. Model Dev. Discuss., 8, 1893–1943, doi:10.5194/gmdd-8-1893-2015, 2015.

Tornow, F., Ackerman, A. S., Fridlind, A. M., et al.: Dilution of Boundary Layer Cloud Condensation Nucleus Concentrations by Free Tropospheric Entrainment During Marine Cold Air Outbreaks, Geophysical Research Letters, 49, e2022GL098 444, doi:10.1029/2022GL098444, e2022GL098444 2022GL098444, 2022.

Wendisch, M., Müller, D., Schell, D., and Heintzenberg, J.: An Airborne Spectral Albedometer with Active Horizontal Stabilization, Journal of Atmospheric and Oceanic Technology, 18, 1856 – 1866, doi:10.1175/1520-0426(2001)018<1856:AASAWA>2.0.CO;2, 2001.

Wendisch, M., Brückner, M., Crewell, S., et al.: Atmospheric and Surface Processes, and Feedback Mechanisms Determining Arctic Amplification: A Review of First Results and Prospects of the (AC)3 Project, Bulletin of the American Meteorological Society, 104, E208 – E242, doi:10.1175/BAMS-D-21-0218.1, 2023.

Wesche, C., Steinhage, D., and Nixdorf, U.: Polar aircraft Polar5 and Polar6 operated by the Alfred Wegener Institute, Journal of large-scale research facilities Facilities, 2, doi:10.17815/jlsrf-2-153, 2016.

Long-term changes and trends of mesosphere/lower thermosphere winds over Collm, Germany

Jacobi, Ch.✉, Karami, K.

Leipzig Institute for Meteorology, Leipzig University, Germany
✉*e-mail: jacobi@uni-leipzig.de*

Summary: We analyse 43 years of mesosphere/lower thermosphere (MLT) horizontal winds obtained from a joint analysis of low frequency (LF) spaced receiver lower ionospheric drift measurements from 1979 through 2006 and very high frequency (VHF) meteor radar wind observations since 2004 at Collm (51°N, 13°E). Due to limitations of the earlier LF measurements, we restrict ourselves to the analysis of monthly mean winds near 90 km, which represents the height of maximum meteor activity as well as LF reflections in the MLT. In the 1980s and 1990s, we observe mainly positive trends of the zonal prevailing wind throughout the year, while the meridional winds tend to decrease in magnitude in both summer and winter. We also analyse interannual variability, in particular with respect to a possible signature of NAO and ENSO. These signals, however, are relatively weak and not stable throughout the time of observations.

Zusammenfassung: Wir analysieren 43 Jahre Messungen horizontaler Winde in der Mesosphäre/unteren Thermosphäre (MLT) über Collm (51°N, 13°E), die aus einer gemeinsamen Analyse von Langwellen (LF) -Driftmessungen in der unteren Ionosphäre von 1979 bis 2006 und VHF-Meteorradar-Windbeobachtungen seit 2004 gewonnen wurden. Aufgrund der Einschränkungen der früheren LF-Messungen beschränken wir uns auf die Analyse der mittleren monatlichen Windgeschwindigkeiten bei 90 km, welches die Höhe maximaler Meteorraten sowie die mittleren nächtlichen LF-Reflexionshöhen in der MLT darstellt. In den 1980er und 1990er Jahren beobachten wir das ganze Jahr über hauptsächlich positive Trends des zonalen mittleren Windes, während die Stärke des meridionalen Windes sowohl im Sommer als auch im Winter tendenziell abnimmt. Wir analysieren auch die Variabilität von Jahr zu Jahr, insbesondere im Hinblick auf eine mögliche Signatur von NAO und ENSO. Diese Signale sind jedoch relativ schwach und nicht über die gesamte Beobachtungszeit stabil nachweisbar.

1 Introduction

It is well known that anthropogenic influences have a cooling effect on the middle atmosphere, including the mesosphere/lower thermosphere (MLT) which has been shown by observations (She et al., 2019) and modeling (Qian et al., 2019; Liu et al., 2020), and which is associated with a shrinking of atmospheric layers from the stratosphere (Pisoft et al., 2021) and mesosphere (Taubenheim et al., 1997; Bremer and Berger, 2002; Peters et al., 2017) to the thermosphere (Emmert et al., 2008; Emmert, 2015). Thermospheric climate change also manifests itself in changes and a decrease in ionospheric layer heights and long-term variability of their plasma parameters (Mielich and Bremer, 2013;

Jakowski et al., 2017; Liu et al., 2021). This has been summarized several times (e.g., Beig et al., 2003; Laštovička et al., 2006, 2008; Beig, 2011). The effect of anthropogenic atmospheric composition change on the MLT wind is less clear. From earlier radar observations there is an indication that, at least during the last decades, the zonal winds change towards more westerly ones both in summer and winter, and that the meridional winds show a decrease in magnitude (Bremer et al., 1997; Jacobi et al., 1997, 2015; Hoffmann et al., 2011). However, winds in the MLT are strongly forced by gravity wave breaking, and the gravity waves are in turn filtered by the middle atmosphere mean winds. This means, that the MLT winds are influenced mainly by middle atmospheric mean wind changes. Possible changes in gravity wave sources and the interaction between mean winds and waves play a minor role as has been shown by Smith et al. (2010). Still, besides further modeling effort, analysis of long wind time series are required.

Apart from the long-term cooling and a decrease in layer heights, changes in trends of various middle and upper atmosphere parameters have been reported. One mechanism possibly responsible for trend changes is the ozone reversal after 1995, and decreasing cooling or even recent warming of the middle atmosphere had been attributed to that (Lübken et al., 2013). Trends of other parameters, such as planetary waves or ozone laminae (Jacobi et al., 2008, 2009b) also had breakpoints near the ozone turnaround date, and MLT wind changes were thought to be connected with that. It is, however, also possible that MLT wind trend changes are connected with long-term trends in the lower atmosphere, e.g. increased temperature trends at high latitudes after the 1990s (Chylek et al., 2022; Wendisch et al., 2023).

MLT wind variability has been also observed at different time scales, including the decadal and quasi-biennial one. Also a possible correlation with tropospheric circulation patterns like the North Atlantic Oscillation (NAO) and El Nino/Southern Oscillation (ENSO) have been proposed based on shorter LF wind time series over Collm (Jacobi and Beckmann, 1999; Jacobi and Kürschner, 2002). All these influences, however, appeared to be not stable at 90 km over several decades, as has been shown by later analyses using an extended LF dataset (Jacobi, 2009). In particular, there are hints that the effect is height dependent (Jacobi et al., 2017; Jacobi and Mewes, 2017). Indeed, there is a clear ENSO and NAO influence on the stratospheric polar vortex in winter (van Loon and Labitzke, 1987; Taguchi and Hartmann, 2006), which extends to the mesosphere (Sassi et al., 2004), but vanishes or even reverses above (Jacobi et al., 2017).

2 Observations

At Collm (51.3°B, 13.0°E), MLT winds had been measured from December 1978 to 2008 by the low frequency (LF) spaced receiver (D1) method using the sky wave of three commercial radio transmitters. LF observations had started even earlier than 1978 (e.g., Sprenger and Schminder, 1967), but early measurements had been performed on single frequencies and they are not used here. Monthly mean zonal and meridional prevailing winds have been calculated from monthly medians with a regression analysis including mean winds and the semidiurnal tide (Jacobi and Kürschner, 2006). Since the reflection height itself has been measured only after late 1982 (Kürschner and Schminder, 1986; Kürschner et al., 1987), the data are attributed to the mean nighttime LF reflection height of about 90 km (Jacobi et al., 2009a).

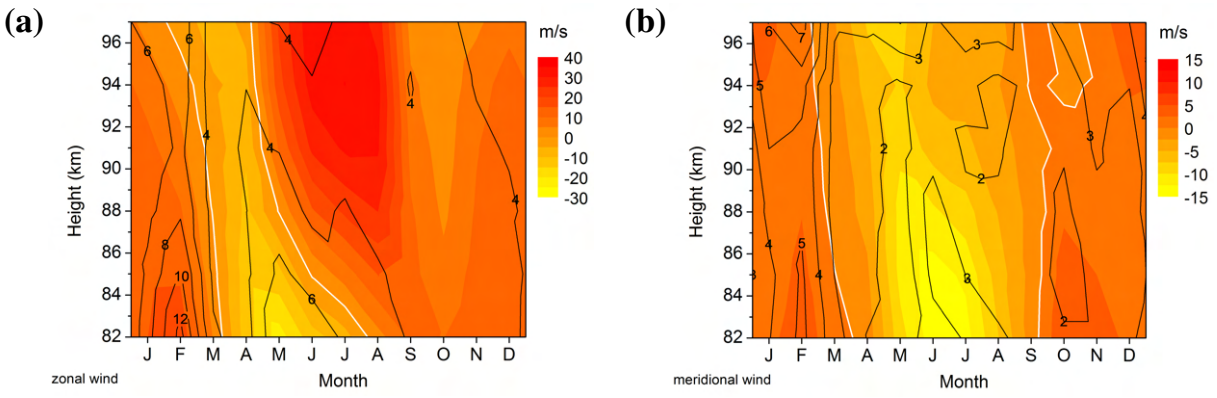

Figure 1: *Color coding: 2005–2021 mean monthly mean (a) zonal and (b) meridional winds over Collm measured by VHF meteor radar. The respective zero lines are given as solid white curves. Contour lines: standard deviations based on the monthly means of each year.*

Since 2004 to date, very high frequency (VHF) meteor radar observations on 36.2 MHz have been performed at Collm (Jacobi et al., 2007). An upgrade of the radar has been made in 2015/2016, including antenna configuration and peak power increase. Details of the radar configuration can be found, e.g., in Stober et al. (2021). The radar delivers winds in the approximate height range of 75 to 105 km. The height information is provided by an interferometer. Mean height-time cross-sections of zonal and meridional VHF radar winds for the years 2005–2021 are shown in Figure 1. In winter, zonal winds are westerly and meridional winds are poleward. In summer, zonal winds are easterly in the upper mesosphere, but westerly in the lower thermosphere, while the meridional winds are southward. Meridional winds, which are driven mainly by gravity wave mean flow interaction in the mesosphere, are considerably weaker than the zonal winds. Similar seasonal cycles of MLT winds have been already shown by earlier observations at Collm and at other midlatitude sites (e.g., Manson and Meek, 1984, 1991; Kashcheyev and Oleynikov, 1994; Schminder et al., 1997; Jacobi, 2012). In the following analysis, we use the VHF winds without the height information. Monthly mean prevailing winds are calculated by a least squares fit of one month of half-hourly mean winds on model winds including the mean (prevailing) wind and the semidiurnal and diurnal tide (Jacobi et al., 2015).

Meteor peak heights are close to 90 km (e.g., Liu et al., 2017) and thus are comparable to the mean LF nighttime reflection heights. Therefore, the LF and VHF wind time series have been combined using a LF D1 speed bias correction and a virtual height correction based on the joint LF/VHF observations from mid 2004 to 2008. The virtual height correction takes into account the group retardation of LF radio waves in the ionospheric D region that leads to greater apparent (virtual) heights. The correction was performed using phase comparisons of the semidiurnal tide (Jacobi, 2011) and resulted in mean nighttime LF real height estimates that are very close to meteor peak heights. The zonal LF and VHF winds during the time interval of joint measurements were close to each other (Jacobi et al., 2015). The meridional LF and VHF winds differed, which was partly due to a spaced receiver speed bias particularly strong in meridional winds (Jacobi et al., 2009a). Therefore, a mean meridional wind bias for each month of the year

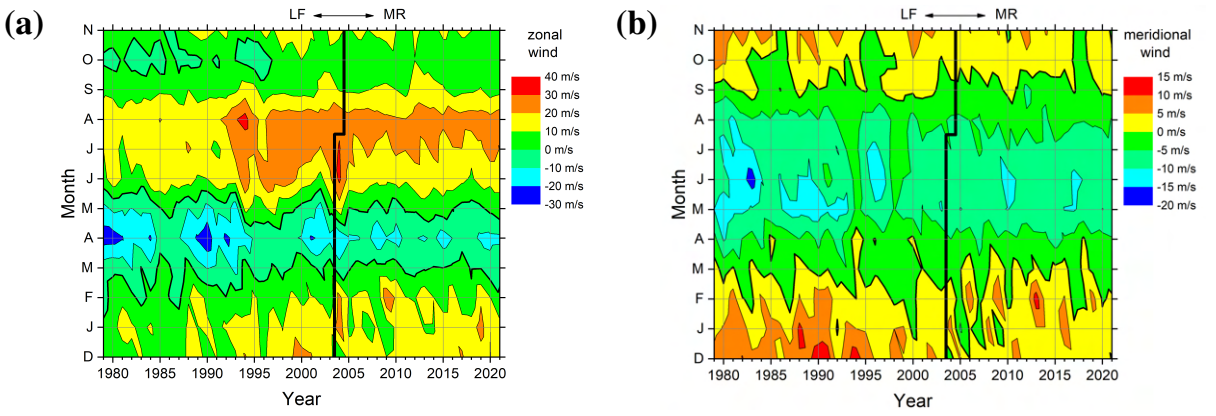

Figure 2: *Monthly mean (a) zonal and (b) meridional winds over Collm at approx. 90 km altitude. Note the different scaling of the two panels. The seasonal change is indicated by the ordinate for each year shown in the abscissa; note that the December values belong to the respective previous year. The solid black line shows the change from LF to VHF observations.*

was determined separately and used to correct the LF meridional winds. The analysis method is described by Jacobi et al. (2015). Here, we use combined LF/VHF data from December 1978 through 2021 for a long-term trend and year-to-year variability analysis.

3 Results

Figure 2 shows the monthly mean zonal and meridional winds from the combined LF and VHF wind analysis. Apart from the seasonal cycle that is also seen in Figure 1, interannual and long-term changes are visible. In particular, the zonal winds, on an average, increase with time in each month, while the meridional winds decrease in winter and increase in summer. Since the summer meridional winds are negative, this actually relates to a decrease in magnitude during both seasons. Particularly in winter, there is considerable wind variability at time scales of a few years. In spring, also a quasi-decadal variability of the zonal wind is visible, although this does not seem to be a stable signature throughout the whole period of observations.

3.1 Long-term trends

In Figure 3, 3-monthly mean zonal and meridional winds over Collm at about 90 km are shown for winter (a, December–February, DJF), spring (b, March–May, MAM), summer (c, June–August, JJA), and autumn (d, September–November, SON). Linear fits are added as solid lines. The trend coefficients for each month of the year are shown in red in Figure 4. As has been visually shown in Figure 2 already, the zonal wind trends are positive throughout the year, and they are statistically significant during most months. The meridional winds trends are positive in summer and negative in winter, which is related to a weakening of the wind in all seasons. Similar results, based on shorter time intervals or earlier observations, have been already shown, e.g., by Bremer et al. (1997); Jacobi et al. (1997).

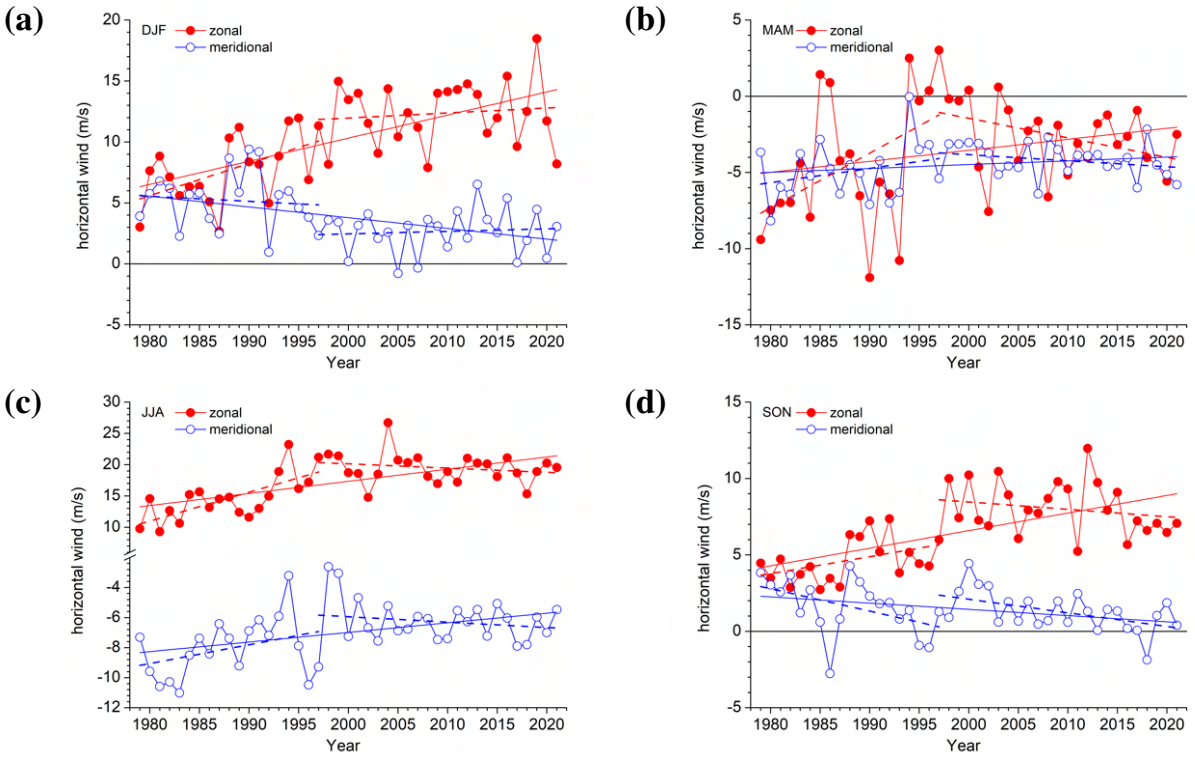

Figure 3: *Seasonal mean zonal (red) and meridional (blue) prevaling winds for (a) DJF, (b) MAM, (c) JJA, and (d) SON over Collm at approx. 90 km altitude. Linear fits are added. Dashed lines show linear fits for the time interval 1979-1997 and 1997-2002.*

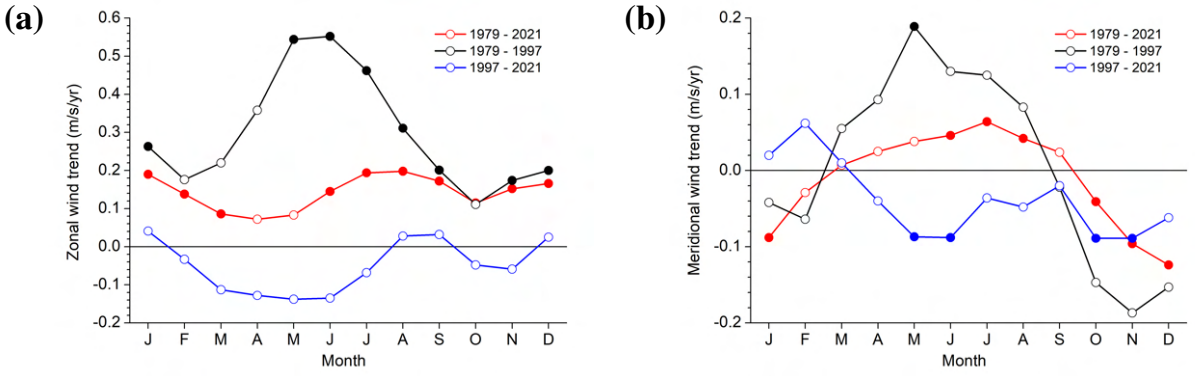

Figure 4: *Trend coefficients for (a) zonal and (b) meridional 3-monthly mean winds over Collm at approx. 90 km altitude for three different time intervals. Solid symbols denote significant trends according to a t-test.*

Visual inspection of Figure 3 reveals that the long-term trends change after the 1990s. This has already been analyzed from shorter time series (Jacobi et al., 2015). Therefore linear fits for the first and second half of the time series are added in Figure 3, and the trend coefficients for each month are added in Figure 4. They show that the long-term increase in zonal wind is mainly due to the first half of the time interval under consideration, while after 1997 the zonal wind trends are small. The meridional wind trends, except for autumn/early winter, actually reverse after the 1990s.

3.2 Interannual variability

Figure 5 shows periodograms, calculated from the zonal (red) and meridional (blue) monthly winds from 12/1978 to 05/2022. While the major peaks are owing to the annual and, for the zonal component, semiannual cycle, there is some variability at the 3 year, 5-6 year, and quasi-decadal time scale, which is more strongly expressed in the zonal wind component than in the meridional one. These variations have time scales of lower atmospheric circulation patterns and the solar cycle. A signature of the latter has been found in Collm time series (e.g., Jacobi et al., 1997; Jacobi and Kürschner, 2006), but inspection of the quasi-decadal variability of the winds in Figure 3 shows that this variation, most strongly expressed in spring, is not stable and changes phase with respect to solar activity, e.g., visible in zonal wind maxima around 1985 and 1995 (solar minimum) and 2015 (solar maximum).

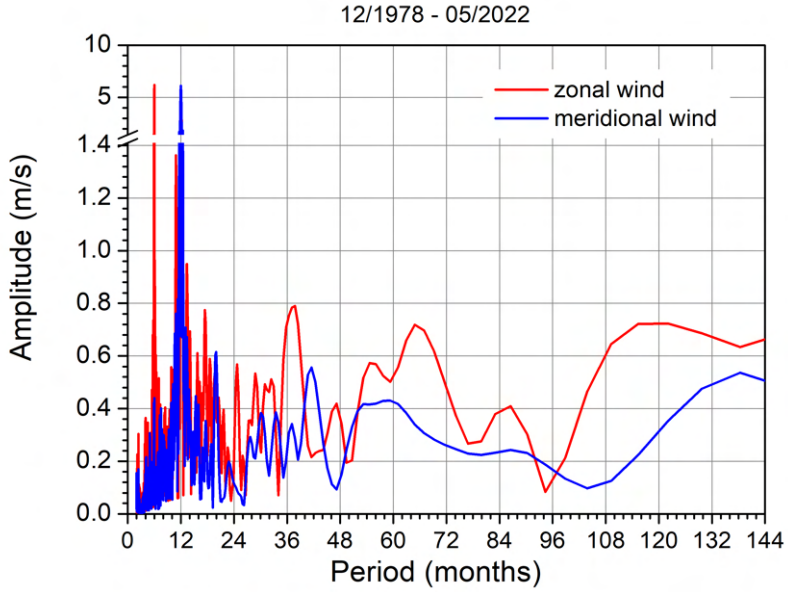

Figure 5: *Periodograms of zonal (red) and meridional (blue) monthly mean winds over Collm.*

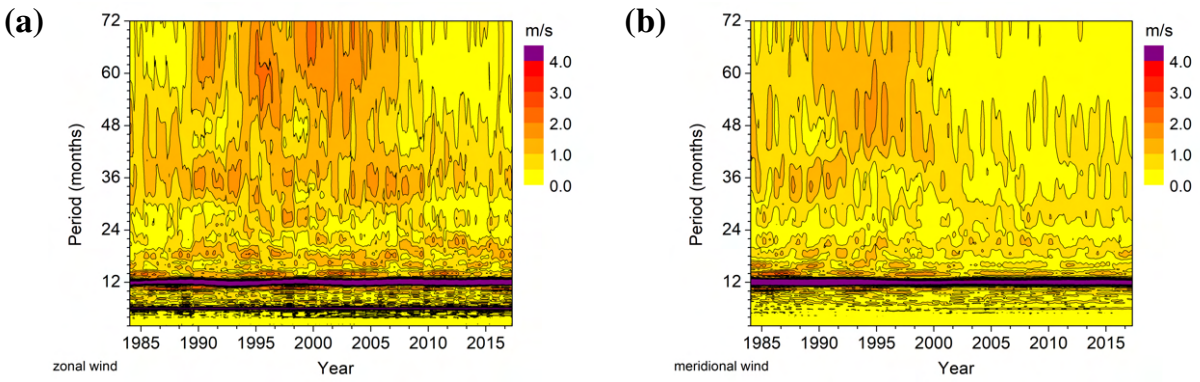

Figure 6: *Running periodograms based on 11 years of 3-monthly mean (a) zonal and (b) meridional winds each.*

Because visual inspection of Figure 2 indicates that the year-to-year variations e.g. at the 3-year and quasi 5-year time scale are intermittent, Figure 6 shows running periodograms, each based on 11 years of data. They show that interannual variations of MLT winds are actually present at time scales that may be connected with circulation patterns such as NAO and ENSO. However, these maxima are not continuously visible throughout the time interval investigated. So a quasi 5-year variability in the zonal wind is only present in the 1990s and early 2000s, while the 3-year oscillations appear to decrease then. Similarly, a 3-year variation in the meridional wind is replaced by a 4-year cycle after 1993.

Thus, in order to analyse the possible ENSO or NAO signature in MLT winds, Figure 7 shows running correlation (Kodera, 1993) coefficients, each based on 11 years of monthly data, between Collm zonal winds and (a) Nino3 sea surface temperature (SST) anomalies (Rayner et al., 2003) as proxy for ENSO and (b) NAO indices (Barnston and Livezey, 1987). Since both ENSO and NAO are most active during boreal winter, we show December, January, and February monthly winds here.

The correlation of zonal MLT wind and ENSO SST is negative in February during the first years of the time series (Figure 7(a)). In the 21st century, this reverses and the correlation is positive then. For December and January, there is a tendency for a negative trend of the correlation coefficient, which reverses to a more positive one for January after the mid 1990s. The correlation with NAO (Figure 7(b)) is positive in January and February until the middle 1990s (see Jacobi and Beckmann, 1999). This correlation actually reverses after the year 2000.

4 Conclusions and outlook

We have analysed 43 years of MLT zonal and meridional mean winds over Collm to show long-term trends, their changes, and interannual and quasi-decadal variability. The zonal wind trends are positive throughout the year and the meridional winds trends are positive in summer and negative in winter, which is related to a meridional wind weakening in all seasons. There is considerable variabiliy of winds at time scales of several years, and a quasi-decadal variation is visible.

There are indications for a trend change in the late 1990s, which is visible in each

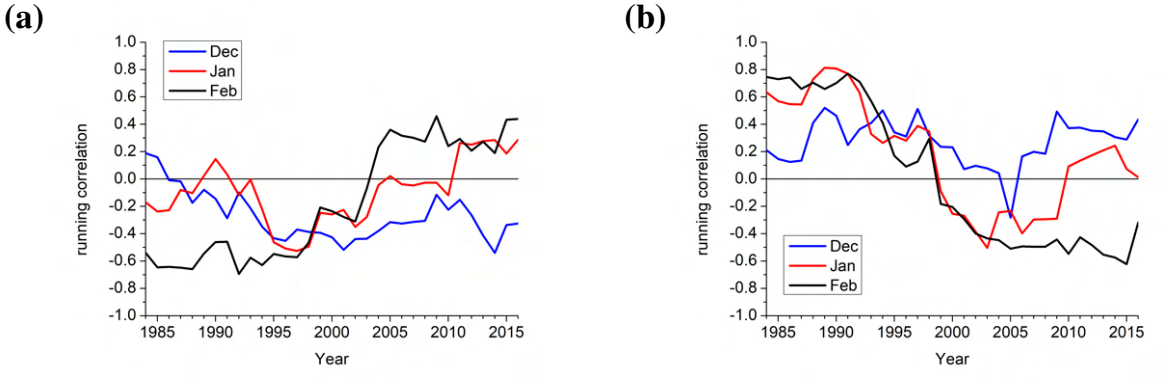

Figure 7: *Running correlation based on 11 years each of Collm monthly mean zonal wind and the (a) Nino3 SST and (b) NAO index.*

month. Such a change, possibly connected with the ozone turnaround after 1995 or lower atmosphere climate change, has been reported earlier (Jacobi et al., 2015). The update of the Collm time series presented here shows that the wind tendencies after the late 1990s, which mainly show a decrease or even a reversal of the trends before that time, continued during the recent years.

The correlation of MLT winds with tropospheric circulation patterns is intermittent, in particular a change even in sign after the 1990s is visible. This is also the case for the quasi-decadal cycle. The reason for this behavior is presently unclear. However, model experiments show that the ENSO and NAO signals in middle atmosphere winds change with height, and tend to reverse in the MLT. Thus, one may speculate that the intermittent lower atmosphere signals in MLT winds are owing to middle atmosphere circulation changes that influence the height up to which circulation patterns influence the mesospheric winds.

After 2004, the VHF wind observations deliver height-resolved time series between approximately 80 and 100 km. An analysis of height-resolved trends of wind parameters, together with modeling of the MLT response to tropospheric variations, will show whether the missing trend after the 1990s as shown in Figure 4(a) is an effect of trends decreasing with height, and possibly reversing. The same is the case with the weak and unstable NAO and ENSO signal at 90 km altitude, and a possible solar cycle effect on the MLT.

Acknowledgements: Nino3 SST anomalies have been provided by NOAA ESRL through https://psl.noaa.gov/gcos_wgsp/Timeseries/Nino3/. NAO indices have been provided by NOAA CPC through https://www.ncei.noaa.gov/access/monitoring/nao/. This work was supported by the German Research Foundation (DFG) through grant JA 836/47-1.

References

Barnston, A. G. and Livezey, R. E.: Classification, Seasonality and Persistence of Low-Frequency Atmospheric Circulation Patterns, Mon. Wea. Rev., 115, 1083 – 1126, doi:https://doi.org/10.1175/1520-0493(1987)115<1083:CSAPOL>2.0.CO;2, 1987.

Beig, G.: Long-term trends in the temperature of the mesosphere/lower thermosphere region: 2. Solar response, J. Geophys. Res.: Space Physics, 116, A00H12, doi:10.1029/2011JA016766, 2011.

Beig, G., Keckhut, P., Lowe, R. P., et al.: Review of mesospheric temperature trends, Rev. Geophys., 41, 1015, doi:10.1029/2002RG000121, 2003.

Bremer, J. and Berger, U.: Mesospheric temperature trends derived from ground-based LF phase-height observations at mid-latitudes: comparison with model simulations, J. Atmos. Sol.-Terr. Phys., 64, 805–816, doi:10.1016/S1364-6826(02)00073-1, 2002.

Bremer, J., Schminder, R., Greisiger, K., et al.: Solar cycle dependence and long-term trends in the wind field of the mesosphere/lower thermosphere, J. Atmos. Sol.-Terr. Phys., 59, 497–509, doi:10.1016/S1364-6826(96)00032-6, 1997.

Chylek, P., Folland, C., Klett, J. D., et al.: Annual Mean Arctic Amplification 1970–2020: Observed and Simulated by CMIP6 Climate Models, Geophys. Res. Lett., 49, e2022GL099 371, doi:https://doi.org/10.1029/2022GL099371, 2022.

Emmert, J. T.: Altitude and solar activity dependence of 1967–2005 thermospheric density trends derived from orbital drag, J. Geophys. Res.: Space Physics, 120, 2940–2950, doi:10.1002/2015JA021047, 2015.

Emmert, J. T., Picone, J. M., and Meier, R. R.: Thermospheric global average density trends, 1967–2007, derived from orbits of 5000 near-Earth objects, Geophys. Res. Lett., 35, doi:10.1029/2007GL032809, 2008.

Hoffmann, P., Rapp, M., Singer, W., and Keuer, D.: Trends of mesospheric gravity waves at northern middle latitudes during summer, J. Geophys. Res.: Atmospheres, 116, D00P08, doi:10.1029/2011JD015717, 2011.

Jacobi, C.: Possible signal of tropospheric circulation patterns in middle atmosphere dynamics, Collm (51.3°N, 13°E) mesosphere lower thermosphere winds 1979-2008, Adv. Space Res., 45, 153–162, URL http://nbn-resolving.de/urn:nbn:de:bsz:15-qucosa2-163684, 2009.

Jacobi, C.: Meteor radar measurements of mean winds and tides over Collm (51.3° N, 13° E) and comparison with LF drift measurements 2005–2007, Adv. Radio Sci., 9, 335–341, doi:10.5194/ars-9-335-2011, 2011.

Jacobi, C.: 6 year mean prevailing winds and tides measured by VHF meteor radar over Collm (51.3°N, 13.0°E), J. Atmos. Sol.-Terr. Phys., 78-79, 8–18, doi:10.1016/j.jastp.2011.04.010, 2012.

Jacobi, C. and Beckmann, B.: On the connection between upper atmospheric dynamics and tropospheric parameters: Correlations between mesopause region winds and the North Atlantic Oscillation, Climatic Change, 43, 629 – 643, doi:10.1023/A:1005451227975, 1999.

Jacobi, C. and Kürschner, D.: A possible connection of mid-latitude mesosphere/lower thermosphere zonal winds and the southern oscillation, Phys. Chem. Earth, Parts A/B/C, 27, 571–577, doi:https://doi.org/10.1016/S1474-7065(02)00039-6, 2002.

Jacobi, C. and Kürschner, D.: Long-term trends of MLT region winds over Central Europe, Phys. Chem. Earth, Parts A/B/C, 31, 16–21, doi:10.1016/j.pce.2005.01.004, 2006.

Jacobi, C. and Mewes, D.: Influence of tropospheric circulation patterns on the winter middle and high-latitude mesosphere, 1st $(AC)^3$ Science Conference on Arctic Amplification, March 26th – 28th, 2017, University of Bremen, 2017.

Jacobi, C., Schminder, R., Kürschner, D., et al.: Long-term trends in the mesopause wind field obtained from LF D1 wind measurements at Collm, Germany, Adv. Space Res., 20, 2085–2088, doi:10.1016/S0273-1177(97)00599-1, 1997.

Jacobi, C., Fröhlich, K., Viehweg, C., Stober, G., and Kürschner, D.: Midlatitude mesosphere/lower thermosphere meridional winds and temperatures measured with meteor radar, Adv. Space Res., 39, 1278 – 1283, doi:10.1016/j.asr.2007.01.003, 2007.

Jacobi, C., Hoffmann, P., and Kürschner, D.: Trends in MLT region winds and planetary waves, Collm (52°N, 15°E), Ann. Geophys., 26, 1221–1232, doi:10.5194/angeo-26-1221-2008, 2008.

Jacobi, C., Arras, C., Kürschner, D., et al.: Comparison of mesopause region meteor radar winds, medium frequency radar winds and low frequency drifts over Germany, Adv. Space Res., 43, 247 – 252, doi:10.1016/j.asr.2008.05.009, 2009a.

Jacobi, C., Hoffmann, P., Liu, R., et al.: Midlatitude mesopause region winds and waves and comparison with stratospheric variability, J. Atmos. Sol.-Terr. Phys., 71, 1540–1546, doi:10.1016/j.jastp.2009.05.004, 2009b.

Jacobi, C., Lilienthal, F., Geißler, C., and Krug, A.: Long-term variability of mid-latitude mesosphere-lower thermosphere winds over Collm (51°N, 13°E), J. Atmos. Sol.-Terr. Phys., 136, 174–186, doi:10.1016/j.jastp.2015.05.006, 2015.

Jacobi, C., Ermakova, T., Mewes, D., and Pogoreltsev, A. I.: El Niño influence on the mesosphere/lower thermosphere circulation at midlatitudes as seen by a VHF meteor radar at Collm (51.3° N, 13° E), Adv. Radio Sci., 15, 199–206, doi:10.5194/ars-15-199-2017, 2017.

Jakowski, N., Hoque, M., Mielich, J., and Hall, C.: Equivalent slab thickness of the ionosphere over Europe as an indicator of long-term temperature changes in the thermosphere, J. Atmos. Sol.-Terr. Phys., 163, 91–102, doi:10.1016/j.jastp.2017.04.008, 2017.

Kashcheyev, B. and Oleynikov, A.: Dynamic regime of the mesopause—lower thermosphere at mid-latitudes of the northern hemisphere by radio meteor observations, J. Atmos. Sol.-Terr. Phys., 56, 1197–1207, doi:10.1016/0021-9169(94)90057-4, 1994.

Kodera, K.: Quasi-decadal modulation of the influence of the equatorial quasi-biennial oscillation on the north polar stratospheric temperatures, J. Geophys. Res: Atmospheres, 98, 7245–7250,

doi:https://doi.org/10.1029/92JD02930, 1993.

Kürschner, D., Schminder, R., Singer, W., and Bremer, J.: Ein neues Verfahren zur Realisierung absoluter Reflexionshöhenmessungen an Raumwellen amplitudenmodulierter Rundfunksender bei Schrägeinfall im Langwellenbereich als Hilfsmittel zur Ableitung von Windprofilen in der oberen Mesopausenregion, Z. Meteorol., 37, 322–332, 1987.

Kürschner, D. and Schminder, R.: High-atmosphere wind profiles for altitudes between 90 and 110 km obtained from D1 LF measurements over Central Europe in 1983/1984, J. Atmos. Sol.-Terr. Phys., 48, 447–453, doi:10.1016/0021-9169(86)90121-2, 1986.

Laštovička, J., Akmaev, R. A., Beig, G., Bremer, J., and Emmert, J. T.: Global Change in the Upper Atmosphere, Science, 314, 1253–1254, doi:10.1126/science.1135134, 2006.

Laštovička, J., Akmaev, R. A., Beig, G., et al.: Emerging pattern of global change in the upper atmosphere and ionosphere, Ann. Geophys., 26, 1255–1268, doi:10.5194/angeo-26-1255-2008, 2008.

Liu, H., Tao, C., Jin, H., and Nakamoto, Y.: Circulation and tides in a cooler upper atmosphere: dynamical effects of CO2 doubling, Geophys. Res. Lett., 47, e2020GL087 413, doi:10.1029/2020GL087413, 2020.

Liu, H., Tao, C., Jin, H., and Abe, T.: Geomagnetic activity effects on CO2-driven trend in the thermosphere and ionosphere: ideal model experiments with GAIA, J. Geophys. Res.: Space Physics, 126, e2020JA028 607, doi:10.1029/2020JA028607, 2021.

Liu, L., Liu, H., Chen, Y., et al.: Variations of the meteor echo heights at Beijing and Mohe, China, J. Geophys. Res.: Space Physics, 122, 1117–1127, doi:10.1002/2016JA023448, 2017.

Lübken, F.-J., Berger, U., and Baumgarten, G.: Temperature trends in the midlatitude summer mesosphere, J. Geophys. Res.: Atmospheres, 118, 13,347–13,360, doi:10.1002/2013JD020576, 2013.

Manson, A. and Meek, C.: Winds and tidal oscillations in the upper middle atmosphere at Saskatoon (52°N, 107°W, L = 4.3) during the year June 1982–May 1983, Planet. Space Sci., 32, 1087 – 1099, doi:10.1016/0032-0633(84)90134-X, 1984.

Manson, A. H. and Meek, C. E.: Climatologies of mean winds and tides observed by medium frequency radars at Tromsø (70°N) and Saskatoon (52°N) during 1987–1989, Can. J. Phys., 69, 966–975, doi:10.1139/p91-152, 1991.

Mielich, J. and Bremer, J.: Long-term trends in the ionospheric F2 region with different solar activity indices, Ann. Geophys., 31, 291–303, doi:10.5194/angeo-31-291-2013, 2013.

Peters, D. H., Entzian, G., and Keckhut, P.: Mesospheric temperature trends derived from standard phase-height measurements, J. Atmos. Sol.-Terr. Phys., 163, 23–30, doi:10.1016/j.jastp.2017.04.007, 2017.

Pisoft, P., Sacha, P., Polvani, L. M., et al.: Stratospheric contraction caused by increasing greenhouse gases, Environ. Res. Lett., 16, 064 038, doi:10.1088/1748-9326/abfe2b, 2021.

Qian, L., Jacobi, C., and McInerney, J.: Trends and solar irradiance effects in the mesosphere, J. Geophys. Res.: Space Physics, 124, 1343–1360, doi:10.1029/2018JA026367, 2019.

Rayner, N. A., Parker, D. E., Horton, E. B., et al.: Global analyses of sea surface temperature, sea ice, and night marine air temperature since the late nineteenth century, J. Geophys. Res.: Atmospheres, 108, doi:https://doi.org/10.1029/2002JD002670, 2003.

Sassi, F., Kinnison, D., Boville, B. A., Garcia, R. R., and Roble, R.: Effect of El Niño–Southern Oscillation on the dynamical, thermal, and chemical structure of the middle atmosphere, J. Geophys. Res.: Atmospheres, 109, doi:https://doi.org/10.1029/2003JD004434, 2004.

Schminder, R., Kürschner, D., Singer, W., et al.: Representative height-time cross-sections of the upper atmosphere wind field over Central Europe 1990–1996, J. Atmos. Sol.-Terr. Phys., 59, 2177 – 2184, doi:10.1016/S1364-6826(97)00062-X, 1997.

She, C.-Y., Berger, U., Yan, Z.-A., et al.: Solar Response and Long-Term Trend of Midlatitude Mesopause Region Temperature Based on 28 Years (1990–2017) of Na Lidar Observations, J. Geophys. Res.: Space Physics, 124, 7140–7156, doi:10.1029/2019JA026759, 2019.

Smith, A. K., Garcia, R. R., Marsh, D. R., Kinnison, D. E., and Richter, J. H.: Simulations of the response of mesospheric circulation and temperature to the Antarctic ozone hole, Geophys. Res. Lett., 37, L22 803, doi:10.1029/2010GL045255, 2010.

Sprenger, K. and Schminder, R.: Results of ten years' ionospheric drift measurements in the l.f. range, J. Atmos. Sol.-Terr. Phys., 29, 183–199, doi:10.1016/0021-9169(67)90132-8, 1967.

Stober, G., Kuchar, A., Pokhotelov, D., et al.: Interhemispheric differences of mesosphere–lower thermosphere winds and tides investigated from three whole-atmosphere models and meteor radar observations, Atmos. Chem. Phys., 21, 13 855–13 902, doi:10.5194/acp-21-13855-2021, 2021.

Taguchi, M. and Hartmann, D. L.: Increased Occurrence of Stratospheric Sudden Warmings during El Niño as Simulated by WACCM, J. Clim., 19, 324 – 332, doi:https://doi.org/10.1175/JCLI3655.1, 2006.

Taubenheim, J., Entzian, G., and Berendorf, K.: Long-term decrease of mesospheric temperature, 1963–1995, inferred from radiowave reflection heights, Adv. Space Res., 20, 2059–2063, doi:10.1016/S0273-1177(97)00596-6, 1997.

van Loon, H. and Labitzke, K.: The Southern Oscillation. Part V: The Anomalies in the Lower Stratosphere of the Northern Hemisphere in Winter and a Comparison with the Quasi-Biennial Oscillation, Mon. Wea. Rev., 115, 357 – 369, doi:https://doi.org/10.1175/1520-0493(1987)115<0357:TSOPVT>2.0.CO;2, 1987.

Wendisch, M., Brückner, M., Crewell, S., et al.: Atmospheric and surface processes, and feedback mechanisms determining Arctic amplification: A review of first results and prospects of the (AC)3 project, Bull. Amer. Meteorol. Soc., 104, E208 – E242, doi:10.1175/BAMS-D-21-0218.1, 2023.

Tethered balloon measurements during Arctic spring conditions in Ny-Ålesund in the framework of HALO-(AC)^3

Lonardi, M.[1,✉], **Ehrlich, A.**[1], **Müller, J.**[1], **Saavedra Garfias, P.**[1], **Wendisch, M.**[1]

[1] *Leipzig Institute for Meteorology (LIM), Leipzig University, Germany*
✉*e-mail: michael.lonardi@uni-leipzig.de*

Summary: The tethered balloon system BELUGA (BalloonbornE moduLar Utility for profilinG the lower Atmosphere) was operated in spring 2022 at the AWIPEV research station (Ny-Ålesund, Svalbard). In-situ profiles of thermodynamic parameters, thermal-infrared radiation, aerosol particle concentrations, and turbulence, were measured and analyzed. Additionally, samples of ice-nucleating particles were collected at various heights. In combination with previous BELUGA datasets, measurements from this campaign provide a solid base for studying the vertical profiles of the radiative energy budget and heating rates in different atmospheric states in the Arctic lower troposphere. Here, example thermal-infrared radiation profiles are presented for a period of persisting cloudless conditions related to a series of marine cold air outbreaks in late March/early April. Measurements in clouds are analyzed for a developing cloud observed on 6 May and display the impact of cloudiness on radiation profiles.

Zusammenfassung: Das Fesselballonsystem BELUGA (BalloonbornE moduLar Utility for profilinG the lower Atmosphere) wurde im Frühjahr 2022 an der Forschungsstation AWIPEV Station (Ny-Ålesund, Svalbard) eingesetzt. In-situ-Profile von thermodynamischen Parametern, terrestrische Strahlung, Aerosolpartikelkonzentrationen und Turbulenz wurden gemessen und ausgewertet. Zusätzlich wurden in verschiedenen Höhen Proben von eiskeimbildenden Partikeln gesammelt. In Kombination mit früheren BELUGA Messungen zu anderen Jahreszeiten und an anderen arktischen Messstandorten bieten die Messungen in Ny-Ålesund eine Grundlage für weitere Untersuchungen des Strahlungsenergiehaushalts und des Einflusses von Wolken auf atmosphärische Heizraten. Profile der Strahlungsbilanz werden für eine anhaltende Kälteperiode zwischen Ende März bis Anfang April 2022 vorgestellt. Über diesen Zeitraum herrschten vor allem wolkenlose Bedingungen. Weitere Beobachtungen unter einer sich entwickelnden Wolkendecke am 6. Mai 2022 zeigen den Einfluss der Bewölkung auf die Strahlungsprofile.

1 Introduction

The tethered balloon system BELUGA (BalloonbornE moduLar Utility for profilinG the lower Atmosphere; Egerer et al., 2019) was deployed at the AWIPEV research station in Ny-Ålesund (Svalbard) in spring 2022. The objective of the measurements was to characterize the profiles of thermal-infrared radiation, aerosol particle concentrations, and turbulence, and their interaction. The spring deployment of BELUGA in Ny-Ålesund

Figure 1: *The balloon site as observed on 28 March 2022. The winch in the foreground controls the vertical release of the balloon. The tether is uncoiled horizontally towards a deflection pulley located underneath the balloon in the background. The extensive snow cover allowed for the use of snowmobiles in logistics operations.*

temporally extends the autumn 2021 observations (Lonardi et al., 2022a), and partially overlapped with the HALO-(AC)^3 airborne campaign (Klingebiel et al., 2023; Walbröl et al., 2023). Aircraft measurements provide the synoptic perspective, while BELUGA observations offer a higher resolution for the atmosphere above Ny-Ålesund. The balloon was operated by a joint team of scientists from Leipzig University, the Institute for Tropospheric Research (TROPOS), and the Free University of Berlin, locally supported by the Alfred Wegener Institute (AWI) and the Institute Paul-Émile Victor (IPEV).

2 Overview

The tethered balloon was deployed from 24 March to 12 May 2022, with a large measurement gap in late April due to the rotation of the field teams. A total of 33 flights was performed typically as profiles (30 flights), while three flights consisted of sampling ice nucleating particles at a fixed height. Most of the observations were obtained in cloudless conditions, which was the dominant atmospheric mode, especially during the first half of the campaign. Clouds occurred more frequently during the second part of the measurement period, but they were often associated with strong winds that inhibited

balloon operations. Similar to the autumn 2021 deployment, the activity of commercial aircraft was an additional factor that limited balloon operations due to the shared airspace.

During the measurement period, temperatures were typically down to -15°C, and slightly increased over the season due to the onset of the polar day. Over the entire period, a horizontally homogeneous snow cover of 0.5-1 m was present. Figure 1 displays the configuration of the measurement site during the initial phase of the campaign.

The balloon-borne instrumental setup primarily consisted of the instruments presented by Lonardi et al. (2022a) for the autumn deployment and was extensively introduced and characterized (Egerer et al., 2019; Lonardi et al., 2022b; Akansu et al., 2023). The thermodynamic measurements were obtained using the extended meteorological package (EP; Egerer et al., 2019). The thermal-infrared up- and downward irradiances were observed with the broadband radiation package (BP; Egerer et al., 2019; Lonardi et al., 2022b). Aerosol concentrations in the 12-150 nm and 150-2500 nm ranges were measured by the Cubic Aerosol Measurement Platform (CAMP; Pilz et al., 2022). High-frequency 1D-wind measurements were obtained from the hot-wire anemometer package (HP; Egerer et al., 2019). The phase of cloud particles was retrieved, for one cloudy case on 6 May 2022, using the Video Ice Particle Sampler (VIPS). In addition to this setup, the high-volume and lightweight balloon-borne filter sampler (HALFBAC) and the newly developed Particle Impactor (IMP) were used to collect INP samples at fixed heights and during profiles, respectively.

3 Thermal-infrared radiation measurements

The focus of LIM operations was the characterization of vertical profiles of thermal-infrared (TIR) radiation using the broadband radiation probe. In total, 17 radiation flights extending at least up to 900 m were obtained. Of these, 12 flights were performed in cloudless atmospheres and 5 in the presence of clouds. The latter were obtained during the same day (6 May 2022), allowing for studying the evolution of a cloud.

Radiative heating rates (ζ) were derived using the method illustrated by Egerer et al. (2019). Figure 2 displays temperature and TIR heating rates observed in Ny-Ålesund during a cold period in early spring (Walbröl et al., 2023). For cloudless days, the profiles indicate a weak but vertically consistent radiative cooling rate extending from the surface to the maximum measurement height. This agrees with previous observations obtained in the same area in spring 2015 (Becker et al., 2020) and over the sea ice in summer 2017 (Egerer et al., 2019). Such features differ significantly from the radiative heating rates simulated (Turner et al., 2018) and observed (Egerer et al., 2019; Lonardi et al., 2022b) for cloudy cases. These recent observations in cloudless atmospheres, combined with the summer 2020 deployment at MOSAiC (Lonardi et al., 2022b) and the autumn 2021 deployment in Ny-Ålesund (Lonardi et al., 2022a), form a comprehensive dataset that can be used to characterize the vertical structure of radiation profiles under different atmospheric conditions (Lonardi et al., 2023).

Example profiles obtained in an evolving cloudy boundary layer on 6 May 2022 are presented in Figure 3. Balloon-borne observations until 20:20 UTC show a strong negative net irradiance above the boundary layer cloud, indicating that the elevated ice cloud does not play a major role in controlling the net irradiance, in agreement with the findings by Turner et al. (2018). In turn, a distinct variation in the net irradiance is

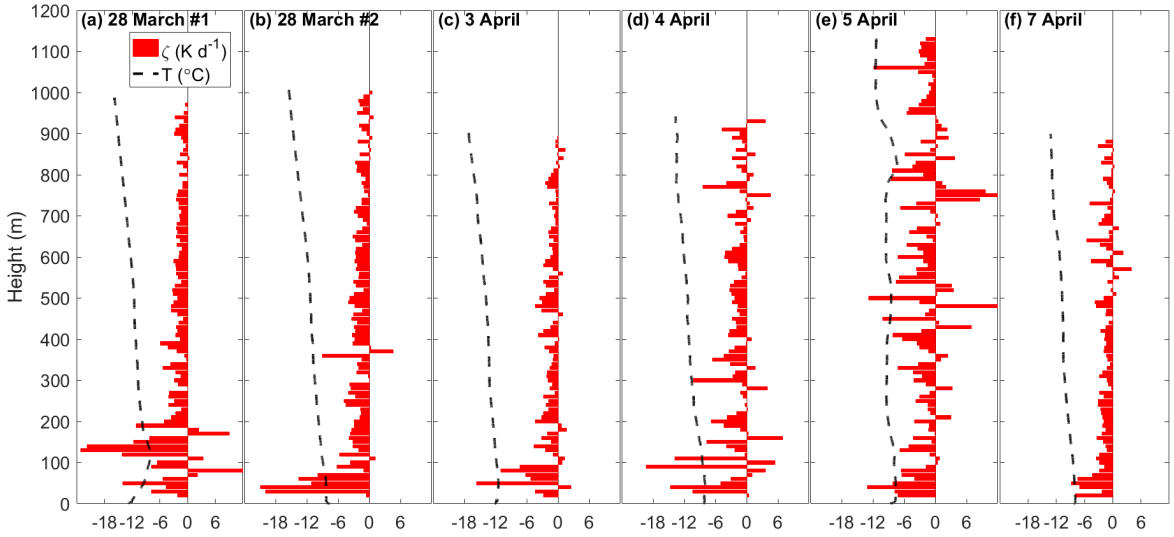

Figure 2: *Profiles of temperature and TIR heating rates (ζ) in cloudless conditions.*

observed while vertically crossing the broken low-level cloud, consistently with a limited amount of liquid water indicated by the radar. Later, the cloud base of the upper cloud decreased significantly. This led to an increased downward emission of TIR irradiance and reduced the cloud top cooling (higher net irradiance) at the boundary layer cloud. Profiles highlight how the liquid-bearing low-level cloud significantly varies the net irradiance throughout the whole profile (Lonardi et al., 2022b) and at the surface (Shupe et al., 2013). In particular, it can be seen how, in comparison to the initial flights, the increase in optical thickness of the cloud results in values of the net irradiance closer to zero.

4 Summary and outlook

The tethered balloon system BELUGA was deployed in Ny-Ålesund between 24 March and 12 May 2022, partially overlapping in time with the HALO-(AC)^3 aircraft campaign. The balloon-borne observations extend the characterization of the local atmospheric column over Ny-Ålesund beyond the available remote sensing retrievals. Combined profiles of thermodynamic properties, TIR radiation, and aerosol particle distribution and their chemical properties were obtained.

The relatively large amount of cloudless scenarios observed with the broadband radiation probe allows to statistically characterize the typical boundary layer structure in Ny-Ålesund for the surveyed period and compare it with similar studies. The comprehensive dataset obtained during the two successive Ny-Ålesund campaigns in 2021-2022, combined with MOSAiC observations in 2020, constitutes an ensemble of cases that allows studying the radiation profiles in the lower troposphere under different conditions and could therefore be used to investigate the radiative structures of the Arctic atmospheric boundary layer.

It was demonstrated how consecutive profiles can provide insights into the evolution of a cloudy atmosphere. A follow-up tethered balloon campaign, in the framework of (AC)^3,

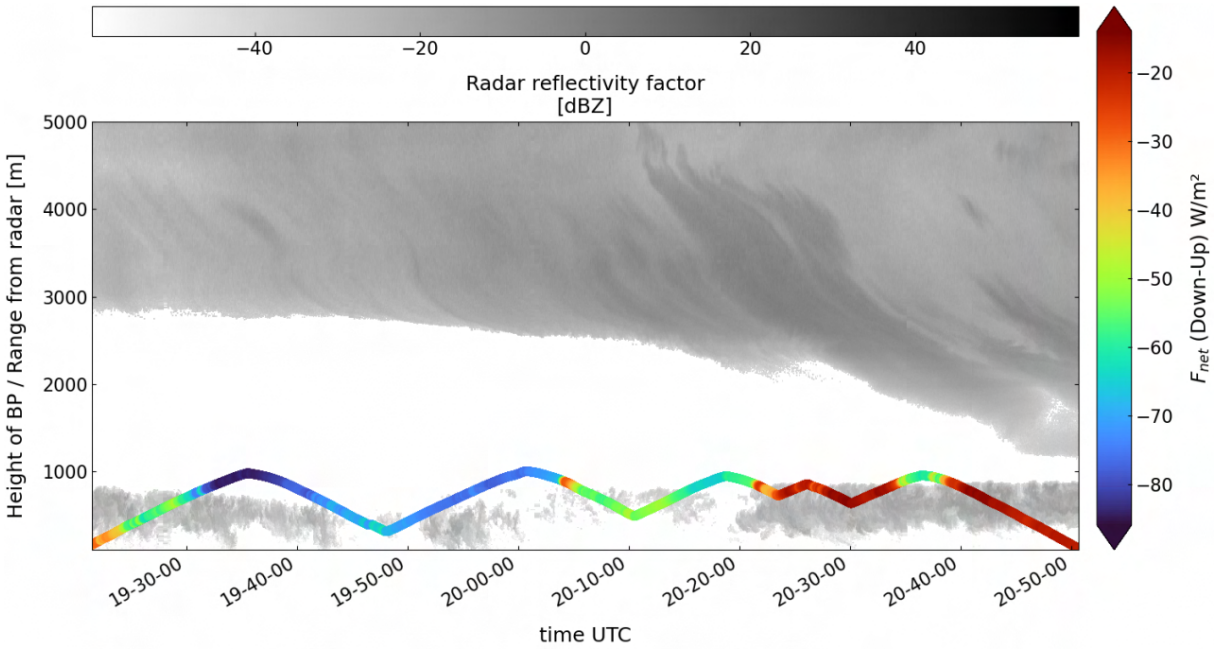

Figure 3: *TIR net irradiances measured during consecutive profiling flights (colored areas). Shaded areas represent the radar reflectivity as retrieved by the radar (94 GHz).*

will therefore aim at characterizing an evolving boundary layer with less instrumentation but with a higher frequency of profiles.

5 Acknowledgements

The authors and the BELUGA team are grateful for the invaluable support provided by AWIPEV and Kings Bay staff. In particular, we wish to personally thank G. Tran, Y. Dulong, and F. Rader for their coordination and on-site support. We also thank S. Jacobsen and V. Sand for their flexibility in ensuring the fundamental airspace clearance, and E. Havenstrøm for the logistic support at the harbor storage site.

References

Akansu, E. F., Dahlke, S., Siebert, H., and Wendisch, M.: Determining the surface mixing layer height of the Arctic atmospheric boundary layer during polar night in cloudless and cloudy conditions, EGUsphere, 2023, 1–22, doi:10.5194/egusphere-2023-629, 2023.

Becker, R., Maturilli, M., Philipona, R., and Behrens, K.: In situ sounding of radiative flux profiles through the Arctic lower troposphere, Bulletin of Atmospheric Science and Technology, 1, 155–177, doi:10.1007/s42865-020-00011-8, 2020.

Egerer, U., Gottschalk, M., Siebert, H., Ehrlich, A., and Wendisch, M.: The new BELUGA setup for collocated turbulence and radiation measurements using a tethered balloon: First applications in the cloudy Arctic boundary layer, Atmospheric Measurement Techniques, 12, 4019–4038, doi:10.5194/amt-12-4019-2019, 2019.

Klingebiel, M., Schäfer, M., Kirbus, B., et al.: Airborne observations of Arctic air mass transformations during the HALO-(AC)^3 campaign, Rep. Inst. Meteorol. Univ. Leipzig, 61, 1–12, 2023.

Lonardi, M., Ehrlich, A., Schäfer, M., Thoböll, J., and Wendisch, M.: Tethered balloon measurements during Arctic autumn conditions in the framework of HALO-(AC)^3, Wiss. Mitteil. Inst. f. Meteorolo.

Univ. Leipzig, 60, 35–40, URL https://www.physgeo.uni-leipzig.de/fileadmin/Fakult%C3%A4t_PhysGeo/Meteorologie/Dokumente/Forschungsbericht/LIM_Bd_60.pdf, 2022a.

Lonardi, M., Pilz, C., Akansu, E. F., et al.: Tethered balloon-borne profile measurements of atmospheric properties in the cloudy atmospheric boundary layer over the Arctic sea ice during MOSAiC: Overview and first results, Elementa, 10, 1–19, doi:10.1525/elementa.2021.000120, 2022b.

Lonardi, M., Akansu, E. F., Ehrlich, A., et al.: Tethered balloon-borne observations of thermal-infrared irradiance and cooling rate profiles in the Arctic atmospheric boundary layer, EGUsphere, 2023, 1–26, doi:10.5194/egusphere-2023-1396, 2023.

Pilz, C., Düsing, S., Wehner, B., et al.: CAMP: An instrumented platform for balloon-borne aerosol particle studies in the lower atmosphere, Atmospheric Measurement Techniques, 15, 6889–6905, doi:10.5194/amt-15-6889-2022, 2022.

Shupe, M. D., Persson, P. O., Brooks, I. M., et al.: Cloud and boundary layer interactions over the Arctic sea ice in late summer, Atmospheric Chemistry and Physics, 13, 9379–9400, doi:10.5194/acp-13-9379-2013, 2013.

Turner, D. D., Shupe, M. D., and Zwink, A. B.: Characteristic atmospheric radiative heating rate profiles in arctic clouds as observed at Barrow, Alaska, Journal of Applied Meteorology and Climatology, 57, 953–968, doi:10.1175/JAMC-D-17-0252.1, 2018.

Walbröl, A., Michaelis, J., Becker, S., et al.: Environmental conditions in the North Atlantic sector of the Arctic during the HALO–(AC)^3 campaign, EGUsphere, 2023, 1–48, doi:10.5194/egusphere-2023-668, 2023.

Clustering and Random Forest approach in the classification of hydrometeors measured by the Thies Laser Precipitation Monitor

Trosits, A.[1,✉] **Foth, A.**[1], **Kalesse-Los, H.**[1]

[1] *Leipzig Institute for Meteorology, Leipzig University, Germany*
✉*e-mail: at58voge@studserv.uni-leipzig.de*

Summary: This article, emerged from a bachelor thesis, focuses on the classification of hydrometeors measured by the Laser Precipitation Monitor by the Adolf Thies GmbH & Co. KG. The optical disdrometer can classify measurements of hydrometeor size and fall velocity spectra concerning the precipitation type. The measurement principle of the disdrometer is explained, as well as the classifications. For reasons of calculation time, mostly six main precipitation types are considered (drizzle, rain, snow, ice grains, hail, mixed). It is the goal to understand the process of a reliable classification and to determine how these classifications are implemented. Therefore, the precipitation measurements from the measurement field of the Leipzig Institute for Meteorology from 2021 are used. An analysis of the spectrum consisting of hydrometeor diameter and fall speed is investigated. Afterwards, two machine learning methods are applied to the dataset. The classification of each sample through grouping similar samples using cluster analysis serves as an unsupervised approach and in particular examines the natural clusters present in the dataset. Contrasting that the purely statistical, nonphysical, supervised Random Forest method is applied as well. The comparison of the unsupervised and supervised approach shows that for the classification the supervised method is more promising.

Zusammenfassung: Dieser Artikel konzentriert sich auf die Klassifizierung von Hydrometeoren, welche durch den Laser Niederschlags Monitor der Adolf Thies GmbH & Co. KG gemessen werden. Das optische Disdrometer kann die Messungen von Fallgeschwindigkeits- und Größenspektren der Niederschlagspartikel eigenständig in Gruppen der Niederschlagsart einsortieren. Das Messprinzip, sowie die Klassifizierungsmechanismen werden erklärt. Auf Grund der Rechenzeit werden im Rahmen der folgenden Untersuchungen hauptsächlich die 6 Hauptniederschlagsarten (Niesel, Regen, Schnee, Eiskörner, Hagel, Gemischt) unterschieden. Das Ziel der Analyse ist es, den Prozess einer zuverlässigen Klassifizierung zu verstehen und die Möglichkeiten der Anwendung abzuschätzen. Dafür werden die Niederschlagsdaten der Wetterwiese des Leipziger Instituts für Meteorologie aus dem Jahr 2021 verwendet. Nach erster grundlegender Betrachtung des Datensatzes werden zwei verschiedene Machine Learning Methoden angewendet. Als unüberwachte Methode dient der Ansatz der Clusteranalyse, welcher alle Samples über Ähnlichkeitskriterien gruppiert und dadurch die natürliche Gruppierbarkeit eines Datensatzes aufzeigt. Im Gegensatz dazu steht die rein statistische, unphysikalische Methode des Random Forest mit überwachtem Lernprozess. Im Vergleich beider Ansätze zeigt sich, dass ein überwachter Machine Learning Methode zufriedenstellendere Ergebisse erzeugt als unüberwachte Prozesse.

1 Introduction

Precipitation is one of the main weather elements and is included in the measurements of every weather station, reporting their observations to larger measurement networks, such as the German weather service (DWD). Since several years the manned measurement stations are transferred into automatic measurement techniques, producing a synoptical weather report with an increased temporal resolution [Merenti-Välimäki et al., 2001]. For simultaneous precipitation measurements and the detection of the precipitation type optical disdrometers started to be developed in the 1990ies. A prototype of an optical disdrometer operating with a laser beam was introduced in detail by Löffler-Mang and Joss [2000]. Starting with measurements of the hydrometeor diameter and velocity the idea to identify the type of precipitation by these measurements arose. Löffler-Mang and Joss [2000] presented this as a goal for future work in their outlook to use optical disdrometers as precipitation monitors. Over time, several types of optical measuring disdrometers were designed e.g., the Laser Precipitation Monitor by the manufacturer Adolf Thies GmbH & Co KG [2015] (in the following named: Thies). The determination of the type of precipitation was developed and added to the output variables.

This precipitation type classification of the disdrometers by Thies is studied in this report. One of the internally determined values provided by the Thies disdrometer is the synop-classification for every sample. How this is executed and how naturally these groups of precipitation types are recognisable in the raw data is analysed here. The aim is to understand the process behind the classification and to reconstruct a reliable classification process close to the one of the disdrometer to potentially apply these methods to other measurements. For this, the precipitation data from 2021 measured by the Thies disdrometer on the measurement field of the Leipzig Institute for Meteorology (51°20'00.5"N, 12°23'20.0"E) is studied with two different machine learning methods. For a better understanding of the methods and results, the theoretical basics are explained, before the analysis is outlined.

2 Theoretical background

Hydrometeors

According to the definition by Kraus [2004], hydrometeors, in general, are defined as aqueous, airborne particles in the air. They may consist of liquid or solid water. Different types of precipitation show different characteristic properties. The relation of fall velocity and diameter for liquid hydrometeors follows the suggestion of Atlas et al. [1973], who derived this equation from the measurements by Gunn and Kinzer [1949]:

$$v = 9.65 - 10.3 \cdot \mathrm{e}^{-0.6D} \tag{1}$$

with v the velocity and D the hydrometeor diameter. In the following, this equation is referred to as Gunn-&-Kinzer-curve. It must be noted, that falling water droplets do not have a spherical shape. The larger the droplet, the stronger the deformation of the original shape. Thus, rain is more non-spherical than drizzle droplets.

For the description of the fall velocity of snow and other light solid particles such as ice crystals and snow grains Locatelli and Hobbs [1974] derived an empirical equation:

$$v = 0.8D^{0.16} \tag{2}$$

Therewith they directly link the velocity v and the diameter D. Hail or ice grains are excluded from this equation because their size and density lead to higher velocities. In addition, they mostly occur in convective precipitation events, so that vertical air motion affects the fall velocity a lot. But there are further descriptions of the relationship between hydrometeor diameter and velocity (e.g. see Ishizaka et al. [2013] as a summary).

Laser Precipitation Monitor

The optical disdrometer by Adolf Thies GmbH & Co KG [2015] (Thies), also called Laser Precipitation Monitor, is a measurement instrument for the optical detection of precipitation. For this an emitter releases a laser beam (wavelength: 785 nm) with a certain volume of 0.75 mm x 20 mm x 228 mm, which then is sampled by the receiver as indicated by the manufacturer's specifications [Adolf Thies GmbH & Co KG, 2015]. As soon as a hydrometeor is located between the emitter and the receiver, the signal of the laser beam gets attenuated. The extent and duration of the reduced signal are used to calculate the size of the object and the velocity (see Fig. 1). Thus, the measurement of size and velocity are independent of each other. For the estimation of hydrometeor size the amplitude of attenuation is crucial and the duration of the weakened signal determines the fall velocity. Every hydrometeor gives a value for each of the variables hydrometeor size and fall velocity. The measured values of velocity are allocated into 22 bins of speed with increasing width of the bins with an increasing velocity ranging from $0\,\mathrm{m\,s^{-1}}$ to $20\,\mathrm{m\,s^{-1}}$. Meanwhile, the diameter is saved into 20 bins of size from 0.125 mm to 8 mm, again with an increase of the width of bins with increasing particle diameter. After the predefined time interval of one minute, the recording of the number of occurrence for every combination of velocity and diameter is saved as spectrum of velocity and diameter for every sample. From this spectrum further variables such as radar reflectivity (dBZ) and the visibility (m) can be calculated. Additionally, the disdrometer classifies every sample into a certain class of precipitation type. Precipitation here is not only differentiated into the six main types like drizzle, rain, snow, hail, soft grains, and a mixture consisting of rain/drizzle/snow-combinations but also in terms of intensity. In the end, there are 17 classes as shown in Tab. 1. There is also one class for 'no precipitation' [Adolf Thies GmbH & Co KG, 2015].

According to information by the manufacturer Thies of the optical disdrometer, the type of precipitation is determined temperature-indepentant via statistical methods. The spectrum of hydrometeor diameter and velocity was studied for certain cases of precipitation observed by eye or other detection techniques apart from the disdrometer itself. Those spectra were transferred into the information of precipitation type then.

Figure 1: *Measurement principle of the optical disdrometer by Thies - Hydrometeors like snow or rain cause an attenuation of the laser beam while falling through the beam. Based on the extent and duration of the attenuation the hydrometeor size and velocity are estimated. [Adolf Thies GmbH & Co KG, 2015]*

Table 1: *Overview of the precipitation classes, which can be identified by the disdrometer including the SYNOP-code*

SYNOP	Description
0	no precipitation
51, 53, 55	light/moderate/heavy drizzle
58, 59	light/moderate drizzle with rain
61, 63, 65	light/moderate/heavy rain
68, 69	light drizzle/rain/moderate drizzle/rain with snow
71, 73, 75	light/moderate/heavy snow
77	light snow grains and needles
87, 88	light/moderate soft hail and graupel
89	moderate hail

As mentioned in the beginning of section 2 (Hydrometeors) scientific relations between fall speed and diameter of precipitation particles are described in the literature. Gunn and Kinzer [1949] induced the relation of the terminal velocity depending on the particle diameter of liquid hydrometeors. Meanwhile, Locatelli and Hobbs [1974] derived such a relation for snow and light ice particles. These equations can help to estimate which hydrometeors are represented in which area of a spectrum of diameter and velocity. A scheme containing the information about the question of which area in the spectrum represents what kind of precipitation type was published by Löffler-Mang and Joss [2000]. Figure 2 shows the “schematic concept for using size and velocity information to detect the different types of hydrometeors” based on Löffler-Mang and Joss [2000].

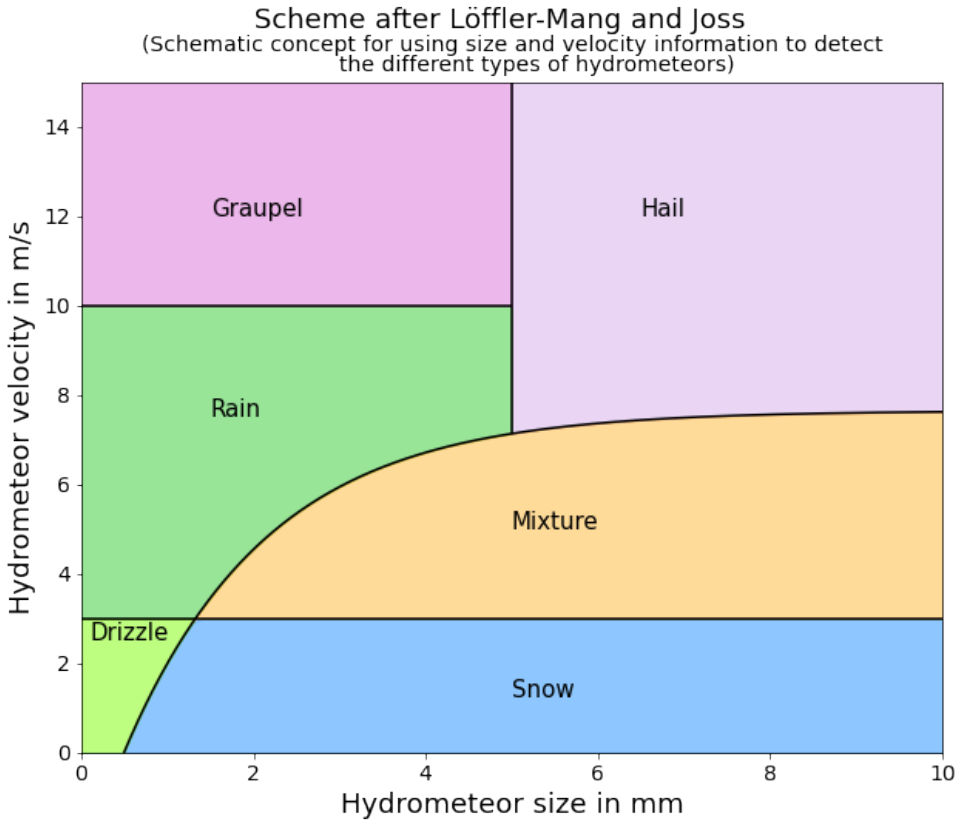

Figure 2: *Scheme for the relation between the precipitation type and the variables diameter and velocity of the corresponding hydrometeor based on Löffler-Mang and Joss [2000]*

Dataset

As previously described, rather than recording the individual velocity and size of each hydrometeor, the number of hydrometeors within certain velocity and size bins are recorded for one minute of sampling time as the size-velocity-spectrum. The dataset used for the analysis arises from the measurement of an optical disdrometer by Thies (Laser precipitation monitor, see section 2) on the measurement field at the Institute for Meteorology at Leipzig University (51°20'00.5"N, 12°23'20.0"E). The time frame of available data ranges over 10 years from January 2012 until December 2022. Since limitations in the amount of data to be analysed the year 2021 was chosen for the contemplation because the amount of precipitation over the year was high and the precipitation type was variable.

For simplicity, the 17 precipitation types given by the disdrometer are combined into six precipitation types neglecting the intensity. Drizzle, rain, snow, soft grains, hail and mixed. Hereby the mixed group contains the mixed types of drizzle with rain and drizzle or rain with snow. For some analysis run-time errors occurred due to the length of the dataset for the whole year 2021. Thus, in some cases smaller sets of data including only nine days of the year 2021 (12.01., 07.02., 12.07., 10.08., 23.08., 17.09., 05.10., 03.11., 03.12.2021) with high precipitation amounts and different precipitation types[1].

[1] Verified with the information from https://monsun.meteo.uni-leipzig.de/remsens

Statistical methods - cluster analysis

A cluster analysis is an explorative procedure for grouping single data points from an uncategorized dataset into natural groups. The segments are set up via the comparison of the similarity of given characteristics. Since there are no predefined categories from the beginning, the characterisation and naming are done after clustering. There are two different main techniques of grouping data; the hierarchical and the flat method [Aggarwal, 2018]. Generally, the flat way describes the gradual correction of a random categorisation of the data points. The other (hierarchical) method uses the appproach of gradual splitting the whole dataset (Top-down-method) or gradual combination of single data points (Bottom-up-method).

For flat clustering, k-means clustering is the most common technique. Here the categorisation of every data point is implemented randomly in the first step. After the calculation of the mean of every group, the nearest neighbours according to a certain linkage criterion are assigned to these mean values as new cluster centres. The rearranging is done until the best combination of groups and group centres is found [Scikit-learn]. The second type of clustering is hierarchical clustering. As visualised in a dendrogram the dataset can successively be combined to obtain a certain, predefined number of clusters. Agglomerative clustering describes the merging of single samples up to one, all data including cluster. Meanwhile, divisive clustering is the opposite. Here the dataset is split until every sample stands alone. For receiving a certain number of clusters both processes are stopped after the fixed number of clusters has been reached.

The linkage criteria for hierarchical clustering between the samples or clusters used for identifying the nearest neighbour can be varied. There are four commonly used types of linkage between single clusters. In general, the minimum of the criterion is used as it is the closest neighbour, what is searched for. Three methods are based on euclidean distances of the closest samples, the average of the clusters or the most distant samples of a cluster [Aggarwal, 2018]. Apart from the euclidean distance, the variance is considered within the ward method. Merging the clusters with a minimal variance is a more robust method, than using e.g. the method of the smallest minimal distance [Scikit-learn, Steinbach et al. [2000]]. The choice of the used method for the clustering in this analysis was made with purpose. As no random clustering is required, but one with groupings of the nearest neighbours, hierarchical clustering is performed. The linkage type “ward” tends to be the most robust linkage type and is additionally more useful for the comparison of multi-variable datasets.

Random Forest

Besides clustering the Random Forest represents a different statistical method applied here. It is a supervised machine learning method consisting of a training and a testing process. During the training, a relation between the given input dataset and the expected output dataset is established. This linkage is created by several, randomly varied decision trees.

A decision tree is a statistical way of classifying an input dataset by following one certain path of the tree, depending on the values of the input. At the first node, it starts with the threshold for one criterion which is exceeded or not. After this first binary decision at the next node the next binary decision is made. Thus, in the end, these decisions lead to a discrete classification. The decisions are purely statistical and not physical.

After training the randomised decision trees the testing can be conducted. To receive a prediction of the classes through the Random Forest the test input is given into the Random Forest. Every tree gives one prediction, but the final classification is determined through the most often occurring output of all decision trees. Thereafter the prediction can be compared to the true classification if available [Liu et al., 2012].

One problem occurring for machine learning methods with a training and prediction part is overfitting. It describes the phenomena when the established linkage of the training dataset is too precise so that slight differences in the new input dataset for the test compared to the input during the training lead to difficulties in the classification through the decision trees [Ying, 2019]. For a Random Forest, the problem can come up when there are more decision trees used than needed. Overfitting is eliminated for the results here, by calculating the accuracy for several numbers of decision trees.

Confusion matrix

A confusion matrix contrasts two different characteristics of a dataset. Both characters (e.g. named x and y) need to exist for every sample of the dataset so that they have the same number of samples. A grid is showing the characters of x on the x-axis and the characters of y on the y-axis, thus representing all combinations of the characters. For each combination of x and y the ratio of character y occurring together with character x is calculated. Later the two compared characteristics are the actual and the predicted values of precipitation type A. It is calculated how often the actual value of A_{actual} corresponds the predicted values of $A_{predicted}$. This gives information about how well the prediction matches the actual values. As it is of interest how good the prediction of the different techniques is representing the actual values the sum of ratios for actual values is 1. This means, that the representability of A_{actual} through $A_{predicted}$ is visualised in a confusion matrix. The colours can support the visualisation of the correlations.

3 Results

Velocity - size - spectrum

To get a first impression of the data used for clustering the spectra of the whole year 2021 are visualised in Fig. 3. The spectra will, later on, represent the input data for all considerations. Here, the x-axis presents the size of the hydrometeor, while the y-axis gives information about the velocity. The main plot shows the number distribution for all combinations of size and velocity intervals through the colours. The two curves included in the main plot visualise the empirical equations by Gunn and Kinzer [1949] (solid) and Locatelli and Hobbs [1974] (dashed) describing the relation between terminal velocity

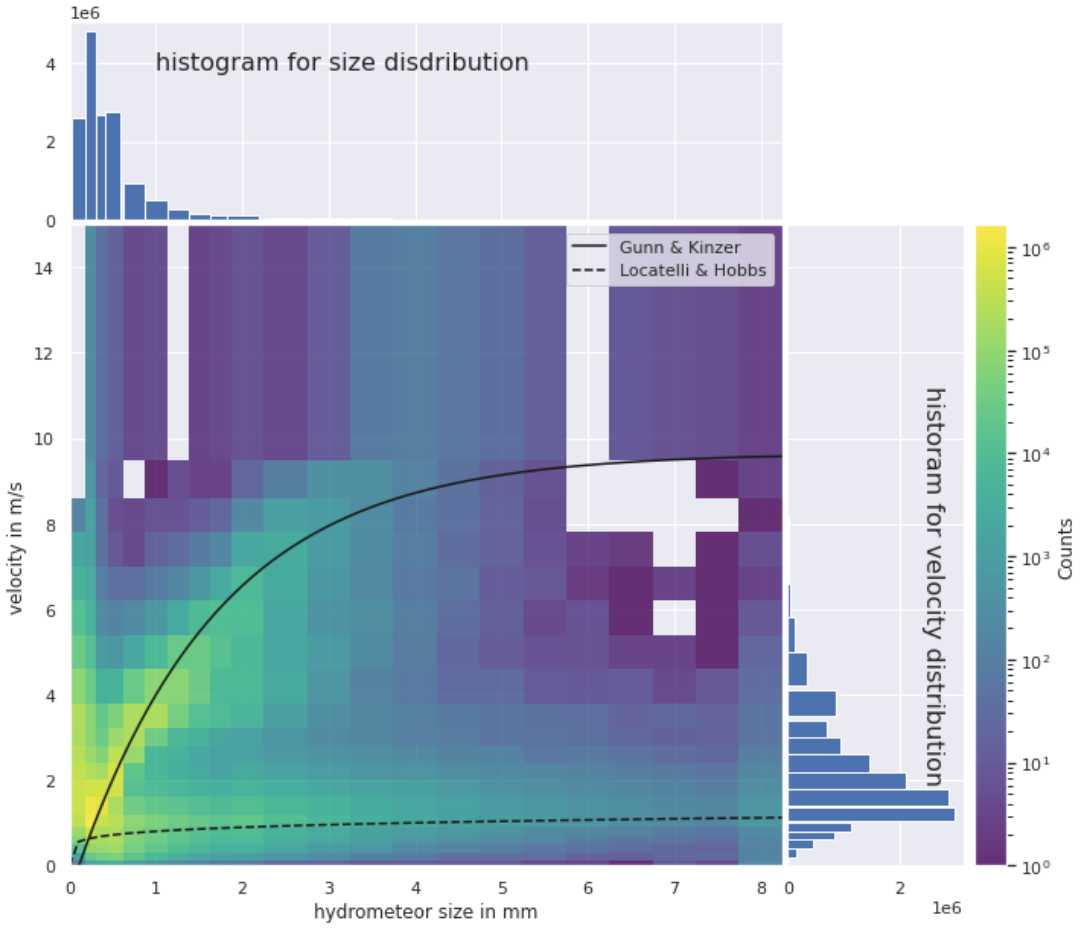

Figure 3: *Measured spectrum of hydrometeor diameter (x-axis) and fall velocity (y-axis) for the whole year 2021 with curves following the equations from Gunn & Kinzer and Locatelli & Hobbs. On the upper x-axis, the distribution of hydrometeor size and on the right y-axis the distribution of fall velocity is shown.*

and size of liquid and solid hydrometeors respectively. The histogram above the upper x-axis shows the size distribution of the measured hydrometeors.

Comparing the scheme by Löffler-Mang and Joss [2000] (Fig. 2) with the values determined by measuring there are maxima of hydrometeor numbers in the region of drizzle, rain and snow. By comparing the visualised data of real measurement with the theoretical curves given by Gunn and Kinzer [1949] and Locatelli and Hobbs [1974], it looks like a good accordance between the areas of higher occurrence and the curves. Rain, having higher velocities and diameters is represented by the nearly diagonal line of yellow-coloured value-couples. The accumulation on the bottom, characterised by low velocities, but diameters up to 8 mm exhibits the properties of snow. Thus, the two precipitation types of rain and snow are derivable from the spectra by eye. The third area of accumulation with high velocities but very small hydrometeor diameters (approximately 0 to 0.2 mm) is not combining the characteristic velocities and diameters of any precipitation type. Physically there is no explanation for the composition of these values. The measurement of those non-physical values correlates with the number of hydrometeor, what suggests splashing as the reason for the wrong values. Meanwhile,

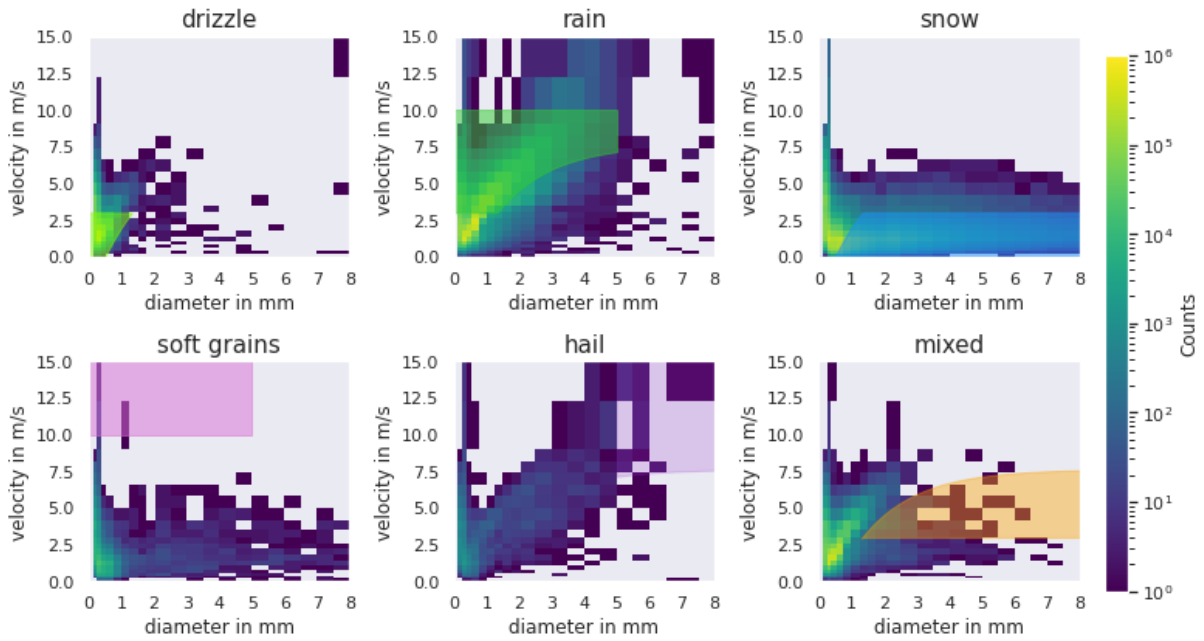

Figure 4: *Spectrum of hydrometeor diameter (x-axis) and fall velocity (y-axis) from the measured precipitation data separated for the six main precipitation types according to the classification by the disdometer*

the declaration of a lower measurement quality failed. According to Angulo-Martínez et al. [2018], these wrong detection results from hydrometeors only falling through the edge of the laser beam, so that not the full size is attenuating the beam.

The histogram of the size distribution shows a clear peak at the diameter interval from 0.312 mm to 0.438 mm. The histogram of the velocity distribution shows a nearly bimodal distribution. The most protruding peak is at the velocity interval form 0.9 $\mathrm{m\,s^{-1}}$ to 1.2 $\mathrm{m\,s^{-1}}$ and a second peak at 3.2 $\mathrm{m\,s^{-1}}$ to 3.8 $\mathrm{m\,s^{-1}}$. These maxima may occur due to a lot of snow and rain with diameters around 1 mm.

Through the separation of the different classifications given by the disdrometer the precipitation type-specific spectra can be presented (Fig. 4). For a better comparison with the expectations by Löffler-Mang and Joss [2000] the coloured areas indicate the corresponding part of the precipitation-type scheme (Fig. 2).

Figure 4 shows, that only the spectrum of snow and soft grains differ clearly from the drizzle, rain and hail, while mixed of course represents the mixture of both main spectra. Because the classification is performed for a whole minute of recorded data the precipitation type and thus, the spectrum could also change within this time range. Additionally, an event of precipitation is not only including one type of precipitation but a mix of some types. The separability of the single precipitation classes is made difficult by that. The biggest difference can be made between light ice particles, including snow and soft hail, and rain-like precipitation types, including hail.

However, in comparison to the scheme by Löffler-Mang and Joss [2000], the classification by the disdrometer shows an acceptable performance at least for drizzle, rain and snow. The class of drizzle is compressed into a small area of the plot with both, small velocities and small diameters. Snow is clearly characterised by low velocities and high diameters. And rain is, as expected, the diagonal accumulation following the curve of Gunn and Kinzer [1949].

Data preparation for clustering

Because clustering only works with 2-dimensional arrays (not 3D) the dimension of the size-velocity-spectrum for every sample of time (3D) needs to be reduced by one. There are different opportunities to conduct this preprocessing. As the number of samples might be contained the two dimensions of size and velocity need to be merged into one array. For that, at first, the distributions of size and velocity can be obtained by integrating over the respective other dimension, and afterwards, just concatenate to receive one array. (For the velocity integrating over the size is necessary, and for the size distribution it was integrated over the velocity.) Here the direct information of the relation between size and velocity gets lost, but the dimension of the dataset is reduced from (t x v x s) to (t x (v+s)) with t the time samples, s the number of size intervals (20) and v the number of velocity intervals (22). The calculation time is the smallest for this input compared to the other possibilities. A second way is to reshape the matrix, by flattening the spectrum matrix into an array with the length of $(s \cdot v)$ per sample. The dimension of the edited matrix is then (t x $(s \cdot v)$). Hereby the information of every combination of size and velocity which can be found in the matrix is transferred into the array. Thus, the loss of information is minimised. To reduce the importance of the total number of hydrometeors and to focus more on the ratios of distributions the datasets are normalised in a following step. As additional information which can help to classify the precipitation type, the temperature can be considered. Therefore the temperature for each sample is also added to the input array. As mentioned in section 2 in some cases a smaller dataset needs to be used. The cluster analysis could not be performed with the whole data from 2021. That is why, the smaller data set consisting of nine days is consulted here. Resulting from that hail is not included in the analysis.

Confusion matrix for clustering

The evaluation of the clustering is visualised via the following confusion matrices in Fig. 5. The cluster output and the classification from the disdrometer are compared. Thus, it describes how often which classification was grouped into which cluster. Starting with the most simple way, using the concatenated input data, led to bad results at first (left). The normalisation (middle) and then the addition of temperature (right) improved the clustering a lot. All invalids are detected and grouped into cluster one (without temperature) or clusters one and two (with temperature). Nearly all of the drizzle samples are included in cluster 6, the samples for rain in cluster 3 and ice grains in cluster 4. By adding the temperature the classification of drizzle is separated more clearly from ice grains. But it is not surprising that the mixed precipitation is combined with rain and drizzle. It suggests that clustering is not recognising the differences between the types

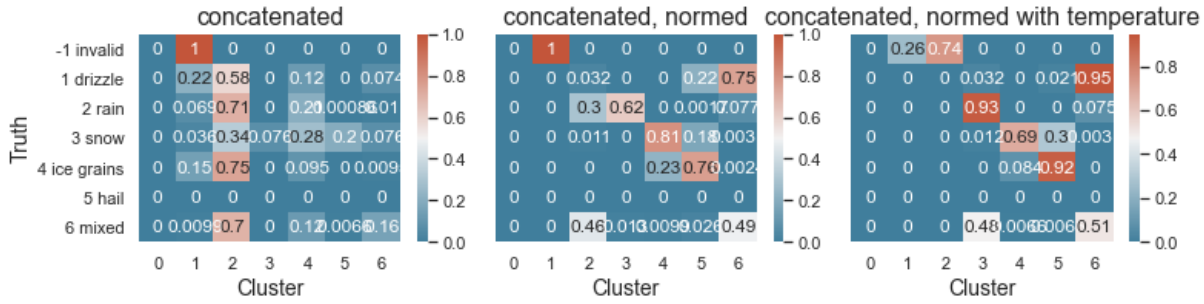

Figure 5: *Confusion matrices for the results from cluster analysis concerning the 6 main precipitation type groups and one group for the invalids with 6 differently edited input datasets, as can be seen in the title of each subplot. The smaller dataset was used here.*

of drizzle, rain and the mixture of both. The results for differently edited datasets deliver worse results and are thus not shown here.

Concluding from these confusion matrices there is a temperature dependency in the clustering, as the best results are delivered by including the temperature. Since the classification of the clusters is conducted after the cluster analysis, there is no order in which the clusters may contain the true classification. To evaluate the diagonal here does not make sense. The results from the clustering are not satisfactory in terms of receiving a classification of the precipitation spectrum which is comparably good as the classification through the disdrometer. This shows that the spectrum is not clearly separable for the different precipitation types. Studying the classification per sample it implies that the measured spectrum for the classification includes precipitation from a whole minute. This leads to variable distributions of size and velocity and thus to imprecise classification.

Random Forest

As a second technique to classify input data into discrete groups a Random Forest can be applied which was explained theoretically before. For training, the Random Forest the size-velocity-spectrum dataset of 2021 is split into training and test datasets. The training dataset consists of 25% of the original data. As expected output the classification of precipitation type is given. The number of decision trees which are used here is 730, chosen in accordance with an overfitting analysis. While linking the spectra with precipitation types through the 730 decision trees, the algorithm learns how to classify certain compositions of size and velocity through fixed thresholds for binary decisions. Testing this Random Forest gives a prediction of the classification of precipitation type for each entered sample. The size-velocity-spectra serve as input for this prediction and are connected to certain precipitation types. This classification can now be compared to the classification by the disdrometer. Therefore, again confusion matrices are used.

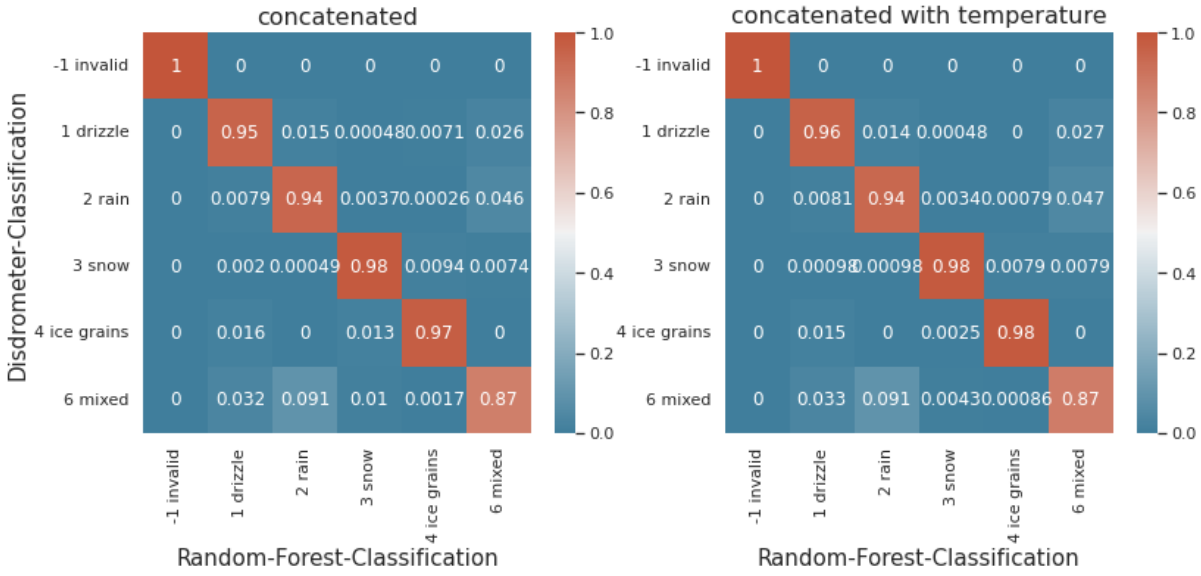

Figure 6: *Confusion matrices for the results from the Random Forest analysis with predefined classes resulting from the training of the Random Forest, for two differently edited input datasets, one without temperature and one with temperature.*

The confusion matrices shown in Fig. 6 convey a different impression than the ones for the cluster evaluation. The training connects existing input and its expected output. Thus, the algorithm does not have to create its own decisions about the possible output. The matrices show that without and with temperature the results are very good. For example, all invalids are detected and classified as invalid by the Random Forest. The other classes are also mainly recognised and correctly classified. The correlation ranging from 94% to 98% excluding the mixed precipitation with 84% shows that the allocations through the random forest are very similar to the evaluation classes through the classification by the disdrometer. For mixed precipitation which can consist of drizzle, rain and snow it is again not surprising that a few spectra detected as mixed by the disdrometer are determined as one of the precipitation types it consists of by the Random Forest. The transitions between these types and their mixture are close. After adding the temperature the results are even better because the transition between the phases is more clear. Even though the Random Forest is operating with purely statistical thresholds and not with physical the influence of the temperature on the precipitation type is trained into the decision trees. Here the quantitative evaluation through accuracy is possible because the expected output and the real output can be declared as true or false. As estimated by eye, the performance of the Random Forest is very good with an accuracy of about 0.99.

Comparison of clustering and Random Forest

The statistical analysis of the precipitation spectra from 2021 shows, that the results with the Random Forest method are more successful in classifying precipitation properly than the cluster analysis. That raises the question why the performance differs so much.

The two used techniques are principally different. Both are machine learning methods, but one is supervised and the other one is unsupervised. This means the application goal of both methods are differing. Of course, both tend to classify data into discrete groups, but for an unsupervised cluster analysis, the similarities between the expected classes are too great here, to separate the expected groups adequately. In general, there are single accumulations recognisable. On the other hand, a classification in terms of more than two or three groups is not delivering good results, because only two main accumulations in the distribution of size and velocity occur as seen in Fig. 3. In the supervised analysis with a Random Forest, the expectations are included in the training of the method. Thus, the groups which may be detected are already predefined. The supervised machine learning is fitting the purposes better than an unsupervised analysis.

The classification by the Thies Laser Precipitation Monitor uses a statistical method. As clustering does not appear useful, the developers of the algorithm for the internal classification probably used a supervised approach. An instantaneous classification by the instrument is possible after training the method (e.g. Random Forest) with an external classification of the measured spectrum and applying it to each measured sample.

4 Conclusion

After all the analysis done for this study, there are some principle conclusions to be made. One of the main conclusions is the performance of the single methods. The approach of cluster analysis appears theoretically useful, but showed that it is not applicable here. The comparison of the cluster analysis and the Random Forest shows that the second technique works much better for the classification of precipitation types through the measured size-velocity-spectrum of the precipitation.

Furthermore, the spectra themselves present the differences between liquid precipitation and light, solid precipitation. The total spectrum is dividable into two separate groups, but more detailed precipitation types do not lead to further accumulations in the spectrum.

In conclusion, it can be said, that the analysis successfully showed the resulting differences between the two approaches with the clear result, that supervised techniques are more useful for work with precipitation spectra concerning the classification of precipitation type. Referring to the overarching aim, the internal hydrometeor classification process of the disdrometer is reconstructed by using a Random Forest. It now can be applied to other instruments which measure the size-velocity-distributions of precipitation. The algorithm can be trained by a short time of parallel measurements, e.g. with the micro rain radar, where the disdrometer data can serve as reference classification.

References

Adolf Thies GmbH & Co KG. *Laser Niederschlags Monitor - Bedienungsanleitung*, 2015. URL https://www.thiesclima.com/db/dnl/5.4110.xx.x00_LNM_deu.pdf.

Charu C. Aggarwal. An introduction to cluster analysis. In *Data Clustering*, pages 1–28. Chapman and Hall/CRC, 2018. doi:10.1201/9781315373515-1.

Marta Angulo-Martínez, Santiago Beguería, Borja Latorre, and Maria Fernández-Raga. Comparison of precipitation measurements by ott parsivel^2 and thies lpm optical disdrometers. *Hydrology and Earth System Sciences*, 22(5):2811–2837, 2018. doi:10.5194/hess-22-2811-2018.

David Atlas, R. C. Srivastava, and Rajinder S. Sekhon. Doppler radar characteristics of precipitation at vertical incidence. *Reviews of Geophysics*, 1973. doi:10.1029/rg011i001p00001.

Ross Gunn and Gilbert D. Kinzer. The terminal velocity of fall for water droplets in stagnant air. *Journal of Meteorology*, 1949. doi:10.1175/1520-0469(1949)006<0243:ttvoff>2.0.co;2.

Masaaki Ishizaka, Hiroki Motoyoshi, Sento Nakai, Toru Shiina, Toshiro Kumakura, and Ken ichiro Muramoto. A new method for identifying the main type of solid hydrometeors contributing to snowfall from measured size-fall speed relationship. *Journal of the Meteorological Society of Japan. Ser. II*, 2013. doi:10.2151/jmsj.2013-602.

Helmut Kraus. *Die Atmosphäre der Erde: Einführung in die Meteorologie*. Springer Berlin Heidelberg, 2004. doi:10.1007/3-540-35017-9.

Yanli Liu, Yourong Wang, and Jian Zhang. New machine learning algorithm: Random forest. In *Information Computing and Applications*, pages 246–252. Springer Berlin Heidelberg, 2012. doi:10.1007/978-3-642-34062-8_32.

John D. Locatelli and Peter V. Hobbs. Fall speeds and masses of solid precipitation particles. *Journal of Geophysical Research*, 1974. doi:10.1029/jc079i015p02185.

Martin Löffler-Mang and Jürg Joss. An optical disdrometer for measuring size and velocity of hydrometeors. *Journal of Atmospheric and Oceanic Technology*, 2000. doi:10.1175/1520-0426(2000)017<0130:aodfms>2.0.co;2.

Hanna-Leena Merenti-Välimäki, Jan Lönnqvist, and Pertti Laininen. Present weather: comparing human observations and one type of automated sensor. *Meteorological Applications*, 2001. doi:10.1017/s1350482701004108.

Scikit-learn. Clustering. URL https://scikit-learn.org/stable/modules/clustering.html#clustering.(accessed:29.11.2022).

Michael Steinbach, George Karypis, and Vipin Kumar. A comparison of document clustering techniques. 2000.

Xue Ying. An overview of overfitting and its solutions. *Journal of Physics: Conference Series*, 2019. doi:10.1088/1742-6596/1168/2/022022.

Melt pond depth retrieval applying airborne spectral imaging and the potential of a new RGB band approach

Rosenburg, S.[1,✉], Jäkel, E.[1], Wendisch, M.[1]

[1] *Institute for Meteorology, Leipzig University, Germany*
✉*e-mail: sophie.rosenburg@uni-leipzig.de*

Summary: Melt ponds are important features on summer Arctic sea ice leading to a surface albedo reduction and thereby altering the energy budget. Besides the spatial pond coverage, the melt pond depth is of importance in context of meltwater volume distribution across the sea ice surface. In this study, the melt pond depth is retrieved based on airborne reflectance measurements performed in the framework of an Arctic field campaign. An already existing approach uses the spectral reflectance slope and is widely independent of the pond ice bottom reflectance contribution. However, the surface coverage of the imaging spectrometer, providing the required spectrally resolved information, is limited due to the narrow field of view. To capture a larger number of melt ponds, a commercial digital camera with fisheye-lens provides reflectances in the red, green, and blue (RGB) spectral ranges. To retrieve the melt pond depth a new RGB band approach was developed and validated by the established spectral retrieval approach. The depth deviation of the approaches ranged between 0.1 cm and 27.6 cm depending on prior information on the pond ice bottom reflectance.

Zusammenfassung: Schmelztümpel stellen wichtige Oberflächenmerkmale des arktischen Meereises im Sommer dar, da sie die Albedo senken und somit Einfluss auf das Energiebudget haben. Neben der Fläche, die die Tümpel bedecken, ist ebenfalls deren Tiefe im Rahmen der Schmelzwasserverteilung relevant. In dieser Studie wird die Schmelztümpeltiefe von flugzeuggetragenen Reflektanzmessungen abgeleitet, die während einer Messkampagne in der Arktis durchgeführt wurden. Ein bereits bestehender Ansatz verwendet den spektralen Reflektanzanstieg und ist weitgehend unabhängig von der Reflexion am Eisboden des Tümpels. Jedoch ist die räumliche Abdeckung des bildgebenden Spektrometers, das spektral aufgelöste Messungen ermöglicht, durch den schmalen Öffnungswinkel des Instruments limitiert. Um eine größere Anzahl von Tümpeln zu beobachten, kann eine kommerzielle Digitalkamera mit Fischaugenlinse verwendet werden, mit welcher Reflektanzen im roten, grünen und blauen (RGB) Spektralbereich bestimmt werden können. Um die Tümpeltiefe abzuleiten, wurde ein neuer RGB Ansatz entwickelt und mit dem bestehenden spektralen Ansatz validiert. Die Abweichungen der abgeleiteten Tiefen variierten zwischen 0.1 cm und 27.6 cm abhängig von den bereitgestellten Informationen zur Reflektanz des Eises am Tümpelboden.

1 Introduction

In global comparison, the Arctic experiences an enhanced warming, which is referred to as Arctic amplification and is connected to feedback mechanisms (Serreze and Francis, 2006; Serreze and Barry, 2011). The positive sea ice surface albedo feedback is an important driver and emphasizes the role of the declining sea ice cover of the Arctic Ocean (Curry et al., 1995; Hall, 2004; Pithan and Mauritsen, 2014). Annual melting processes comprise the snow melting, melt pond formation, and the total ice decay in case of first-year sea ice (Perovich and Polashenski, 2012). Melt ponds are important surface features altering the surface energy budget as less reflective areas. The reflection by a melt pond is depending on the reflective behavior of the pond ice bottom and the pond depth (Malinka et al., 2018). As melt ponds represent a significant portion of the ice surface meltwater balance (Perovich et al., 2021), the melt pond depth is a crucial factor determining the accumulated meltwater volume. To obtain large-scale information on melt ponds and their depths, remote sensing approaches as airborne photogrammetry (Divine et al., 2016) and spaceborne laser altimetry (Fricker et al., 2021) can be applied. Based on the melt pond albedo, Malinka et al. (2018) developed a radiative transfer scheme, which allows to inversely retrieve the melt pond depth. Other approaches rely on spectral reflectance ratios (Legleiter et al., 2014) or a spectral reflectance slope embedded in a linear equation (König and Oppelt, 2020) to retrieve the melt pond depth. König and Oppelt (2020) developed their linear model by widely eliminating the dependence on the pond ice bottom reflectance. In this study, their approach is applied to airborne measurements of the remote sensing reflectance, which is defined as

$$R_{\mathrm{rs}}(\lambda) = \frac{I^{\uparrow}(\lambda)}{F^{\downarrow}(\lambda)}, \tag{1}$$

with the spectral downward irradiance $F^{\downarrow}(\lambda)$ in units of $\mathrm{W\,m^{-2}\,nm^{-1}}$ and the spectral upward radiance $I^{\uparrow}(\lambda)$ in units of $\mathrm{W\,m^{-2}\,nm^{-1}\,sr^{-1}}$. These measurements were performed during the Arctic field campaign ACLOUD (Arctic CLoud Observations Using airborne measurements during polar Day) carried out in May/June 2017 with an imaging spectrometer and a spectral albedometer (Ehrlich et al., 2019). The aircraft was further equipped with a fisheye-lens digital camera, which measured upward radiances in RGB (red, green, blue) bands. Compared to the limited spatial coverage of the imaging spectrometer with a field of view (FOV) of 36°, the camera enables observations of a larger surface area. Transferring the reflectance resolution from spectral to broadband information, an RGB band approach was developed and evaluated by the linear model of König and Oppelt (2020) in terms of its performance and limitations.

Here, a summary of the approach development and the results presented in the master thesis Rosenburg (2022) is given. The airborne measurements and simulations are introduced in Sect. 2. The basis and application of the retrieval approaches are described in Sect. 3, followed by an analysis of the retrieval results (Sect. 4). Retrieval uncertainties are discussed in Sect. 5 leading to a conclusive summary (Sect. 6).

2 Reflectance measurements and simulations

The linear model by König and Oppelt (2020) and the new RGB band approach are based on measurements of melt pond reflectance with different spectral resolutions. Furthermore, both approaches rely on radiative transfer simulations of the pond reflectance. The airborne measurements and the simulation setup are introduced in the following.

2.1 Airborne measurements

The ACLOUD campaign was carried out from 23 May to 26 June 2017 with research flights traversing the sea ice edge in the north-west of Svalbard (Wendisch et al., 2019). The *Polar 5* aircraft of the Alfred Wegener Institute, Helmholtz Centre for Polar and Marine Research (Wesche et al., 2016) was equipped with remote sensing instrumentation comprising the Spectral Modular Airborne Radiation measurement sysTem (SMART) albedometer, the imaging spectrometer AisaEagle, and the digital Canon camera with fisheye-lens (Ehrlich et al., 2019).

The SMART albedometer provided spectral measurements of the upward and downward irradiance. The optical inlets were actively stabilized in a pitch and roll angle range of ±4.5°. The measurements covered the spectral range from 400 nm to 2150 nm temporally resolved with 2 Hz (Wendisch et al., 2001; Bierwirth et al., 2009; Ehrlich et al., 2019). Uncertainties arised from the cosine correction, the sensor tilt, the wavelength accuracy, and the radiometric calibration. A total measurement uncertainty of ±5.7 % was estimated for the downward irradiance (Jäkel et al., 2021).

The across-track pushbroom imaging spectrometer AisaEagle measured the spectral upward radiance in a wavelength range from 400 nm to 990 nm with a FOV of 36° and a temporal resolution of 20 Hz (Ehrlich et al., 2019). The sensor swath is divided into 1024 spatial pixels. Assuming a flight altitude of 100 m, an aircraft speed of 60 m s^{-1}, and 0.05 s integration time, the average pixel area and thereby minimum resolvable pond size is about 0.06 m × 3 m (across × along track). The calibration procedure was performed applying an integrating sphere, which introduced an uncertainty of ±6 % affecting the radiance measurements.

Furthermore, a commercial digital Canon camera equipped with a fisheye-lens (180° FOV) was used to measure the upward radiance with an image resolution of 3908 × 2600 pixels every 6 s. The camera was calibrated spectrally, radiometrically, and geometrically (Ehrlich et al., 2019). The RGB bands have their center wavelengths λ_c at 611 nm, 550 nm, 484 nm, respectively, and a full width at half maximum (FWHM) ranging between 61 nm and 86 nm.

To permit comparability of the two applied approaches, the linear model by König and Oppelt (2020) and the newly developed RGB band approach were applied on AisaEagle radiance data only. In addition, the new approach is still depending on the linear model, which is based on spectrally resolved information. Therefore, the reflectances measured by AisaEagle and SMART were transferred to the RGB resolution.

2.2 Simulations

Melt pond reflectance spectra were also simulated and analyzed with the Water Color Simulator (WASI), providing a tool for in-water radiative transfer calculations (Gege, 2004; Gege and Albert, 2006). In the forward mode the simulations are based on user-defined input. Inversely, also measured reflectance spectra can be analyzed and water properties are derived. The reflectance of a shallow water body, i.e. a melt pond, is composed of the water reflectance itself and contributions of the pond ice bottom. The ice bottom reflectance spectrum can be described in WASI as a linear combination of different areal bottom fractions with respective reflective characteristics. In general, the pond water and bottom reflectances are attenuated due to extinction, depending on pond depth and angular observation as well as solar geometry, yielding the melt pond reflectance (Gege, 2021). Here, the pond water was assumed to be pure without any dissolved matter to avoid additional absorption processes.

The diffuse in-water radiative transport is not implemented in WASI and, therefore, only cloud-free conditions were regarded. Concerning the blue and partly also green spectral range, atmospheric Rayleigh scattering causes diffuse incidence, whose radiative transfer in water cannot be represented. This aspect could introduce further uncertainties regarding this spectral range. Nevertheless, Rayleigh scattering taking place in water is often assumed to be negligible in modelling as liquid water is primarily an absorbing medium (Malinka et al., 2018).

3 Melt pond depth retrieval approaches

3.1 Linear model by König and Oppelt (2020)

To disentangle the dependence of the melt pond reflectance on pond ice bottom reflectance and pond depth, König and Oppelt (2020) simulated pond reflectance spectra varying both properties with WASI and analyzed their contributions. They found that the spectral slope of the log-scaled reflectance at $\lambda = 710\,\mathrm{nm}$ is almost independent of the ice bottom reflectance and highly correlated with the pond depth z_{lin} (in units of cm) via

$$z_{\mathrm{lin}} = a(\theta_{\mathrm{Sun}}) + b(\theta_{\mathrm{Sun}}) \left[\frac{\partial \log R_{\mathrm{rs}}(\lambda)}{\partial \lambda} \right]_{\lambda=710\,\mathrm{nm}}, \tag{2}$$

with the parameters a and b being dependent on the solar zenith angle θ_{Sun}. This linear model is applicable under cloud-free conditions, ensuring computable radiative in-water pathways and taking the WASI setup into account, and pond depths reaching at maximum 1 m because of increasing attenuation (König and Oppelt, 2020).

3.2 New RGB band approach

Visually, the color of melt ponds ranges from bright blue to almost black and may therefore be an indicator for specific pond characteristics. Lu et al. (2018) evaluated the dependence of the pond color on the ice bottom thickness, inherent optical properties, pond depth, and incident solar radiation. Separated into RGB bands, only in the red

channel a partial dependence on pond depth could be found whereas overall mainly the ice bottom thickness predominates.

As a disentanglement in RGB band observations is not feasible, both factors have to be taken into account. The new RGB band approach is based on look-up-tables (LUTs) simulated with WASI for varying ice bottom brightness (from dark with 10 % to bright with 100 %), as a measure of reflectance, and pond depth (0 – 100 cm). The reflectance in all three channels depends on the ice bottom brightness, but only the red channel reflectance ($R_{\mathrm{rs}}^{\mathrm{R}}$) shows a superposition of sensitivity to depth and ice bottom brightness. Thus, applying a reflectance ratio of the green and red channel ($R_{\mathrm{rs}}^{\mathrm{G}}/R_{\mathrm{rs}}^{\mathrm{R}}$), the ice bottom effect is weakened combined with a more distinct depth dependence.

3.3 Approach application

The flowchart in Figure 1 provides a general overview of the approach application. First, the measurement cases were selected according to specific criteria. Melt ponds observed under cloud-free conditions had to cover at least the area of an AisaEagle pixel to be resolvable and to avoid mixed pixels with ice and pond fractions. Furthermore, darker melt ponds were excluded to reduce the probability of mixing with ocean water, violating the pure water assumption. Therefore, only light blue ponds were selected for case studies. In addition, atmospheric effects within the layer between flight altitude and surface could have altered the measured quantities. However, this aspect was neglected as atmospheric radiative transfer simulations showed no significant effect and as flight altitudes of the selected cases did not exceed 128 m. This way, single melt pond pixels were selected and the remote sensing reflectance spectra were calculated according to Eq. 1 in step 1.

For step 2, the application of the linear model by König and Oppelt (2020), the measured reflectance spectra were smoothed and log-scaled. To determine the first derivative at $\lambda = 710$ nm, a Savitzky-Golay filter was applied to a 9 nm window fitting a second order polynomial, of which the spectral slope was determined. Based on this slope and the solar zenith angle, the melt pond depth z_{lin} was retrieved with the linear model according to Eq. 2.

In step 3, the pond ice bottom reflectance spectrum was estimated by the inverse mode of WASI. The pond reflectance spectrum measured by SMART and AisaEagle was fitted with the areal weighting of two default ice reflectance spectra (one bright, one dark taken from König and Oppelt (2019)) as fitting parameters. The already retrieved pond depth z_{lin} and the solar zenith angle served as input information. As a result, WASI determined an estimated pond ice bottom reflectance spectrum that served as a boundary condition for the new RGB band approach.

However, for a practical approach application an estimation for the spectral ice bottom reflectance should also be derivable from measurements (step 4). Thus, it was assumed that the melt pond edge ice and the pond bottom ice experienced similar melting processes and are comparable in their reflective behavior. Therefore, an ice pixel at the melt pond edge was selected providing an estimated reflectance spectrum of the pond ice bottom. Depending on the selection criteria for that ice pixel, the method is subdivided into two experiments: (i) With a prior comparison of the ice pixel reflectance spectrum to the estimated spectrum by WASI in step 3, the guided experiment is based on a validated

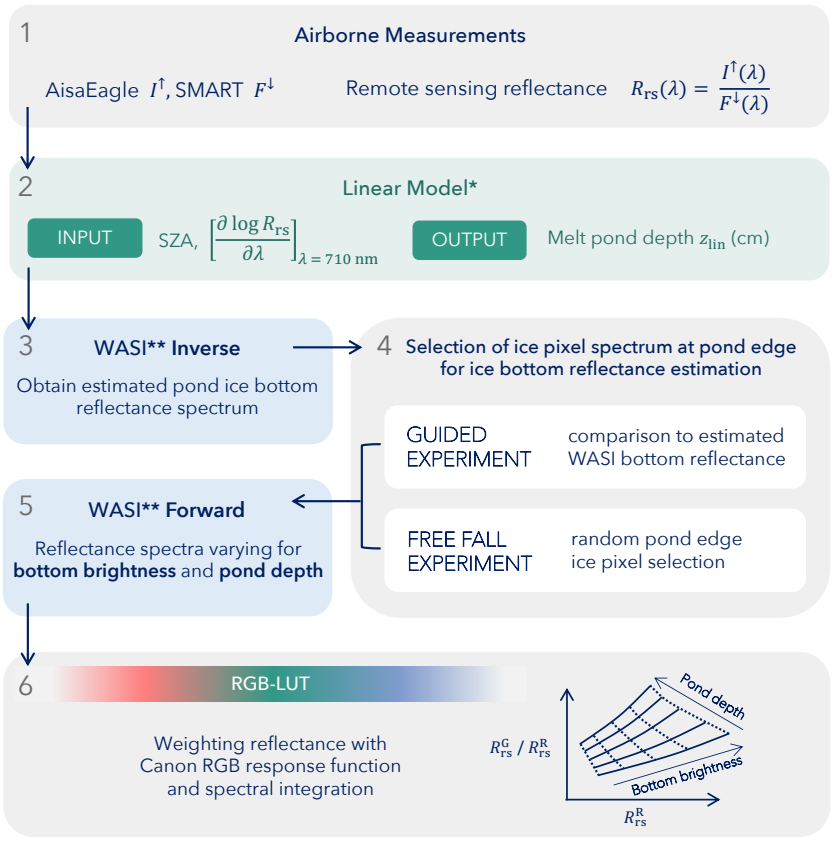

Figure 1: *Flowchart visualizing the application of the RGB band approach in steps 1 to 6. The procedure comprises the application of the linear model by König and Oppelt (2020)* and WASI simulations according to Gege (2021)**.*

pond edge ice pixel choice. (ii) However, to represent realistic conditions without prior knowledge and independence of the linear model, the free fall experiment is based on a randomly chosen pond edge ice pixel.

In step 5, reflectance spectra were simulated based on the estimated pond ice bottom reflectance spectrum and the solar zenith angle with the WASI forward mode for varying pond depth (0 – 100 cm) and bottom brightness by scaling the estimated ice bottom reflectance spectrum. These simulated spectra were then weighted with the relative spectral response function of the Canon camera and integrated to obtain the RGB reflectances generating the respective LUTs described in Sect. 3.2 (step 6). The final LUTs had a resolution of 1 % pond bottom brightness and 1 cm pond depth.

4 Retrieval results

For each of the five selected melt ponds P1 to P5, overflown on 25 June 2017, the linear model by König and Oppelt (2020) as well as the RGB band approach were applied to one pixel reflectance spectrum retrieving a melt pond depth. The results are shown in Figure 2. Due to the lack of in situ depth measurements, the linear model, as already validated approach, was considered as a reference for the RGB band approach. Overall, the depths retrieved by the guided RGB experiment show a better agreement with the linear model with deviations ranging in absolute values from 0.1 cm to 10.1 cm. Contrary,

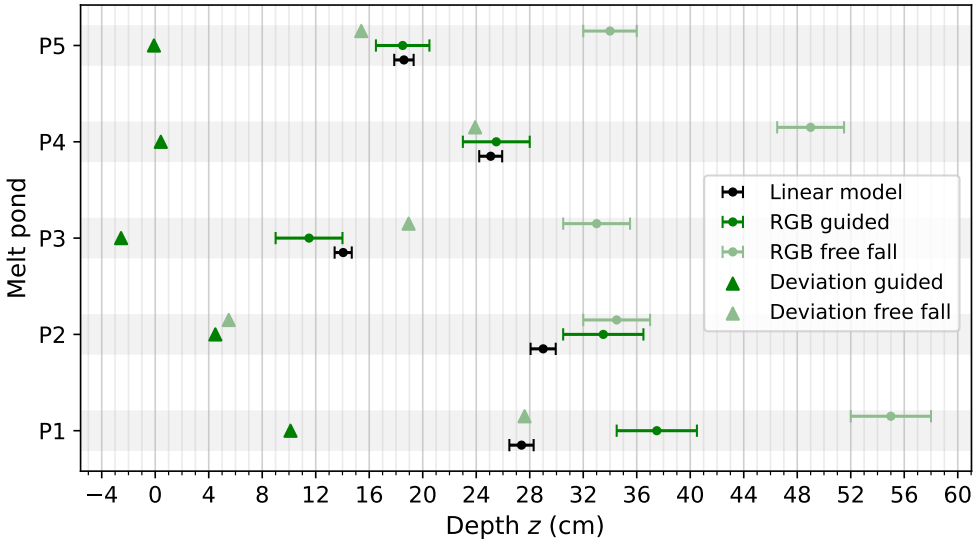

Figure 2: *Comparison of retrieved melt pond depths. The results of the linear model are shown in black with the measurement uncertainty range. The pond depths for the RGB guided/free fall experiment are shown in dark/light green within the range of the respective standard deviation. The deviations from the linear model pond depths are indicated by triangles, which are colored accordingly.*

deviations of the free fall experiment varied between 5.5 cm and 27.6 cm with a partly strong overestimation of the melt pond depth.

To analyze these deviating results, Figure 3a illustrates shifts of the LUT and the measurement itself in the grid of ratio $R_{\mathrm{rs}}^{\mathrm{G}}/R_{\mathrm{rs}}^{\mathrm{R}}$ and red channel reflectance $R_{\mathrm{rs}}^{\mathrm{R}}$. The first and second shift can be attributed to the selected pond ice bottom reflectance spectrum. In the free fall experiment this spectrum was chosen randomly and showed often a distinct deviation from the ice bottom spectrum estimated by WASI. This is also the case for melt pond P4 in Figure 3b regarding the light blue spectrum with a sum of squared deviations from the estimated WASI spectrum $d_{\mathrm{square}} = 7 \times 10^{-2}\,\mathrm{sr}^{-2}$ in comparison to the red spectrum, selected according to the guided experiment, with $d_{\mathrm{square}} = 9 \times 10^{-4}\,\mathrm{sr}^{-2}$. The randomly chosen ice reflectance spectra for the free fall experiment showed in all cases P1 to P5 an underestimation in the blue to green spectral range whereas the red spectral range displayed an overestimated reflectance. Thus, the LUT is shifted horizontally to larger reflectances and vertically to smaller ratios leading to a shift to larger retrieved pond depths for a fixed position of the measurement in the grid. In general, a higher degree of similarity of WASI ice bottom and randomly picked edge ice reflectance spectrum was connected to a better agreement with the linear model depth.

The third shift is connected to the measurement itself and the flight conditions under which it was obtained. The flight altitude was about 120 m for P1 to P3 and about 55 m for P4 and P5. A higher altitude implies a larger surface coverage of possibly also ice surfaces surrounding the regarded melt pond. Therefore, reflections from neighboring bright ice pixels could be scattered into the FOV of the selected pond pixel, also in the green spectral range due to atmospheric Rayleigh scattering. This would have caused measurements of higher spectral reflectances. This overestimation probably led to a

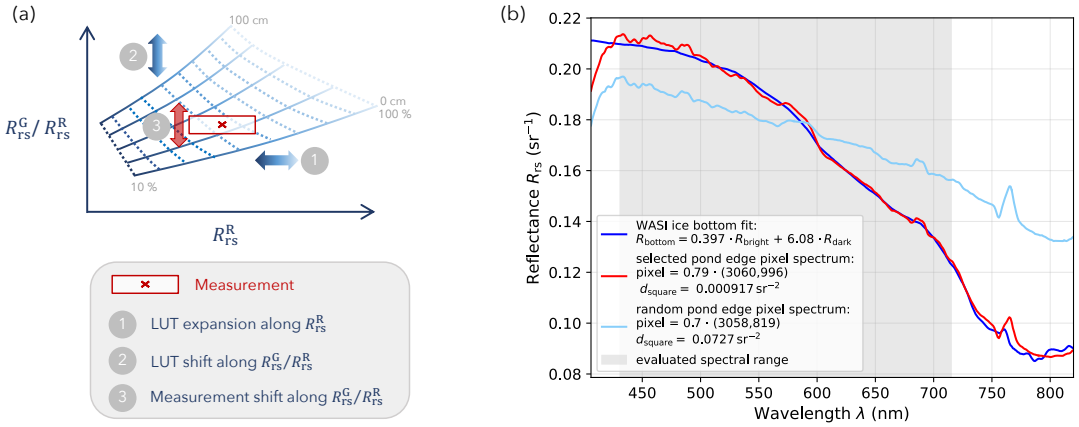

Figure 3: *(a) An illustration of possible causes for depth deviations of the RGB band approach from the linear model. (b) Comparison of near-pond ice reflectance spectra (red - guided, light blue - free fall) to the estimation from the WASI simulations (dark blue) in step 3 of Figure 1 with* d_{square} *as sum of the squared deviations of the evaluated spectral range (grey shaded section), exemplarily for melt pond P4.*

larger reflectance ratio and therefore too high placement of the measurement in the LUT yielding a depth overestimation, even for the guided experiment. This could be the case for melt pond pixels P1 and P2. For P3 the pond depth was underestimated by the guided experiment probably due to fractured sea ice and extensive dark ocean surfaces in the pond environment. For the melt pond pixels P4 and P5 a good agreement was yielded between guided experiment and linear model possibly related to the lower flight altitude.

5 Discussion of uncertainties

5.1 Linear model by König and Oppelt (2020)

The linear model by König and Oppelt (2020) was applied as a reference for the melt pond depth retrieved with the RGB band approach. In the studies by König and Oppelt (2020) and König et al. (2020) maximum melt pond depths of 35 cm were measured with a folding ruler on 10 June 2017. During the Multidisciplinary drifting Observatory for the Study of Arctic Climate (MOSAiC, Shupe et al. (2022)) campaign in situ measured mean melt pond depths in late June 2020 were about 10 cm to 15 cm (Webster et al., 2022). As ice surface and pond characteristics may vary locally, these measurements can only provide a general indication of magnitude. In our comparison, the resulting depths of the linear model are assumed to be reasonable.

In general, the linear model is restricted to cloud-free conditions and the complete independence of the ice bottom reflectance cannot be guaranteed. Furthermore, pure pond water was assumed. The combined measurement uncertainty of AisaEagle and SMART (about ±11.7 %) was applied to the measured reflectance spectra, but did not have any significant impact on the spectral reflectance slope, which determined the retrieved pond depth. In addition, a spectral ±2 % uncertainty, resulting from the transfer calibration, was applied to the slope of the log-scaled reflectance spectrum and yielded depth deviations of less than 1 cm. Another uncertainty aspect concerns the smoothing procedure for

the measured data and the application of the Savitzky-Golay filter to determine the first derivative (Sect. 3.3). Both may affect the slope of the reflectance spectrum depending on the selected scanned window size. Therefore, the smoothing should be a compromise between removing noise as well as artificial features and preserving spectral characteristics. Selecting a 9 nm wide window for the Savitzky-Golay filter appeared in that context as an adequate choice. Quantitatively, the resulting pond depth was compared to a retrieval with a 3 nm window, i.e. applying no smoothing with the Savitzky-Golay filter, and a maximum deviation about 11 cm was determined. Consequently, smoothing is a necessary step in data processing, but has to be applied carefully and should be adapted to measurement conditions and instrument specifications.

5.2 RGB band approach

The RGB band approach is depending on both factors, the pond ice bottom reflectance and the pond depth. Due to the specific ice bottom characteristics, an individual LUT is required for each pond pixel. For the guided and free fall experiments, ice pixels at the melt pond edge were selected. In the guided case, this spectrum was compared to the estimated WASI ice bottom reflectance. To allow a wider range of spectral shapes, more default spectra would be beneficial to match the real ice spectra. Furthermore, in WASI simulations the diffuse in-water transport is not represented. The simulations were performed assuming a nadir viewing geometry to limit computation time. This assumption can be justified according to the almost isotropic reflection of ponded sea ice in the regarded narrow angular range of AisaEagle, which was observed by Goyens et al. (2018). The performance of the RGB band approach is limited by the uncertainty of the linear model, which is part of retrieval and final validation. In the LUTs, the measurement uncertainty of ±11.7 % is considered for the reflectance in the red spectral range whereas the reflectance ratio is regarded in the ±2 % range arising from the transfer calibration. Therefore, a mean melt pond depth was determined with a respective standard deviation about ±2 cm to ±3 cm. Overall, only a comparison to in situ pond depth measurements would allow an adequate validation of the presented new RGB band approach. Additional observations of the reflective characteristics of the pond ice bottom would be required to apply the approach independently and isolated from the linear model by König and Oppelt (2020), which should allow an unbiased comparison of both approaches.

6 Summary and conclusions

In this study, the melt pond depth was retrieved by two retrieval approaches based on airborne reflectance measurements performed during the ACLOUD campaign in May/June 2017. The linear model by König and Oppelt (2020) is a well established and validated approach relying solely on the slope of the log-scaled reflectance spectrum at $\lambda = 710$ nm and the solar zenith angle. This approach is almost independent of the pond ice bottom reflectance, which is an important advantage. As the linear model is applied spectrally, an RGB perspective considers the broadband reflectance in the red, green, and blue spectral ranges, i.e. the visual pond color. In this case, the dependence on the melt pond depth and the ice bottom reflectance, which is predominant, cannot be disentangled and both have to be considered. This was done in LUTs based on reflectances in the

red and green channel, which were simulated with the water color simulator WASI (Gege, 2021). For an estimation of the ice bottom reflectance, reflectance spectra of ice pixels near the melt pond edge were evaluated (guided experiment) or selected randomly (free fall experiment). By a comparison of simulations and measurements the depth was determined for selected pond pixels. The mean absolute deviations from the linear model of the guided and free fall experiment were about 3.5 cm and 18.3 cm, respectively. These results emphasize the importance of detailed observations of pond ice bottom characteristics, which would provide essential information. In general, in situ pond depth measurements would be required for an adequate validation of the new approach. The RGB band approach, applied to radiances measured by the digital camera with fisheye-lens, would allow a spatially more extensive observation of more melt ponds compared to the imaging spectrometer AisaEagle with a rather narrow FOV. Exploiting the full potential, the meltwater distribution on sea ice surfaces could be observed and analyzed in context of the changing melting settings in the Arctic.

References

Bierwirth, E., Wendisch, M., Ehrlich, A., et al.: Spectral surface albedo over Morocco and its impact on radiative forcing of Saharan dust, Tellus B, 61, 252, doi:10.1111/j.1600-0889.2008.00395.x, 2009.

Curry, J. A., Schramm, J. L., and Ebert, E. E.: Sea Ice-Albedo Climate Feedback Mechanism, J. Climate, 8, 240–247, doi:10.1175/1520-0442(1995)008<0240:siacfm>2.0.co;2, 1995.

Divine, D. V., Pedersen, C. A., Karlsen, T. I., et al.: Photogrammetric retrieval and analysis of small scale sea ice topography during summer melt, Cold Reg. Sci. Technol., 129, 77–84, doi:https://doi.org/10.1016/j.coldregions.2016.06.006, 2016.

Ehrlich, A., Wendisch, M., Lüpkes, C., et al.: A comprehensive in situ and remote sensing data set from the Arctic CLoud Observations Using airborne measurements during polar Day (ACLOUD) campaign, Earth Syst. Sci. Data, 11, 1853–1881, doi:10.5194/essd-11-1853-2019, 2019.

Fricker, H. A., Arndt, P., Brunt, K. M., et al.: ICESat-2 Meltwater Depth Estimates: Application to Surface Melt on Amery Ice Shelf, East Antarctica, Geophys. Res. Lett., 48, e2020GL090 550, doi:https://doi.org/10.1029/2020GL090550, e2020GL090550 2020GL090550, 2021.

Gege, P.: The water color simulator WASI: an integrating software tool for analysis and simulation of optical in situ spectra, Computers Geosciences, 30, 523–532, doi:10.1016/j.cageo.2004.03.005, 2004.

Gege, P.: The Water Colour Simulator WASI, User manual for WASI version 6, DLR, 2021.

Gege, P. and Albert, A.: A TOOL FOR INVERSE MODELING OF SPECTRAL MEASUREMENTS IN DEEP AND SHALLOW WATERS, in: Remote Sensing and Digital Image Processing, pp. 81–109, Springer Netherlands, doi:10.1007/1-4020-3968-9_4, 2006.

Goyens, C., Marty, S., Leymarie, E., et al.: High Angular Resolution Measurements of the Anisotropy of Reflectance of Sea Ice and Snow, Earth and Space Science, 5, 30–47, doi:https://doi.org/10.1002/2017EA000332, 2018.

Hall, A.: The Role of Surface Albedo Feedback in Climate, J. Climate, 17, 1550–1568, doi:10.1175/1520-0442(2004)017<1550:trosaf>2.0.co;2, 2004.

Jäkel, E., Carlsen, T., Ehrlich, A., et al.: Measurements and Modeling of Optical-Equivalent Snow Grain Sizes under Arctic Low-Sun Conditions, Remote Sens., 13, 4904, doi:10.3390/rs13234904, 2021.

König, M. and Oppelt, N.: Optical measurements of bare ice and melt ponds on Arctic sea ice acquired during POLARSTERN cruise PS106, doi:10.1594/PANGAEA.908075, 2019.

König, M. and Oppelt, N.: A linear model to derive melt pond depth on Arctic sea ice from hyperspectral data, The Cryosphere, 14, 2567–2579, doi:10.5194/tc-14-2567-2020, 2020.

König, M., Birnbaum, G., and Oppelt, N.: Mapping the Bathymetry of Melt Ponds on Arctic Sea Ice Using Hyperspectral Imagery, Remote Sens., 12, doi:10.3390/rs12162623, 2020.

Legleiter, C. J., Tedesco, M., Smith, L. C., Behar, A. E., and Overstreet, B. T.: Mapping the bathymetry of

supraglacial lakes and streams on the Greenland ice sheet using field measurements and high-resolution satellite images, The Cryosphere, 8, 215–228, doi:10.5194/tc-8-215-2014, 2014.

Lu, P., Leppäranta, M., Cheng, B., et al.: The color of melt ponds on Arctic sea ice, The Cryosphere, 12, 1331–1345, doi:10.5194/tc-12-1331-2018, 2018.

Malinka, A., Zege, E., Istomina, L., et al.: Reflective properties of melt ponds on sea ice, The Cryosphere, 12, 1921–1937, doi:10.5194/tc-12-1921-2018, 2018.

Perovich, D., Smith, M., Light, B., and Webster, M.: Meltwater sources and sinks for multiyear Arctic sea ice in summer, The Cryosphere, 15, 4517–4525, doi:10.5194/tc-15-4517-2021, 2021.

Perovich, D. K. and Polashenski, C.: Albedo evolution of seasonal Arctic sea ice, Geophys. Res. Lett., 39, doi:10.1029/2012GL051432, 2012.

Pithan, F. and Mauritsen, T.: Arctic amplification dominated by temperature feedbacks in contemporary climate models, Nat. Geosci., 7, 181–184, doi:10.1038/ngeo2071, 2014.

Rosenburg, S.: Melt Pond Depth Retrieval applying Airborne Hyperspectral Imagery and the Potential of a New RGB Band Approach, Master's thesis, Leipzig University, Leipzig Institute for Meteorology, 2022.

Serreze, M. C. and Barry, R. G.: Processes and impacts of Arctic amplification: A research synthesis, Global Planet. Change, 77, 85–96, doi:https://doi.org/10.1016/j.gloplacha.2011.03.004, 2011.

Serreze, M. C. and Francis, J. A.: The Arctic Amplification Debate, Climatic Change, 76, 241–264, doi:10.1007/s10584-005-9017-y, 2006.

Shupe, M. D., Rex, M., Blomquist, B., et al.: Overview of the MOSAiC expedition: Atmosphere, Elementa: Science of the Anthropocene, 10, 00 060, doi:10.1525/elementa.2021.00060, 2022.

Webster, M. A., Holland, M., Wright, N. C., et al.: Spatiotemporal evolution of melt ponds on Arctic sea ice, Elementa: Science of the Anthropocene, 10, doi:10.1525/elementa.2021.000072, 2022.

Wendisch, M., Müller, D., Schell, D., and Heintzenberg, J.: An Airborne Spectral Albedometer with Active Horizontal Stabilization, J. Atmos. Ocean Tech., 18, 1856–1866, doi:10.1175/1520-0426(2001)018<1856:aasawa>2.0.co;2, 2001.

Wendisch, M., Macke, A., Ehrlich, A., et al.: The Arctic Cloud Puzzle: Using ACLOUD/PASCAL Multiplatform Observations to Unravel the Role of Clouds and Aerosol Particles in Arctic Amplification, B. Am. Meteorol. Soc., 100, 841–871, doi:10.1175/bams-d-18-0072.1, 2019.

Wesche, C., Steinhage, D., and Nixdorf, U.: Polar aircraft Polar5 and Polar6 operated by the Alfred Wegener Institute, Journal of large-scale research facilities, 2, doi:10.17815/jlsrf-2-153, 2016.

Forschungsbericht 2022
Bearbeitete Forschungsprojekte

Institut für Meteorologie

Allgemeine Meteorologie; Manfred Wendisch
AG Atmosphärische Strahlung

Koordination des Schwerpunktprogramms 1294 "Atmosphären- und Erdsystemforschung mit dem Forschungsflugzeug HALO (High Altitude and Long Range Research Aircraft)"
HALO coordination project

Schlagworte: flugzeuggetragene Forschung

Projektleiter: M. Wendisch (m.wendisch@uni-leipzig.de)
Professor Dr. Joachim Curtius, Goethe-Universität Frankfurt am Main, Institut für Atmosphäre und Umwelt

Projektmitarbeiter: Anja Schwarz, Jörg Schmidt

Projektbeginn: 2010
Projektende: 2027

Beschreibung
Das Ziel des Antrages ist die zentrale Koordination des SPP 1294 'Atmosphären- und Erdsystemforschung mit HALO' (HALO: HighAltitude and Long Range Research Aircraft, Hochfliegendes und weitreichendes Forschungsflugzeug). Das Projekt dient der Förderung der Zusammenarbeit und Kommunikation innerhalb der HALO Missionsteams und den individuellen Projektpartnern, die im SPP eingebunden sind. Die drei Koordinatoren (M. Wendisch, Universität Leipzig; J. Curtius, Universität Frankfurt am Main; M. Scheinert, Technische Universität Dresden) vertreten den SPP gegenüber der DFG, dem Wissenschaftlichen Lenkungsausschuss (WLA) für HALO, dem HALO Projektteam des Deutschen Zentrums für Luft- und Raumfahrt (DLR-FX) und der Öffentlichkeit. Der DFGAnteil an den Missionskosten wird an der Universität Leipzig zentral verwaltet. Die Finanzmittel für Maßnahmen zur Förderung der Gleichstellung werden verwaltet, und die Ausbildung der jungen Wissenschaftler wird koordiniert. Monatliche Telefonkonferenzen der drei Koordinatoren, jährlich Statusseminare und thematische Workshops werden organisiert. Spezielle Sitzungen auf internationalen Konferenzen und Veröffentlichungen von Spezialausgaben in internationalen Zeitschriften werden initiiert und befördert. Die SPP Internet-Seite wird überarbeitet, fortlaufend aktualisiert und gewartet. Um die Arbeit der Koordinatoren zu unterstützen, werden eine halbe Position eines Wissenschaftlichen Administrators und eine Stelle für einen HALO Nutzerkoordinator beantragt.

Description
The goal of this proposal is the central coordination of the SPP 1294 'Atmospheric and Earth System Research with HALO' (HALO: High Altitude and Long Range Research Aircraft). The project serves the promotion of cooperation and communication among the HALO mission teams and the

individual project participants involved in the SPP. The three coordinators (M. Wendisch, University of Leipzig; J.Curtius, University of Frankfurt am Main; M. Scheinert, Dresden University of Technology) represent the SPP at the DFG, the scientific steering committee of HALO (WLA: Wissenschaftlicher Lenkungsausschuss), the HALO project team of the German Aerospace Center (DLR-FX), and the public. The DFG share of the mission costs will be centrally administered by the University of Leipzig. The funds for measures to promote gender equality are managed, and the training of young researchers is coordinated. Monthly teleconferences of the three coordinators, annual status seminars, and topical workshops will be organized. Special sessions at international conferences and publications of special issues are initiated and pursued. The SPP web page will be revised, continuously updated, and maintained. To support the three coordinators in conducting these tasks, funding of a half-time position of a Scientific Administrator and a HALO User Coordinator is applied for.

Mittelgeber: DFG WE 1900/24-1, Projekt number 179953493 and Projekt number 316646266

Kampagnenantrag für die HALO-(AC)^3 Mission: Arktische Luftmassentransformationen während Warmlufteinschüben und Kaltluftausbrüchen
Umbrella Proposal for the HALO-(AC)^3 Mission: Arctic Air-Mass Transformations During Warm Air Intrusions and Marine Cold Air Outbreaks

Schlagworte: flugzeuggetragene Forschung

Projektleiter: M. Wendisch (m.wendisch@uni-leipzig.de)

Projektmitarbeiter: N.N.

Projektbeginn: 2020
Projektende: 2023

Beschreibung
Das Ziel des Antrages ist die zentrale Koordination des SPP 1294 'Atmosphären- und Erdsystemforschung mit HALO' (HALO: HighAltitude and Long Range Research Aircraft, Hochfliegendes und weitreichendes Forschungsflugzeug). Das Projekt dient der Förderung der Zusammenarbeit und Kommunikation innerhalb der HALO Missionsteams und den individuellen Projektpartnern, die im SPP eingebunden sind. Die drei Koordinatoren (M. Wendisch, Universität Leipzig; J. Curtius, Universität Frankfurt am Main; M. Scheinert, Technische Universität Dresden) vertreten den SPP gegenüber der DFG, dem Wissenschaftlichen Lenkungsausschuss (WLA) für HALO, dem HALO Projektteam des Deutschen Zentrums für Luft- und Raumfahrt (DLR-FX) und der Öffentlichkeit. Der DFG-Anteil an den Missionskosten wird an der Universität Leipzig zentral verwaltet. Die Finanzmittel für Maßnahmen zur Förderung der Gleichstellung werden verwaltet, und die Ausbildung der jungen Wissenschaftler wird koordiniert. Monatliche Telefonkonferenzen der drei Koordinatoren, jährlich Statusseminare und thematische Workshops werden organisiert. Spezielle Sitzungen auf internationalen Konferenzen und Veröffentlichungen von Spezialausgaben in internationalen Zeitschriften werden initiiert und befördert. Die SPP Internet-Seite wird überarbeitet, fortlaufend aktualisiert und gewartet. Um die Arbeit der Koordinatoren zu unterstützen, werden eine halbe Position eines Wissenschaftlichen Administrators und eine Stelle für einen HALO Nutzerkoordinator beantragt.

Description
So far, observations of air-mass transformations in the Arctic have mostly been conducted from a fixed local position. Only few aircraft-based samplings of air-mass properties over a limited regional area have been reported. This Eulerian point of view does not permit the observations of air-mass modifying processes along their meridional pathway, which are required for model validations. Therefore, we propose a quasi-Lagrange approach following air-masses to and from the Arctic to observe the air-mass transformation processes during warm air intrusions and cold air outbreaks, whereby we focus on warm air intrusions, which have been observed much less frequently in the past. This quasi-Lagrange approach requires a long-endurance airborne facility, which may carry the necessary equipment for the observations. HALO with its exceptional endurance and high lifting capacity is most suited for these observations.

Mittelgeber: DFG Projekt number 442647689

Einfluss der Eiskristallform auf den Strahlungseffekt von arktischen Zirren: Messungen und Repräsentation in numerischen Wettervorhersagemodellen
Influence of the ice crystal shape on radiative effects of Arctic cirrus: Observations and representation in numerical weather prediction models

Schlagworte: flugzeuggetragene Messungen, Wolken, Strahlungsantrieb, Zirren

Projektleiter: M. Wendisch (m.wendisch@uni-leipzig.de)

Projektmitarbeiter: Johannes Röttenbacher

Projektbeginn: 2021
Projektende: 2023

Beschreibung
Flugzeuggetragenen Messungen der solaren und thermisch-infraroten atmosphärischen Strahlung sollen verwendet werden, um den Strahlungseffekt von Zirren in hohen Breiten zu quantifizieren und dessen Repräsentation in numerische Wettervorhersagemodellen zu evaluieren. Diese Zielstellung basierend auf den Erkenntnissen des vorangegangenen Projektes, in dem eine hohe Sensitivität des Strahlungsschemas im ECMWF Integrated Forecast System (IFS) bezüglich der Parametrisierung der Strahlungseigenschaften von Eiskristallen nachgewiesen werden konnte. Für arktischen Zirrus muss diese Analyse auf das Strahlungsbudget im thermisch-infraroten Wellenlängenbereich erweitert werden, da in der Arktis (Polarnacht), die solare Strahlung einen geringen bis nicht-vorhanden Anteil am Energiebuget ausmacht. Das Projekt ist in den HALO Missionen Cirrus-HL (High Latitude) und HALO-(AC)^3 (ArctiC Amplification: Climate Relevant Atmospheric and SurfaCe Processes, and Feedback Mechanisms) eingebunden. Beide Missionen nutzen das Forschungsflugzeug HALO, um arktische Wolken mit neuesten aktiven und passiven Fernerkundungsmethoden sowie in situ Messungen der Wolkeneigenschaften zu charakterisieren. In diesem Projekt werden Messungen der von den Wolken reflektierten solaren und der emittierten thermisch-infraroten Strahlung durchgeführt. Dazu wird ein neues breitbandiges Radiometersystem, ein spektrales Albedometer und ein abbildendes Infrarotkamera verwendet, um das Strahlungsbudget oberhalb und unterhalb der Zirren zu quantifizieren. Basierend auf

diesen Messungen, wird der Strahlungseffekt der Zirren berechnet und in Abhängigkeit der Wolkeneigenschaften analysiert. Besonders wird hier untersucht, in wie weit sich typisch arktische Randbedingungen wie das reflektierende Meereis und langlebige niedrige Wolken auf den Strahlungseinfluss der Zirren auswirken. Des Weiteren wird untersucht, wie diese Strahlungseffekte von arktischen Zirren in numerischen Wettervorhersagemodellen repräsentiert werden. Dazu werden die im Modell vorhergesagten Strahlungseffekte mit den Messungen verglichen. In mehreren Schritten, werden Strahlungstransfermodellen mit unterschiedlichen Parametrisierungen der Strahlungseigenschaften von Eiskristall verwendet, um die Unsicherheiten in Bezug auf das Strahlungsschema und die prognostizieren Wolkeneigenschaften zu separieren.

Description
Based on the sensitivity of the ECMWF radiation scheme to the parametrization of ice crystal radiative properties observed in the completed project for ice clouds in mid-latitudes, the continuation of the project aims to extends this model evaluation for the radiative effects of cirrus in high-latitudes. For Arctic cirrus, the analysis needs to be extended to the thermal-infrared radiation budget, which dominates due to the lag of solar radiation and depends on cloud altitude, thickness and ice crystal properties. Therefore, the project is embedded in the proposed HALO missions Cirrus-HL (High Latitude) and HALO-$(AC)^3$ (ArctiC Amplification: Climate Relevant Atmospheric and SurfaCe Processes, and Feedback Mechanisms), which both aim to investigate Arctic clouds by state of the art airborne remote sensing (active and passive) and cloud microphysical in situ observations. Within this project, measurements of the cloud-reflected solar and emitted thermal infrared radiance and irradiance with a new broadband radiometer system, a spectral albedometer, and a thermalinfrared imager are proposed to quantify the radiative energy budget above and below Arctic cirrus. Based on the observations, the cirrus radiative effect will be derived and evaluated with respect to its dependence on cloud macrophysical and microphysical properties, and the special Arctic environment (sea ice, persistent low clouds). We will evaluate how well the cirrus and their radiative effects are represented in numerical weather prediction models. The comparison will be performed in the observational space of irradiances and radiances instead of cloud properties. Therefore, the output of the numerical weather prediction (NWP) models will be converted by radiative transfer models into the observed radiation quantities. Operational and experimental radiation schemes will be tested and compared to the observed radiation quantities to identify the reasons of potential differences between model and observation. The airborne observations and the radiative transfer simulations will be used to corroborate the hypothesis: “The radiative effects of Arctic cirrus, which significantly depend on their macrophysical and microphysical properties such as the ice crystal shape, can be used to validate numerical weather prediction models.” To address this hypothesis, the proposed study will focus on five specific science questions: (A) How variable are the radiative effects by Arctic cirrus on different horizontal scales (e.g., contrail cirrus, cirrus in air mass transformation)? (B) How strong the radiative effects depend on the presence of sea ice and low clouds? (C) Do observed ice crystal shapes of Arctic cirrus lead to a significant change of cloud radiative effects? (D) Do NWP models realistically represent the radiative effects of Arctic cirrus? (E) Can we use spectral solar and thermal-infrared radiation measurements to constrain potential uncertainties of NWP models?

Mittelgeber: DFG, SPP 1294, Projekt number 316500630

SFB/Transregio 172 „Arktische Verstärkung“
Zentrale Dienstleistungen, Verwaltung und Koordinierung (Z01)

Central services, administration and coordination (Z01)

Schlagworte: Arktis

Projektleiter:
M. Wendisch (m.wendisch@uni-leipzig.de)
Prof. Dr. Susanne Crewell, Universität zu Köln, Institut für Geophysik und Meteorologie
Prof. Dr. Justus Notholt, Universität Bremen, Institut für Umweltphysik

Projektmitarbeiterin: Dr. Marlen Brückner

Projektbeginn: 2016
Projektende: 2023

Beschreibung
Innerhalb des TR 172 Antrages werden Mittel für die zentrale Koordinierung beantragt. Dieses Teilprojekt dient dazu, die Kooperationen und Kommunikation im Verbund unter den einzelnen wissenschaftlichen Projekten und Clustern zu fördern. Aus diesem Grund werden monatliche Videokonferenzen, halbjährliche Meetings, jährliche wissenschaftliche Konferenzen, als auch spezielle Workshops organisiert und durchgeführt. Die Mittel für Gleichstellungsmaßnahmen werden dazu verwendet um junge Wissenschaftler/innen in Zusammenarbeit mit lokalen Graduiertenschulen zu trainieren. Die internationale Präsenz des TR 172 wird etabliert. Eine Internetseite wird erstellt und implementiert. Die logistische Organisation und wissenschaftliche Planung von intensiven Messkampagnen innerhalb des TR 172 werden durch das Projekt Z01 unterstützt. Öffentlichkeitsarbeit zwischen den verschiedenen Partnern wird organisiert und koordiniert.

Description
Funds for the central coordination of TR 172 are requested within this proposal. The project serves the promotion of cooperation and communication among the individual scientific projects and clusters. Monthly video conferences, biannual general assemblies, annual scientific conferences, as well as topical workshops will be organized and conducted. The funds for measures to promote gender equality are managed the training of young researchers is coordinated, in collaboration with local graduate schools. The international visibility of TR 172 will be fostered. A web page will be set up and maintained. The logistic organization and scientific planning of the extensive observational campaigns within TR 172 will be supported by project Z01. Public outreach activities will be organized and coordinated between the different partners.

Mittelgeber: DFG, TRR 172, Projekt number 268020496

SFB/Transregio 172 „Arktische Verstärkung“
Modul integriertes Graduiertenkolleg (MGK*)
Integrated Research Training Group (MGK*)

Schlagworte: Arktis

Projektleiter:

M. Wendisch (m.wendisch@uni-leipzig.de)
Prof. Dr. Susanne Crewell, Universität zu Köln, Institut für Geophysik und Meteorologie
Prof. Dr. Justus Notholt, Universität Bremen, Institut für Umweltphysik

Projektmitarbeiterin: Dr. Marlen Brückner

Projektbeginn: 2020
Projektende: 2023

Beschreibung
Ziel des Projektes ist es eine Integrated Research Training Group (IRTG) innerhalb von (AC) 3 einzurichten, um junge Forscher (Doktoranden und Postdocs) bei der Entwicklung ihrer wissenschaftlichen Unabhängigkeit zu unterstützen und sie auf den Arbeitsmarkt in Wissenschaft, in verschiedenen Bereichen der Industrie, oder in der wissenschaftlichen Verwaltung vorzubereiten. Das im Rahmen der IRTG geplante Qualifizierungsprogramm wird dazu beitragen, das Wissen und die Fähigkeiten junger Forscher zu vertiefen und ihre Unabhängigkeit zu fördern.

Description
The project will establish an Integrated Research Training Group (IRTG) within (AC)3 to support young researchers (Phd students and Postdocs) in their development of scientific independence, and prepare them for positions in academia, industry, in various fields, or in administration. The qualification programme planned within the IRTG will help to deepen their knowledge and skills of young researchers and promote their independence.

Mittelgeber: DFG, TRR 172, Projekt number 268020496

SFB/Transregio 172 „Arktische Verstärkung“
Fesselballongetragene Messungen des Energiebudgets in der wolkenbedeckten Zentralarktis (A02)
Tethered balloon-borne energy budget measurements in the cloudy central Arctic (A02)

Schlagworte: Arktis, ballongetragene Messungen, Energiebilanz, Strahlungsabkühlung

Projektleiter: M. Wendisch (m.wendisch@uni-leipzig.de)
Dr. Holger Siebert, Leibniz-Institut für Troposphärenforschung e.V. (TROPOS)

Projektmitarbeiter: Michael Lonardi

Projektbeginn: 2016
Projektende: 2023

Beschreibung
Während der Expedition MOSAiC im Frühsommer (April bis Juni) 2020 werden fesselballongetragene Messungen von einer Eisschollenstation analysiert. Basierend auf den gewonnenen Messungen werden wir typische Werte und Profile von Turbulenz, Strahlung, Aerosolpartikeln und wolkenmikrophysikalische Eigenschaften während der Entstehung von stratiformen Grenzschichtwolken in der Zentralarktis sammeln. Wir fokussieren uns hier auf lokale

Aspekte der bewölkten Grenzschicht auf die Arktische Verstärkung, wobei auch entfernte Prozesse wie Advektion berücksichtigt werden.

Description
Tethered balloon-borne measurements from an ice-floe camp during the MOSAiC expedition in early summer (April-June) 2020 will be analysed. On the basis of the collected data we will quantify typical values and profiles of turbulence, radiation, aerosol particle and cloud microphysical properties during the life-time of stratiform ABL clouds in the central Arctic. Here we focus on local aspects of the cloudy ABL on Arctic amplification, although remote processes such as advection will also be considered.

Mittelgeber: DFG, TRR 172, Projekt number 268020496

SFB/Transregio 172 „Arktische Verstärkung“
Einfluss von tiefen Wolken auf die arktische atmosphärische Grenzschichtturbulenz und -Strahlung (A03)
Impact of low-level clouds on Arctic atmospheric boundary layer turbulence and radiation (A03)

Schlagworte: Arktis, flugzeuggetragene Messungen, Energiebilanz, Strahlungsabkühlung

Projektleiter: M. Wendisch (m.wendisch@uni-leipzig.de)
Dr. Christof Lüpkes, Alfred-Wegener-Institut Helmholtz-Zentrum für Polar- und Meeresforschung

Projektmitarbeiter: Sebastian Becker

Projektbeginn: 2016
Projektende: 2023

Beschreibung
Um den Einfluss von atmosphärischen Grenzschichtwolken auf die Arktische Verstärkung zu verstehen, sind detaillierte Studien der wolkenbedingten Prozesse, welche die arktische Grenzschicht und das Energiebudget beeinflussen, unabdingbar. Wir schlagen zwei Hauptziele für die zweite Phase vor. Ersteres bezweckt ein besseres Verständnis des Einflusses der Jahreszeit auf Wolken und deren verbundene Grenzschichtprozesse und das Energiebudget. Zweites Ziel beinhaltet die Untersuchung der Wolken während eines Lagrangeschen Luftmassentransports. Um diese Ziele zu erreichen, werden drei Messkampagnen mit den Polar5/6 Flugzeugen sowie mit HALO (High Altitude and Long Range Research Aircraft) durchgeführt.

Description
To understand the role of atmospheric boundary layer clouds in Arctic amplification, detailed studies of cloud–related processes influencing the ABL and the atmospheric energy budget are indispensable. We propose two major goals for phase II. The first one aims at a better understanding of the seasonal dependence of the cloud impact on the ABL processes and energy budget. The second objective includes to investigate the changing cloud impact during Lagrangian air mass transports. To reach these goals, we will perform three campaigns using the AWI Polar 5/6 aircraft and the High Altitude and Long Range Research Aircraft (HALO).

Mittelgeber: DFG, TRR 172, Projekt number 268020496

SFB/Transregio 172 „Arktische Verstärkung“
Einfluss von Bodenheterogenität auf den Strahlungsantrieb und Ableitung von Aerosol- und Wolkeneigenschaften in der Arktis (C01)
Influence of surface heterogeneity on radiative forcing and retrieval of aerosol and cloud properties in the Arctic (C01)

Schlagworte: Arktis, flugzeuggetragene Messungen, Eis- und Schneealbedo, BRDF

Projektleiter: M. Wendisch (m.wendisch@uni-leipzig.de)
Dr. Georg Heygster (bis 12/2019), Universität Bremen, Institut für Umweltphysik (IUP)
Dr. Marcel Nicolaus (Seit 01/2020), Alfred-Wegener-Institut Helmholtz-Zentrum für Polar- und Meeresforschung
Dr. Gunnar Spreen, (seit 01/2020), Universität Bremen, Institut für Umweltphysik Abteilung für Erdfernerkundung

Projektmitarbeiterin: Dr. Evelyn Jäkel

Projektbeginn: 2016
Projektende: 2023

Beschreibung
Die Bodenheterogenität und zeitliche Entwicklung der Bodeneigenschaften des Arktischen Ozeans beeinflussen den Strahlungsenergietransfer durch die Kopplung von Atmosphäre, Meereis und Ozean im arktischen Klimasystem. Strahlungseffekte durch Interaktionen dieser Komponenten sind nicht gut verstanden, allerdings können sie eine entscheidende Rolle im arktischen Klimasystem spielen. Wir werden Flugzeugmessungen der vorangegangenen Kampagnen ACLOUD, PAMARCMiP, und AFLUX analysieren und neue Messungen während MOSAiC und HALO-(AC) hoch 3 sammeln. Zusätzlich werden wir Satellitendaten (MERIS, Sentinel-3) für unsere Analyse verwenden.

Description
The spatial heterogeneity and temporal evolution of surface properties of the Arctic Ocean influence the radiative energy transfer through the coupled compartments (atmosphere, sea ice, open ocean) of the Arctic climate system. Radiative effects of interactions between these components are not well studied, however, they may play an important role in the Arctic climate system. We will analyse airborne data from the previous ACLOUD, PAMARCMiP, and AFLUX campaigns, and collect new measurements during the planned MOSAiC and HALO-(AC) observations. In addition, we will use satellite data (MERIS, Sentinel-3) in our analysis.

Mittelgeber: DFG, TRR 172, Projekt number 268020496

SFB/Transregio 172 „Arktische Verstärkung“
Charakterisierung von arktischen Mischphasenwolken durch flugzeuggetragene in-situ Messungen und Fernerkundung (B03)

Characterization of Arctic mixed-phase clouds by airborne in-situ measurements and remote sensing (B03)

Schlagworte: Arktis, flugzeuggetragene Messungen, Mischphasenwolken

Projektleiter: Dr. André Ehrlich (a.ehrlich@uni-leipzig.de)
Professor Dr. Susanne Crewell, Universität zu Köln, Institut für Geophysik und Meteorologie
Professor Dr. Andreas Macke, Leibniz-Institut für Troposphärenforschung e.V. (TROPOS)

Projektmitarbeiter: Marcus Klingebiel

Projektbeginn: 2016
Projektende: 2023

Beschreibung
Dieses Teilprojekt kombiniert flugzeuggetragene Fernerkundung der Vertikalsäule und den Strahlungseffekt von Wolken mittels in-situ mikrophysikalischen Messungen von Wolken- und Aerosolpartikeln. Da die vorangegangenen Kampagnen lediglich Momentaufnahmen der arktischen Bedingungen geliefert haben, werden wir diese Messungen mit zwei weiteren Kampagnen ausbauen, um die saisonalen und regionalen Unterschiede von Wolken- und Aerosoleigenschaften und deren Beitrag zur Arktischen Verstärkung systematisch zu untersuchen. Die beobachteten Wolken- und Aerosoleigenschaften werden untereinander verlinkt und für unterschiedliche Aspekte kategorisiert, um Änderungen der Aerosol-Wolken-Wechselwirkung unter verschiedenen Bedingungen zu identifizieren, welche mehr oder weniger häufig bedingt durch die Arktische Verstärkung zu beobachten sind.

Description
We aim to combine airborne remote sensing of the vertical column and the radiative impact of clouds with in–situ microphysical measurements of cloud and aerosol properties. As the completed campaigns represent only a snapshot of Arctic conditions, we aim to extend these measurements by two major campaigns to systematically investigate seasonal and regional differences of cloud and aerosol properties and their contribution to Arctic amplification. The observed cloud and aerosol properties will be linked to each other and categorized for different issues to identify changes of aerosol-cloud interaction under different conditions, which are expected to occur more/less frequently due to Arctic amplification.

Mittelgeber: DFG, TRR 172, Projekt number 268020496

SFB/Transregio 172 „Arktische Verstärkung“
Analyse und Vorhersage des Transports und der Transformation von Arktischen Luftmassen (Warmlufteinschübe und Kaltluftausbrüche)
Analysis and forecast of transport and transformation of Arctic air masses (warm air intrusions, cold air outbreaks)

Schlagworte: Arktis, Luftmassentransport

Projektleiter: Dr. Michael Schäfer (michael.schaefer@uni-leipzig.de)

Projektmitarbeiter: Benjamin Kirbus

Projektbeginn: 2020
Projektende: 2023

Beschreibung
Im Frühjahr 2022 werden Messungen mit dem deutschen Forschungsflugzeug HALO (High Altitude and Long Range Research Aircraft) im Rahmen von HALO- (AC) ³ (www.halo-spp.de) durchgeführt. Ziel sind Fernerkundungsmessungen, um die Auswirkungen von Wolken auf atmosphärische Grenzschichtprozesse und den Energiehaushalt in der Arktis zu untersuchen. Mit HALO wollen wir einen Lagrange-Ansatz verfolgen, um dasselbe Wolkensystem innerhalb von mehreren Tagen zu untersuchen und die Entwicklung der eingebetteten Wolken zu charakterisieren. In diesem Zusammenhang sind Warmlufteinschübe und Kaltluftausbrüche von besonderem Interesse. Sie bleiben in der Regel mehrere Tage bestehen und können große Mengen an Wärme und Feuchtigkeit über große Entfernungen in die Arktis oder aus der Arktis transportieren, wodurch die Wolkenmorphologie auf ihrem Weg beeinflusst wird. Um die Wolkenbildung / -entwicklung entlang solcher Transportwege von Anfang an zu erfassen, müssen Warmlufteinbrüche und Kaltluftausbrüche rechtzeitig vorhergesagt werden. Der Kern dieses Projekts besteht darin, ein Prognosetool zu entwickeln, es während der HALO- (AC) 3-Kampagne anzuwenden und anschließend zu validieren. Darüber hinaus werden die Luftmasseneigenschaften, die Wolkenentwicklung und ihr Einfluss auf die Strahlungseigenschaften analysiert.

Description
In spring 2022 airborne remote sensing in the Arctic will be used to study the cloud impact on atmospheric boundary layer processes and the energy budget. The measurements will be performed using the German research aircraft HALO (High Altitude and Long range research aircraft) within the framework of HALO-(AC)³ (www.halo-spp.de). With HALO, we aim to follow a Lagrangian approach to sample the same cloud system in the course of several days to investigate the embedded cloud evolution. In this regard, warm air intrusions and cold air outbreaks are of special interest. They usually persist for several days and are capable to transport large amounts of heat and moisture over huge distances into the Arctic or out of it, influencing the cloud morphology on its way. To capture the cloud formation/evolution along such transport paths from the very beginning, it is necessary to forecast warm air intrusions and cold air outbreaks in time. The core of this project is to develop a forecast tool, apply it during the HALO-(AC)3 campaign, and to validate it afterwards. Furthermore, the air-mass characteristics, the cloud evolution, and their influence on radiative properties will be evaluated.

Mittelgeber: Universität Leipzig, Doktorandenförderung

SFB/Transregio 172 „Arktische Verstärkung“
Evaluierung der ECMWF und ICON Vorhersagequalität von arktischen Wolkeneigenschaften mit Hilfe von flugzeuggetragenen Messungen
Evaluation of ECMWF and ICON forecast quality of cloud properties using airborne dropsonde and cloud measurements in the Arctic

Schlagworte: Arktis, flugzeuggetragene Messungen, Mischphasenwolken

Projektleiter: Dr. Michael Schäfer (michael.schaefer@uni-leipzig.de)

Projektmitarbeiter: Hanno Müller

Projektbeginn: 2021
Projektende: 2024

Beschreibung
In den letzten Jahren hat sich die Leistung numerischer Wettervorhersagemodelle wie ECMWF oder ICON stetig verbessert. Ihre horizontale und vertikale Auflösung wurde erhöht, während die Unsicherheit ihrer vorhergesagten Parameter und die erforderliche Rechenzeit verringert werden konnten. Daher wurden solche Modelle zu einem wertvollen Instrument, um das Auftreten verschiedener Wolkentypen in bestimmten synoptischen Situationen zu untersuchen, was insbesondere in arktischen Regionen mit spärlichen lokalen Beobachtungen von entscheidender Bedeutung ist. Darüber hinaus helfen die Modelle in wissenschafltich interessante synoptische Situationen zu identifizieren und unterstützen die Planung geeigneter Flugmuster zur Untersuchung von arktischen Wolken. In früheren Kampagnen (ACLOUD, AFLUX oder MOSAiC-ACA) wurden zahlreiche Dropsonden- und Wolkenmessungen (in-situ, Fernerkundung) erfasst. Das Ziel dieses Projekts ist es, diese Daten zu verwenden, um die ECMWF- und ICON-Prognosequalität von Wolkeneigenschaften in der Arktis in unterschiedlichen synoptischen Situationen zu bewerten.
Es sind Profildaten von Temperatur und Luftfeuchtigkeit aus Dropsonde-Messungen zu verwenden, die während mehrerer Forschungsflüge nördlich von Spitzbergen in früheren Kampagnen erfasst wurden. Zusätzliche Kamera-, Radar- und Lidar-Messungen stehen zur Verfügung, um die Wolkensituation während der Flüge zu charakterisieren. Die Ergebnisse sollen zu einer quantitativen Bewertung der Vorhersagequalität von EZMW und ICON führen, die 2022 in weiteren Luftkampagnen wie HALO- (AC) 3 getestet wird.

Description
During the past years, the performance of numerical weather prediction models like ECMWF or ICON improved steadily. Their horizontal and vertical resolution have been increased, while the uncertainty of their predicted parameters and the required computational time could be reduced. Therefore, such models became a valuable tool to investigate the occurrence of different cloud types in specific synoptic situations, which is crucial especially in Arctic regions, where local observations are sparse. Furthermore, in such regions, they help to identify interesting upcoming cloud situations and to design most suited flight patterns for airborne campaigns. During past campaigns (ACLOUD, AFLUX, or MOSAiC-ACA) numerous dropsonde and cloud (in-situ, remote sensing) measurements have been collected. The objective of this project is to use these data to evaluate the ECMWF and ICON forecast quality of cloud properties in the Arctic in different synoptic situation.
Profile data of temperature and humidity from dropsonde measurements shall be used, which were captured during several research flights North of Svalbard during past campaigns. Additional image data, radar, and lidar measurements are available to further characterize the cloud situation during the flights. The results shall lead to a quantitative evaluation of the prediction quality of ECMWF and ICON, which will be tested during further airborne campaigns like HALO-(AC)3 in 2022.

Mittelgeber: Universität Leipzig, Doktorandenförderung

SFB/Transregio 172 „Arktische Verstärkung“
Bestimmung der Variabilität der Abkühlungsraten am Oberrand von arktischen Wolken mit einer flugzeuggetragenen Infrarotkamera und deren Abhängigkeit von Wolkeneigenschaften
Variability of Arctic cloud top cooling as a function of cloud microphysical properties derived from airborne thermal infrared imagery

Schlagworte: Arktis, flugzeuggetragene Messungen, Mischphasenwolken

Projektleiter: Dr. Michael Schäfer (michael.schaefer@uni-leipzig.de)

Projektmitarbeiter: Sophie Rosenburg

Projektbeginn: 2022
Projektende: 2025

Beschreibung
Arktische Wolken weisen eine signifikante Abkühlung an der Wolkenoberkante auf, die Turbulenz- und Mischungsprozesse hervorruft und damit für die lange Lebensdauer arktischer Grenzschichtwolken entscheidend ist. Allerdings weist die Wolkenoberkante in der Regel erhebliche horizontale Inhomogenitäten auf. Diese kleinräumigen Inhomogenitäten können zur Abkühlung der Wolkendecke beitragen, je nachdem, ob sie sich innerhalb, oberhalb oder unterhalb der Temperaturinversion der Wolkendecke befinden. Daher kann die unterschiedliche Abkühlung der Wolkendecke die Inhomogenitäten der Wolkendecke abpuffern oder verstärken. Diese horizontalen kleinräumigen Inhomogenitäten liegen jedoch weit unter der räumlichen Auflösung der meisten Satellitensensoren. Daher werden flugzeuggestützte Beobachtungen analysiert, um den Einfluss räumlicher Wolkeninhomogenitäten auf die Abkühlungsraten der Wolkenoberkante zu quantifizieren.
Ziel dieses Projekts ist die Verwendung einer nach unten gerichteten flugzeuggetragenen thermischen Infrarotkamera zur Untersuchung der Wolkenoberkantentemperatur. Diese soll in hoher räumlicher (< 10 m Pixelgröße) und zeitlicher (100 Hz) Auflösung, sowie in verschiedenen Spektralkanälen gemessen werden. Eine Infrarot-Kamera ist an Bord des High Altitude and Long Range Research Aircraft (HALO) installiert. Mit dieser Kamera wurden während der HALO-(AC)3-Kampagne im März/April 2022 von Kiruna, Schweden, aus erste Messungen in arktischen Regionen durchgeführt. Die beobachtete Wolkentemperatur soll als Funktion der optischen und mikrophysikalischen Wolkeneigenschaften für verschiedene Zustände der Inhomogenität der Wolkendecke bewertet werden. Dazu sind optische und mikrophysikalische Ableitungen der Wolken auf der Grundlage von thermischen Infrarot-Wellenlängen erforderlich. Neben den Messungen werden die notwendigen Daten aus Strahlungstransfersimulationen gewonnen. Zusätzliche Wolkeninformationen werden von Lidar, Radar, abbildenden Spektrometern im solaren Spektralbereich und Breitbandradiometern zur Verfügung stehen.

Description

Arctic clouds are known to possess a significant cloud top cooling, which induces turbulence and entrainment processes and is crucial for the long life time of Arctic boundary layer clouds. However, the cloud top typically shows significant horizontally inhomogeneous structures. These small-scale inhomogeneities may feedback to the cloud top cooling depending on the position within, above or below the cloud top temperature inversion. Therefore, the differential cloud top

cooling may buffer or enhance the cloud top inhomogeneities. However, those horizontal small-scale inhomogeneities are far below the spatial resolution of most of the satellite sensors. Therefore, airborne observations will be analysed to quantify the influence of spatial cloud inhomogeneities on the cloud top cooling.
The aim of this project is to use downward viewing airborne thermal infrared imagery to investigate the cloud top temperature with high spatial (< 10 m pixel size) and temporal (100 Hz) resolution, measured within different spectral channels. The infrared imager is installed on board of the High Altitude and Long Range Research Aircraft (HALO). Using this imager, first airborne measurements in Arctic regions were performed out of Kiruna, Sweden during the HALO-(AC)3 campaign in March/April 2022. The observed cloud top temperature shall be evaluated as a function of the optical and microphysical cloud properties for different states of cloud top inhomogeneity. For this, cloud optical and microphysical retrievals based on thermal infrared wavelengths are required. Besides the measurements, necessary input for the retrievals will be obtained from radiative transfer simulations. Additional cloud information will be available from lidar, radar, imaging spectrometers in the solar spectral range and broadband radiometer.

Mittelgeber: Universität Leipzig, Doktorandenförderung

Fernerkundung und Strahlungsantrieb von Inhomogenen Passatwind-Cumuli
Remote Sensing and Radiative Forcing of Inhomogeneous Trade-Wind Cumuli

Schlagworte: Passatwind-Cumuli, atmosphärische Strahlung, flugzeuggetragene Fernerkundung

Projektleiter: M. Wendisch (m.wendisch@uni-leipzig.de)

Projektmitarbeiterin: Anna Luebke

Projektbeginn: 2019
Projektende: 2024

Beschreibung
Das Hauptziel des Projektes besteht in der Quantifizierung des großskaligen Strahlungsantriebes von flachen Passatwind Cumulus-Wolken als Funktion der makro- und mikrophysikalischen Wolkeneigenschaften, der räumlichen Anordnung der Wolken, und der mesoskaligen Vertikalbewegung. Wir kombinieren makro-, mikrophysikalische und Strahlungseigenschaften von Passatwindwolken, welche von flugzeuggetragenen Fernerkundungsbeobachtungen und in-situ Strahlungsmessungen abgeleitet werden. Diese Messungen werden an Bord von HALO (High Altitude and Long Range Research Aircraft) während der Messkampagne EUREC4A (ElUcidating the Role of Cloud-Circulation Coupling in ClimAte) östlich von Barbados im Februar 2020 gewonnen. Um die relevanten Wolken- und Strahlungsdaten ableiten zu können, werden wir die Instrumentierung von HALO erweitern durch (i) eine multispektrale thermisch-infrarote Kamera, und (ii) auf- und abwärts gerichtete, halbräumliche Breitband-Pyranometer und Pyrgeometer. Die breitbandigen Radiometer werden solare und terrestrische Strahlungsflussdichtemessungen liefern, um den atmosphärischen Strahlungshaushalt in Flughöhe zu quantifizieren. Die thermisch-infrarote Kamera wird die Helligkeitstemperatur in verschiedenen Spektralbändern mit hoher räumlicher (5 Meter) und zeitlicher (20 Hz) Auflösung bestimmen. Diese Geräte wurden noch nicht auf HALO eingesetzt. Deshalb besteht ein wichtiger Teil des vorgeschlagenen Arbeitsplanes in intensiven Tests und Kalibrierungen der neuen Geräte und der Entwicklung von Software zur

Handhabung und Auswertung der Daten. Die thermisch-infrarote Kamera wird verwendet, um Wolkenprodukte abzuleiten. Dies umfasst Felder der Temperatur am Wolkenoberrand, Flüssigwasserpfad und Effektivradien. Die Felder werden statistisch analysiert, um den Bedeckungsgrad, den Grad der Organisation, und die Wolkengrößenverteilung zu erhalten. Die Daten werden mit atmosphärischen Parametern (Temperatur-/Feuchteprofile, Hintergrundaerosol, großskalige Divergenz) korreliert. Die Beobachtungen mit den Breitband-Radiometern werden in Kombination mit den Feldern der Wolkeneigenschaften, die von den Messungen mit der thermisch-infraroten Kamera abgeleitet werden, analysiert. Die Quantifizierung des Wolken-Strahlungsantriebes für unterschiedliche Wolkenbedeckungen sowie Wolkenoberkantentemperaturen wird zeigen, wie empfindlich der Wolken-Strahlungsantrieb im Hinblick auf makroskopische Eigenschaften und die Anordnung der Passatwolken ist. Eine Parametrisierung dieser Empfindlichkeiten hilft bei der Beschreibung von Passatwind-Wolken in numerischen Wettervorhersage- und globalen Klimamodellen.

Description
The core objective of the project is to quantify the large-scale radiative forcing of shallow trade-wind cumuli as a function of the cloud macrophysical and microphysical properties, the cloud spatial organization, and the mesoscale vertical motion. We will combine macrophysical, microphysical, and radiative properties of trade-wind cumuli obtained from airborne remote sensing cloud observations and in situ irradiance measurements aboard the High Altitude and Long Range Research Aircraft (HALO) during the EUcidating the Role of Cloud-Circulation Coupling in ClimAte (EUREC4A) campaign east of Barbados in February 2020.To retrieve the relevant cloud and radiation data, we will extend the instrumentation of HALO by (i) a multi-wavelength thermal infrared (IR) imager, and (ii) pairs of upward and downward looking, hemispheric broadband pyranometers and pyrgeometers. These broadband radiometers will provide solar and terrestrial irradiance measurements to quantify the atmospheric radiation budget at flight level. The thermal IR imager will map the cloud top brightness temperatures at different thermal IR spectral bands with high spatial (5 m) and temporal (20 Hz) resolution. The instruments were not operated on HALO yet. Therefore, a crucial part of the proposed work plan is related to extensive tests and calibrations of the new instruments and developing tools for handling and post processing the data. The thermal IR imager will be used to develop an IR-based cloud product, providing maps of cloud top temperature, cloud liquid water path and cloud effective droplet size. The maps will be analysed statistically to obtain the cloud fraction, degree of clustering, and cloud size distributions. The data will be correlated with atmospheric parameters (temperature/humidity profiles, background aerosol, large-scale divergences). The observations of the broadband radiometers will be analysed in combination with the maps of cloud properties derived from the thermal IR imager. Quantifying the cloud radiative forcing for scenes of trade-wind cumuli with different cloud fraction, degree of clustering, and cloud top temperatures will indicate how sensitive the cloud radiative forcing is with respect to the macroscopic properties and organization of trade-wind cumuli. Parameterizing this sensitivity provides a tool to evaluate the representation of trade-wind cumuli in numerical weather prediction models and global climate models.

Mittelgeber: DFG Projekt Nummer 422897361

EUREC4A Rahmenantrag - Untersuchung der Bedeutung der Koppelung zwischen Wolken und Zirkulation im Klimasystem
EUREC4A mission proposal - Elucidating the Role of Cloud-Circulation Coupling in Climate

Schlagworte: Passatwind-Cumuli, atmosphärische Strahlung, flugzeuggetragene Fernerkundung

Projektleiter: Felix Ament (Univeristät Hamburg), M. Wendisch (m.wendisch@uni-leipzig.de)

Projektmitarbeiterin: Anna Luebke

Projektbeginn: 2019
Projektende: 2022

Beschreibung
Das Project finanziert den univesitären Anteil der Missionskosten der HALO Mission EUcidating the Role of Cloud-Circulation Coupling in ClimAte (EUREC4A) in dem die Universität Leipzig mit einem Einzelprojekt (siehe „Fernerkundung und Strahlungsantrieb von Inhomogenen Passatwind-Cumuli“, DFG Projekt Nummer 422897361) vertreten ist.

Description
The project funds the university part of the mission cost of the HALO mission EUcidating the Role of Cloud-Circulation Coupling in ClimAte (EUREC4A) in which the Leipzig University participates with a research project (see “Remote Sensing and Radiative Forcing of Inhomogeneous Trade-Wind Cumuli” DFG Project Number 422897361).

Mittelgeber: DFG Projekt Nummer 423239633

Anwendung von Eisoberflächen- und Strahlungsdaten in der Luft basierend auf MOSAiC Beobachtungen für Oberflächenalbedoparametrisierungen der zentralen Arktis
Application of airborne ice surface and radiation data based on MOSAiC observations for surface albedo parameterizations of the central Arctic (ALIBABA)

Schlagworte: Arktis, Oberflächenalbedo, hubschraubergetragene Messungen, MOSAiC

Projektleiter: M. Wendisch (m.wendisch@uni-leipzig.de)

Projektmitarbeiter: Tim Sperzel

Projektbeginn: 2021
Projektende: 2024

Beschreibung
Das Ziel des Projekts ALIBABA ist die direkte Anwendung der fluggestützten Strahlungs- und Kameradaten, die mit der Hubschrauber-Schleppsonde „HELiPOD“ während MOSAiC erhoben werden. Damit soll der Einfluss von Wolken-Inhomogenitäten auf die Eigenschaften der Rückstreuung solarer Strahlung von arktischen Eisflächen quantifiziert werden. Es werden verschiedene Skalen von 0.25 km bis 10 km betrachtet, die für regionale Klimamodelle und die horizontale Auflösung von Satelliten charakteristisch sind. Für diese räumlichen Skalen stellen die Oberflächen-Reflexionseigenschaften oft eine Mischung von verschiedenen Oberflächen-Arten dar, wie z.B. offenes Wasser, pures Eis, mit Schnee bedecktes Eis -und Schmelztümpel. Dreidimensionale

(3D) Strahlungstransportsimulationen sollen mit den Messungen der komplexen Oberflächen-Reflexionseigenschaften kombiniert werden. Die Albedo und die direktionale Reflexion der individuellen Oberflächenarten sollen aus den großflächigen Beobachtungen unter Berücksichtigung der von Einstrahlungsänderungen (Wolkenbedeckung, Sonnenstand) abgeleitet werden. Dadurch soll die zeitliche Entwicklung der Reflexionseigen-schaften der verschiedenen Ober-flächenarten über einen längeren Zeitraum dokumentiert werden (MOSAiC-Messungen Mai bis August 2020). Damit können Parametrisierungen der Oberflächen-Albedo für Klimamodelle wie HIRHAM-NAOSIM und ICON evaluiert und verbessert werden.

Description
The aim of the project ALIBABA is the direct application of the airborne radiation and camera data obtained with the helicopter borne meteorological sonde “Helipod” during MOSAiC (Multi-disciplinary drifting Observatory for the Study of Arctic Climate). The data are used to quantify the impact of cloud inhomogeneity on the solar reflection properties of Arctic surfaces on typical spatial scales (0.25 – 10 km) covered by regional climate models and satellite footprint sizes. For such spatial scales, the surface reflection properties may feature a mixture of different surface types such as open water, bare ice, snow covered ice, and melt ponds. Three-dimensional (3D) radiative transfer modeling will be combined with measurements of such complex surface reflection properties. The subtype albedo and directional reflection will be extracted from areal surface observations considering effects of illumination changes (cloud occurrence, solar zenith angle). By that, the temporal evolution of the individual subtypes of reflection properties during the course of MOSAiC (May – August 2020) will be documented. That will help to evaluate and improve the surface albedo parameterization scheme of climate models such as HIRHAM-NAOSIM and ICON.

Mittelgeber: BMBF Projekt Nummer 232101570

Wechselwirkungen zwischen Vegetation und Wolken Klimaextremen und deren Effekte auf die spektrale Albedo und Auswirkungen auf die Energiebilanz
Interactions between vegetation and clouds in climate extrems and their effect on the spectral albedo and the energy budget

Schlagworte: Oberflächenalbedo, Vegetation, Wolken, Strahlungsbilanz

Projektleiter: M. Wendisch (m.wendisch@uni-leipzig.de), Alexandra Weigelt

Projektmitarbeiter: Sudhanshu Shekhar Jha

Projektbeginn: 2022
Projektende: 2024

Beschreibung
Die Oberflächenalbedo moduliert den atmosphärischen Energiehaushalt und bestimmt somit die vertikalen Strömungs-, Energie- und Massenflüsse. Daher modifiziert die Oberflächenalbedo die lokalen und regionalen Auswirkungen der Klimaerwärmung. Über einem Wald und wahrscheinlich auch über anderen biologischen Oberflächen hängt die Oberflächenalbedo hauptsächlich vom

Blattzustand ab, der sich mit der meteorologischen Jahreszeit ändert. Auch extreme Wetter-/Klimaverhältnisse wie Dürren, Überschwemmungen oder Kälteperioden beeinflussen den physiologischen und morphologischen Zustand der Blätter auf kürzeren Zeitskalen. Dies kann sich auf die Oberflächenalbedo auswirken, die wiederum in den atmosphärischen Energiehaushalt zurückfließt. Außerdem hat sich gezeigt, dass sich die Oberflächenalbedo bei bestimmten Oberflächentypen, wie z. B. Schnee, in Abhängigkeit von der Bewölkung ändert. Wenn ein ähnlicher Effekt für die Vegetationsoberflächen nachgewiesen werden könnte, wären die potenziellen Rückkopplungsschleifen zwischen der Vegetation und dem Klima wesentlich komplexer. Als Ausgangspunkt für die Untersuchung dieser Effekte und möglicher Rückkopplungen wurden Langzeitmessungen am Leipziger Auenwaldkran installiert, um die Albedo der Baumkronen unter verschiedenen saisonalen und extremen Wetterbedingungen zu beobachten. Die Messungen an einem festen Standort an der Spitze des Krans umfassen Strahlungsmessungen zur Ableitung der spektralen und breitbandigen Waldalbedo. Die Bewölkung wird mit einer Wolkenkamera erfasst. Das Ziel des Projekts ist es, diese bestehenden Messsysteme zu nutzen, sie anzupassen und zu verbessern. Die Daten werden im Hinblick auf die Identifizierung von Wolken-Albedo-Effekten über dem Wald unter verschiedenen meteorologischen und jahreszeitlichen Bedingungen mit einem aktuellen Schwerpunkt auf Klimaextremen analysiert.

Description
The surface albedo modulates the atmospheric energy budget and, thus, it determines vertical radiation, energy, and mass fluxes. Therefore, the surface albedo modifies the local and regional effects of climate warming. Over a forest canopy (and probably other biological surface types), the surface albedo mainly depends on the leaf state, which changes with meteorological season. Also extreme weather/climate conditions such as droughts, floods or cold spells influence the physiological and morphological state of leaves on shorter time scales. This can affect surface albedo, which in turn feeds back to the atmospheric energy budget. Furthermore, for certain surface types, such as snow, it has been shown that the surface albedo changes as a function of cloud cover. If a similar effect could be demonstrated over plant canopy surfaces, potential feedback loops between canopy surfaces and climate would be much more complex. As a starting point to investigate these effects and possible feedbacks, long-term measurements have been installed at the Leipzig floodplain crane to observe the forest canopy albedo under different seasonal and extreme weather conditions. The measurements at a fixed location at the top of the crane include radiation observations to derive the spectral and broadband forest albedo. Cloudiness is recorded remotely by sky-viewing cameras. The project aims to use these existing measurement system, adapt and improve it. The data will be analyzed with respect to identify cloud-albedo effects over the forest canopy under different meteorological and seasonal conditions with a topical focus on climate extremes.

Mittelgeber: Universität: Anstoßfinanzierung Breathing Nature

Hochatmosphäre, Christoph Jacobi
Upper Atmosphere

Large-scale dynamical impacts on regional Arctic climate change
Der Einfluss großräumiger Dynamik auf regionale arktische Klimaänderungen

Schlagworte: Arktische Verstärkung, Klimavariabilität

Projektleiter: Prof. Dr. Christoph Jacobi (jacobi @ rz.uni-leipzig.de), Prof. Dr. Johannes Quaas (johannes.quaas @ uni-leipzig.de)

Projektmitarbeiter: Sina Mehrdad

Projektbeginn: 1.1.2016
Projektende: 31.12.2023

Beschreibung
Das Projekt umfasst die Wechselwirkung zwischen der variablen großskaligen Zirkulation und regionalen arktischen Klimaänderungen und der Diagnose der arktischen Verstärkung auf regionaler Skala als Reaktion auf Variationen großskaliger Zirkulation in der Vergangenheit sowie in Klimaszenarien zukünftigen Klimwandels. Es werden hierzu Reanalysedaten und CMIP5-Modellergebnisse herangezogen und eigene Modellsimulationen durchgeführt. Die Kopplung von Troposphäre und Stratosphäre als wichtiger Bestandteil der Variabilität der polaren Atmosphäre wird auch mit numerischen Simulationen untersucht.

Mittelgeber: Deutsche Forschungsgemeinschaft, SFB-Transregio 172

Lokaler Schwerewellenantrieb auf die mittlere Atmosphäre: Bildung, Auswirkungen, und Langzeittrends
Middle atmosphere localized gravity wave forcing: Formation, impact and longterm evolution (MATELO-FILE)

Schlagworte: Schwerewellen, mittlere Atmosphäre, Brewer-Dobson-Zirkulation, Klimawandel

Projektleiter: Prof. Dr. Christoph Jacobi (jacobi @ rz.uni-leipzig.de)

Projektmitarbeiter: Dr. K. Karami

Projektbeginn: 1.5.2021
Projektende: 30.4.2024

Beschreibung

MATELO-FILE beinhaltet die Bestimmung, Analyse und Simulation von Schwerpunkten stratosphärischer Schwerewellenaktivität sowie deren Auswirkungen auf die Dynamik der mittleren Atmosphäre. Zu diesem Zweck werden die relevanten Regionen auf Basis von Beobachtungs-, Reanalyse- und Modelldaten identifiziert, indem Schwerewellenparameter sowie die Hintergrundzirkulation untersucht werden. Aus diesen Analysen werden die Auslöser der erhöhten Schwerewellenaktivität sowie meteorologische Bedingungen, die solche Schwerpunkte hervorrufen, abgeleitet. Darauf aufbauend wird mit Hilfe mehrjähriger Zeitreihen aus ERA5 und CMIP6-Datensätzen untersucht, ob sich die Aktivität solcher Schwerpunktregionen verändert hat. Um die Wechselwirkung von lokal verstärkter Schwerewellenaktivität mit der Zirkulation der mittleren Atmosphäre zu untersuchen, was die Anregung atmosphärischer Wellen sowie mögliche Kompensationsmechanismen umfasst, werden Experimente mit dem UA-ICON GCM sowie einem weiteren mechanistischen Zirkulationsmodell durchgeführt. Derartige Herangehensweisen ermöglichen es zu untersuchen, (i) wie Bereiche verstärkter Schwerewellenaktivität in Klimamodellen reproduziert werden, (ii) was der Einfluss von Schwerewellen auf die Zirkulation ist und (iii) wie diese sich in einem sich ändernden Klima anpassen. Das Projekt ist eine Kooperation zwischen dem LIM und dem Department Atmosphärenphysik, Karls-Universität Prag.

Description
The MATELO-FILE project focuses on the detection, analysis, and modelling of stratospheric gravity wave (GW) hotspots and their effect on the dynamics of the middle atmosphere. To this end, we will identify GW hotspots on the basis of observations, reanalysis data and model output by analysing different GW parameters, and also background conditions. From these analyses we will deduce possible GW sources as well as meteorological conditions that favour the generation of GW hotspots. Based on these results fromthe datasets partly covering several decades, we will also investigate the temporal development of these GW hotspots to investigatein how far the GW hotspot activity has changed during the last decades. To analysethe interactionprocessesof these GW hotspots with the circulation of the middle atmosphere (the wave forcing itself as well as a compensation mechanism), experiments with the UA-ICON global circulation model and a further mechanistic circulation modelwill be performed. This will enable us toinvestigate (i) how the GW hotspots and their effects are reproduced in climate models, (ii) their influence on circulation changes in a changing climate, and (iii) how they react on a changing climate. The project is a cooperation between LIM and the Department of Atmospheric Physics, Charles University in Prague.

Mittelgeber: Deutsche Forschungsgemeinschaft (DFG JA 836/47-1)

Verzögerte Antwort der Ionosphäre auf Variationen des solaren EUV II (DRIVAR II)
Delayed response of the ionosphere to solar EUV variability II (DRIVAR II)

Schlagworte: Ionosphäre, solare Variabilität

Projektleiter: Prof. Dr. Christoph Jacobi (jacobi @ rz.uni-leipzig.de)

Projektmitarbeiter: R. Vaishnav

Projektbeginn: 1.5.2022
Projektende: 30.04.2025

Beschreibung

Die Variabilität der oberen Atmosphäre der Erde wird durch die Schwankungen in der Absorption solarer UV- und EUV-Strahlung die Ionosphäre hervorgerufen. Dabei tritt jedoch eine Verzögerung auf, die durch das Zusammenspiel verschiedener physikalischer und chemischer Prozesse verursacht wird. So haben die bestimmenden Ionisations- und Rekombinationsprozesse in den verschiedenen Schichten der Ionosphäre, aber auch Transportprozesse einen entscheidenden Einfluss. Die Rolle dieser Prozesse wurde in verschiedenen Studien untersucht, jedoch haben sich diese Analysen bisher nur mit einzelnen Aspekten der Verzögerung beschäftigt. Im Projekt DRIVAR II werden jene Aspekte der Verzögerung untersucht werden, die bisher nicht in Studien aufgenommen wurden. Dies beinhaltet die Variation der Verzögerung in hohen und niedrigen Breiten und die Rolle von Kopplungsprozessen zwischen Thermosphäre und Ionosphäre. Aufbauend auf diesen Ergebnissen und vorangegangenen Studien wird im Rahmen des Projektes eine globale Beschreibung der Verzögerung bereitgestellt. Die Analyse wird dabei einerseits auf etablierten Datensätzen (z.B. SDO-EVE, GOES, GUVI, Ionosonde oder TEC-Karten) aufbauen, aber andererseits auch neue Daten berücksichtigen (z.B. GOLD und ICON). Diese Vielzahl an solaren, thermosphärischen und ionosphärischen Parametern wird eine detaillierte Beschreibung der ionosphärischen Verzögerung ermöglichen. Hinzu kommen Modelluntersuchungen mit dem Coupled Thermosphere Ionosphere Plasmasphere Electrodynamics (CTIPe) Modell und dem Thermosphere-Ionosphere- Electrodynamics General Circulation (TIE-GCM) Modell. Die Untersuchungen mithilfe dieser Modelle werden die verantwortlichen Prozesse ionosphärischer Variabilität zu bestimmen. Mit den Ergebnissen der Untersuchungen sollen dann ggf. auch Vorschläge für die Optimierung dieser Modelle formuliert werden und empirische Modelle ergänzt werden. Mit dem DRIVAR-II-Projekt werden die ionosphärischen und thermosphärischen Prozesse, welche die verzögerte Reaktion der Ionosphäre bestimmen umfassender und genauer analysiert. Diese Untersuchungen werden auch das generelle Verständnis von Prozessen in der oberen Atmosphäre verbessern und sind für das Vorhersagen von ionosphärischen Bedingungen interessant. Das Projekt ist eine Kooperation zwischen dem Institut für Solar-Terrestrische Physik in Neustrelitz und dem Institut für Meteorologie der Universität Leipzig.

Description

In Earth’s upper atmosphere, the absorption of solar UV and EUV radiation causes the creation of the ionosphere, which varies following the variations of solar radiation at these wavelengths of the solar spectrum. However, a delay occurs between these variations caused by the interaction of various physical and chemical processes. Especially the different ionization and recombination processes in the layers of the ionosphere but also transport processes have a significant influence on the delay. The role of these processes has been investigated in various studies, but so far these analyses have only studied separate aspects of the delay. The DRIVAR II project will investigate the aspects of the delay that have not been included in studies so far. This includes the variation of the delay at high and low latitudes or the role of coupling processes between thermosphere and ionosphere. Based on these results and previous studies, the project will provide a global and 3-dimensional description of the delay. The analysis will be based on established data sets (e.g., SDO-EVE, GOES, GUVI, radiation and Ionosonde data, or GNSS TEC maps), but will also consider new data such as GOLD and ICON observations. This variety of solar, thermospheric and ionospheric parameters will allow a detailed description of the delay. In addition, the Coupled Thermosphere Ionosphere Plasmasphere Electrodynamics (CTIPe) model and the Thermosphere-Ionosphere Electrodynamics General Circulation (TIE-GCM) model will be used for more detailed studies defining the processes responsible for the delay. The results of these investigations will then be used to make suggestions for optimizing these models as well as empirical models, if necessary.

DRIVAR II is a joint project of the DLR Institute for Solar-Terrestrial Physics in Neustrelitz (DLR-SO) and the Leipzig Institute for Meteorology (LIM). The DRIVAR II project will provide a more comprehensive and detailed analysis of the ionospheric and thermospheric processes that define the delayed ionospheric response. The studies will also improve the general understanding of processes in the upper atmosphere and are of interest for predicting ionospheric conditions.

Mittelgeber: Deutsche Forschungsgemeinschaft (DFG JA 836/48-1)

Nicht-zonale Strukturen der Dynamik der Mesosphäre/unteren Thermosphäre in mittleren Breiten (NOSTHEM)
Non-zonal Structures of Mesosphere/lower Thermosphere Dynamics at Middle Latitudes (NOSTHEM)

Schlagworte: mittlere Atmosphäre; Radarmessungen

Projektleiter:
Prof. Dr. Christoph Jacobi (jacobi @ rz.uni-leipzig.de)

Projektmitarbeiter: F. Lilienthal, K. Kandieva

Projektbeginn: 1.9.2018
Projektende: 31.12.2022

Beschreibung
In NOSTHEM sollen zonale Unterschiede des mittleren Windes, Gezeitenparameter, planetarer Wellen und Schwerewellen in der Mesosphäre und unteren Thermosphäre untersucht und erklärt werden. Ihr Einfluss auf die Repräsentativität einzelner Messungen für ein zonales Mittel von mittlerem Wind und Wellen wird bestimmt werden. Dies soll eine quantitative Einschätzung der Unsicherheiten von mittlerer Klimatologie, Langzeittrends und Maßen für die Variabilität auf der Basis einzelner Messungen ermöglichen. Der Beitrag nicht-zonaler Strukturen auf die mittlere Zirkulation und ihre Variabilität wird bestimmt. Hemisphärische Analysen von Wellen und Zirkulation in der unteren und mittleren Atmosphäre werden verwendet, um deren Rolle bei der Bildung longitudinaler Unterschiede zu klären. Dies wird auch die Frage beantworten, ob die schon seit langem beobachteten Unterschiede des mesosphärischen Windes über Mittel- und Osteuropa signifikant sind und wenn ja, welche Prozesse zu deren Auftreten beitragen.
In NOSTHEM werden Beobachtungen zweier praktisch identischer VHF-Meteorradare auf ähnlicher geographischer Breite, aber mit 36° Längenunterschied herangezogen. Daher kann daraus der Beitrag nicht-zonaler Strukturen zur lokalen Klimatologie und Variabilität ermittelt werden. Um ein umfassendes hemisphärisches Bild zu erhalten, werden die lokalen Radarmessungen durch Satellitenbeobachtungen und Reanalysedaten ergänzt, sowie numerische Simulationen mit einem Zirkulationsmodell der mittleren Atmosphäre durchgeführt.
Die Hauptziele von NOSTHEM sind (1) eine quantitative Darstellung von Ähnlichkeiten und Unterschieden der mesosphärischen/thermosphärischen Zirkulation an zwei Längengraden, (2) eine Erweiterung dieser Analyse durch hemisphärische Daten und (3) eine Quantifizierung der Rolle von Wellen bei der Ausprägung der Zirkulation an einzelnen Orten. Als Endziel werden nicht-zonale Strukturen und ihre Gründe und die zu ihnen führenden Prozesse geklärt, und auch

Hinweise für die Interpretation von Klimatologie und Variabilität an einzelnen Orten in Bezug auf die gesamthemisphärische Dynamik gegeben.
NOSTHEM wird als Kooperation des Instituts für Meteorologie, Universität Leipzig und des radiophysikalischen Departments, Universität Kasan gemeinsam durchgeführt.

Description
During NOSTHEM, longitudinal differences of mean winds, tidal parameters, and planetary and gravity waves in the mesosphere/lower thermosphere (MLT) will be analyzed and interpreted. The influence of these differences on the representativeness of single sites for describing zonal means of winds and wave parameters will be quantified. This will allow us to quantitatively estimate the uncertainty of mean climatology, long-term trends, and measures of interannual variability observed at single sites. The contribution of non-zonal structures to mean circulation and its variability will be determined. Hemispheric analyses of lower and middle atmosphere waves and circulation parameters will be used to analyze the role of these in establishing longitudinal differences. This will then resolve the question whether there is a significant difference between the mid-latitude MLT wind regimes in Western and Eastern Europe, and which are the underlying processes leading to these differences.
The NOSTHEM project will make use of the two very similar VHF meteor radar observations at similar latitude, but with a 36° difference in longitude in order to specify quantitatively the influence of non-zonal structures on mean circulation, waves and tides. In order to obtain a comprehensive picture of non-zonal structures in the MLT dynamics, the concurrent observations of winds and temperatures using VHF radars at Collm and Kazan will be completed by numerical modeling using a circulation model of the middle atmosphere, satellite observations, and reanalyses.
Main goals of NOSTHEM are (1) a quantitative description of similarities and differences of MLT circulation parameters at two longitudes, (2) an extrapolation of this analysis to the full hemispheric view based on satellite observations and modeling, and (3) a quantitative estimation of the role of waves in the specific characteristic of circulation parameters at single sites. As a final goal, we shall explain longitudinal differences through their underlying processes, and also provide guidelines for the interpretation of both mean climatology and trend analyses made at single sites in terms of their representativeness for hemispheric dynamics.
NOSTHEM is carried out in cooperation between the Institute for Meteorology, Universität Leipzig and the Department of Radiophysics, Institute of Physics, Kazan Federal University, Russian Federation.

Mittelgeber: Deutsche Forschungsgemeinschaft (DFG JA 836/38-1)

Wellenkopplung der mittleren und oberen Atmosphäre: Jahr-zu-Jahr-Variabilität und Langzeittrends (VACILT)
Wave coupling processes of the middle and upper atmosphere: Interannual and long-term variability (VACILT)

Schlagworte: mittlere Atmosphäre; Hochatmosphäre, Langzeittrends

Projektleiter: Prof. Dr. Christoph Jacobi (jacobi @ rz.uni-leipzig.de)

Projektmitarbeiter: A. Kuchar

Projektbeginn: 1.5.2019
Projektende: 31.12.2022

Beschreibung
Die langfristigen Änderungen in der Hochatmosphäre werden durch dynamische Prozesse der darunterliegenden Schichten beeinflusst. Diese meteorologischen Einflüsse werden vor allem durch Wellen hervorgerufen, die sich von der unteren Atmosphäre in die Thermosphäre ausbreiten. Indem sie Energie und Impuls transportieren, modifizieren sie thermosphärische und ionosphärische Parameter. Wellen in der Atmosphäre werden nicht nur vom Zustand der unteren und mittleren Atmosphäre beeinflusst, sondern weisen auch Langzeittrends auf. Daher trägt nicht nur die bekannte Abkühlung durch die Zunahme von Treibhausgasen zu langfristigen Änderungen in der Thermosphäre bei, sondern auch Trends der Wellenaktivität, so dass eine umfassende Beschreibung hochatmosphärischer Variabilität auch Trends der Wellen beinhalten muss.
Um die Auswirkung von Wellen auf die Kopplung von mittlerer und oberer Atmosphäre zu quantifizieren, zielt das Projekt VACILT auf die Beobachtung und Simulation von Wellen, sowie die Quantifizierung ihrer Variabilität und die Analyse ihrer Auswirkungen auf die Thermosphäre. Dazu werden langfristige (> 30 Jahre) Radarbeobachtungen herangezogen und Ergebnissen einer Langzeitsimulation mit dem GAIA-Erdsystemmodell gegenübergestellt, welche wiederum durch Beobachtungen thermosphärischer Parameter gestützt werden.
Die GAIA-Analysen erlauben es, die Auswirkungen atmosphärischer Wellen in der Thermosphäre zu quantifizieren und mit der Variabilität der atmosphärischen Zirkulation in Verbindung zu bringen. Die Ergebnisse werden mit Hilfe von Sensitivitätsstudien unter Verwendung eines mechanistischen Zirkulationsmodells gestützt.
Die Ziele von VACILT sind demnach die folgenden: (1) Quantifizierung der Variabilität der Wellen in der mittleren Atmosphäre auf der Basis von Radarbeobachtungen und GAIA-Analysen (2) quantitative Bestimmung der Auswirkung von Wellenkopplung auf die Hochatmosphäre und (3) die umfassende Analyse des Beitrags von Wellen auf Trends in der Thermosphäre/Ionosphäre, gegenüber dem Beitrag von Treibhausgasen und deren Änderung. Das Erreichen dieser Ziele wird die Rolle von Wellen auf die Thermosphäre/Ionosphäre klären, und hat damit direkte Anwendung z.B. in der Vorhersage der Genauigkeit von Kommunikations-/Navigationssignalen.
VACILT ist ein gemeinsames Projekt der Universität Leipzig mit dem Leibniz-Institut für Atmosphärenphysik, Kühlungsborn und dem Department of Earth and Planetary Sciences, Universität Kyushu, Japan. Damit können die Ressourcen der jeweiligen Partner, nämlich Radarbeobachtungen und mechanistische Modelle auf deutscher, Erdsystemmodellierung und thermosphärischer Satellitenanalysen auf japanischer Seite, optimal kombiniert werden.

Description
The long-term variations of the upper atmosphere are influenced by dynamical processes in the underlying atmosphere. These meteorological influences are mainly due to atmospheric waves propagating from the lower atmosphere to the thermosphere. Transferring energy and momentum, they modify thermospheric and ionospheric parameters. Atmospheric waves not only reflect dynamical features of the lower/middle atmosphere, but also exhibit long-term trends. Consequently, not only the widely known greenhouse gas cooling contributes to thermospheric long-term changes, but atmospheric wave trends also, and a comprehensive description of upper atmosphere trends will have to include this wave variability and trends.

To quantify the effect of lower and middle atmosphere wave coupling on upper atmosphere dynamics, VACILT aims at observing, modeling, and rigorously quantifying interannual and long-term changes of lower and middle atmosphere waves and their effects in the upper atmosphere. To this end, long-term (> 30 years) radar observations will be analyzed with respect to waves and

mean circulation trends. These analyses will be compared with results of a long-term, lower atmosphere driven simulation of the GAIA Earth System Model, which in turn will be supported by the analysis of thermospheric observations.

From the GAIA analyses, the lower atmosphere forcing on the thermosphere due to waves will be quantified. The variability of this forcing will be determined and interpreted in the context of lower atmosphere variability. To substantiate the results, sensitivity experiments with a mechanistic model will be performed.

Main goals of VACILT are (1) a quantitative description of interannual and long-term variability and trends in the middle atmosphere and thermosphere by analyzing the mean circulation and wave parameters from Earth System Model, supported by ground-based and satellite observations. (2) Quantitative estimates of the degree of wave coupling effects in the upper atmosphere . (3) comprehensive analysis of the role of middle-upper atmosphere wave coupling in forcing upper atmosphere long-term trends and variations, in relation to other drivers like greenhouse gas cooling.

Reaching these goals will elucidate the role of waves for the thermosphere/ionosphere and can for example be applied to predicting the accuracy of communication/navigation signals. VACLIT is a joint project between Universität Leipzig and the Leibniz Institute of Atmospheric Physics, Kühlungsborn, Germany and the Department of Earth and Planetary Sciences, University of Kyushu, Japan.

Mittelgeber: Deutsche Forschungsgemeinschaft (DFG JA 836/43-1)

Theoretische Meteorologie; Johannes Quaas
AG Wolken und globales Klima

Probabilistic attribution of extreme precipitation to aerosol perturbations (PATTERA)

Schlagworte: Attribution, Klima-Extremereignisse, Aerosol-Konvektions-Wechselwirkung

Projektleiter:
Koordinator: Andreas Hense, Universität Bonn (ahense@uni-bonn.de)
J. Quaas (johannes.quaas@uni-leipzig.de)

Projektmitarbeiter: Dr. Ribu Cherian (ribu.cherian@uni-leipzig.de)

Projektbeginn: 1.3.2020
Projektende: 28.2.2023

Beschreibung
Der Klimawandel wirkt sich insbesondere über Änderungen in Extermereignissen auf die Gesellschaft aus; hierbei stellen Extremniederschläge und Blitzeinschläge aus hochreichender Konvektion (Gewitter) besondere Gefahren dar. Anthropogene Änderungen der Atmosphärenzusammensetzung können Veränderungen in solchen Ereignissen bewirken. Anders

als Treibhausgase und globale Erwärmung haben Emissionen von Aerosolpartikeln möglicherweise einen unmittelbaren Einfluss auf Konvektion. Das Projekt PATTERA wird (i) die Einflüsse von Aerosolen auf Konvektion, wie sie im ICON-Atmosphärenmodell simuliert werden, evaluieren, wobei vorhandene hochaufgelöste Simulationen, Multi-Modell-Ensembles und bodengebundene Beobachtungen als Referenz genutzt werden. Es wird weiterhin (ii) mit dem Ansatz probabilistischer Ursachenzuordnung (attribution; Ensemblesimulation tatsächlicher und hypothetischer – faktischer und kontrafaktischer – Bedingungen) die Auswirkungen von anthropogenen Aerosolen auf Extremniederschlag und Blitze untersuchen. In einer möglichen zweiten Phase können diese Untersuchungen auf die globale Skala ausgeweitet werden.

Mittelgeber: BMBF

Contrast between hemispheres in aerosol impact on cloud erosion (CHANCE)

Schlagworte: Neuseeland, Aerosol-Wolken-Wechselwirkungen, Hemisphärischer Unterschied

Projektleiter:
Koordinator: J. Quaas (johannes.quaas@uni-leipzig.de)
Gilles Bellon, University of Auckland (gilles.bellon@auckland.ac.nz)

Projektmitarbeiter: Samuel Kwakye (samuel.kwakye@uni-leipzig.de), Alice Henkes (alice.henkes@uni-leipzig.de)

Projektbeginn: 1. 4. 2020
Projektende: 31.12.2022

Beschreibung
Die Frage, wie anthropogene Verschmutzungspartikel, sogenannte Aerosole, Wolken, und dadurch die Energiebilanz des Erdsystems beeinflussen, ist eine der wichtigsten Fragen bezüglich der Physik des Klimawandels. Hierbei spielen vor allem niedrige Wolken eine Rolle, und der wichtigste Wolkentyp bezüglich des Einflusses auf die Strahlung sind Stratokumuluswolken. Besonders interessant und mit besonders großer Unsicherheit behaftet ist dabei, inwiefern Stratokumulus auf einen anfänglichen Anstieg der Wolkentröpfchenkonzentration, Nd, aufgrund der anthropogenen Aerosolemissionen, reagieren (Wolkenanpassungen). Dabei sind zwei gegenläufige Senkenprozesse zu untersuchen: (i) Wolkenauflösung via Niederschlagsbildung – höhere Nd führen zu verzögerter Niederschlagsbildung, längerer Wolkenlebensdauer und damit zu einem stärkeren abkühlenden Effekt der Wolken. (ii) Wolkenauflösung durch turbulente Mischung mit der Umgebung und Tröpfchenverdunstung. Bei höhrerer Nd verdunsten die Tröpfchen durch größeres Oberfläche-Volumen-Verhältnis schneller – der gegenteilige Effekt. CHANCE baut auf neuen, komplementären Entwicklungen in Neuseeland und Deutschland auf: Neue Ansätze für die Darstellung und Untersuchung des Wolkenlebenszyklus anhand von hochaufgelösten Modelle (Auckland/NZ) sowie die führende universitäre Rolle in den Entwicklungen des ICON-Atmosphärenmodells (Leipzig/D). Dies ermöglicht wolkenauflösende – mit realistischer Darstellung der Wolkensenkenprozesse – bis globale Simulationen. CHANCE verbindet die Modellierung mit eingehenden Analysen von Beobachtungsdaten insbesondere von Satelliten und wird Stratokumulus für eine große Bandbreite an Wetterbedingungen und Aerosolkonzentrationen in den beiden unterschiedlichen Hemisphären simulieren; die beiden Wolkenauflösungsprozesse eingehend analysieren; die

Modelle prozessorientiert mit Satellitendaten evaluieren und damit Modellverbesserungen vorschlagen; und schließlich den Aerosol-Wolken-Strahlungsantrieb quantifizieren.

Mittelgeber: BMBF

---

innovative MachIne leaRning to constrain Aerosol-cloud CLimate Impacts (iMIRACLI)

Schlagworte: Aerosol-Wolken-Wechselwirkungen, Maschinelles Lernen, Datenwissenschaften

Projektleiter:
Koordinator: Philip Stier, Universität Oxford (philip.stier@physics.ox.ac.uk)
J. Quaas (johannes.quaas@uni-leipzig.de)

Projektmitarbeiter: Jessenia Gonzalez Villarreal (jessenia.gonzalezv@uni-leipzig.de)
Julien Lenhardt (julien.lenhardt@uni-leipzig.de)

Projektbeginn: 1.1.2020
Projektende: 31.12.2023 verlängert bis 30.6.2024

Beschreibung
Climate change is one of the most urgent problems facing mankind. Implementation of the Paris climate agreement relies on robust scientific evidence. Yet, the uncertainty of non-greenhouse gas forcing associated with aerosol-cloud interactions limits our constraints on climate sensitivity. Radically new ideas are required. While the majority of radiative forcing estimates are model based, model uncertainties remain too large to achieve the required uncertainty reductions. The quantification of aerosol cloud climate interactions in Earth Observation data is thus one of the major challenges of climate science. Progress has been hampered by i) the difficulty to disentangle aerosol effects on clouds and climate from their covariability with confounding factors, ii) retrieval issues, iii) a very low signal-to-noise ratio and on the other hand computationally, due to the scale of the “big” datasets (100s of Tb) and their heterogeneity.
Such “big data” challenges are not unique to climate science but occur across a wide range of data sciences. However, innovative techniques and tools developed by the data mining and machine learning community have not yet found their way into climate sciences and climate scientists are currently not trained to capitalise on these advances.
This Marie Curie ITN will train the next generation of climate & data scientists through synergies between climate research and modern data sciences. Its innovative training plan will match students (and supervisors) from climate and data backgrounds, provide them with training in state of the art data and climate science techniques which will be applied to key uncertainties in current climate research. Partners from the data-science and space industry will be closely involved in the projects and provide real-world training opportunities in a commercial context. This will produce a new generation of climate and data scientists, ideally trained for employment in science or commercial data applications.

Mittelgeber: Europäische Union, Horizon 2020, Marie Curie Innovative Training Network

---

Advancing the Science for Aviation and ClimAte (ACACIA)

Schlagworte: Einfluss von Flugverkehr auf Klima, Aerosol – Wolken – Wechselwirkungen, Kondensstreifen

Projektleiter:
Koordinator: Robert Sausen, Deutsches Zentrum für Luft- und Raumfahrt, Institut für Physik der Atmosphäre (Robert.Sausen@dlr.de)
J. Quaas (johannes.quaas@uni-leipzig.de)

Projektmitarbeiterin: Sajedeh Marjani (sajedeh.marjani@uni-leipzig.de)

Projektbeginn: 1.1.2020
Projektende: 31.12.2023

Beschreibung
Non-CO2 emissions of aviation may impact climate as much as aviation's carbon dioxide (CO2) emissions do. However, the impact the non-CO2 effects (e.g., ozone and methane from NOx emissions, contrails, indirect aerosol effects) is associated with much larger uncertainties, some of these effects might result in a relatively large cooling. ACACIA has four aims for scientifically based and internationally harmonised policies and regulations for a more climate-friendly aviation system. (1) We will improve scientific understanding of those impacts that have the largest uncertainty, in particular, the indirect effect of aviation soot and aerosol on clouds. (2) We will identify needs for international measurement campaigns to constrain our numerical models and theories with data and we will formulate several design options for such campaigns. (3) Putting all aviation effects on a common scale will allow providing an updated climate impact assessment. Uncertainties will be treated in a transparent way, such that trade-offs between different mitigation strategies can be evaluated explicitly. This helps our final aim (4) to provide the knowledge basis and strategic guidance for future implementation of mitigation options, giving robust recommendations for no-regret strategies for achieving reduced climate impact of aviation. To this end, ACACIA brings together research across scales (from plume to global scale), from the laboratory experiments to global models, and it proceeds from fundamental physics and chemistry to the provision of recommendations for policy, regulatory bodies, and other stakeholders in the aviation business. Additionally, ACACIA will cooperate with international partners, both research institutions and organisations.

Mittelgeber: Europäische Union, Horizon2020

Modellierung von Aerosolen und Aerosol-Wolken-Wechselwirkungen in der Arktis (D02)
Modelling aerosols and aerosol-cloud interactions in the Arctic (D02)

Schlagworte: Arktischer Klimawandel, Aerosol-Wolken-Wechselwirkungen, Modellierung

Projektleiter: Johannes Quaas, Universität Leipzig (johannes.quaas@uni-leipzig.de)

Projektmitarbeiterin: Iris Papakonstantinou-Presvelou (i.presvelou@uni-leipzig.de)

Projektbeginn: 1.1.2016
Projektende: 31.12.2023

Beschreibung
In diesem Beitrag zum SFB/Transregio (AC)³ soll mit Hilfe von globaler Modellierung in Kombination mit verschiedenen Beobachtungen der Einfluss anthropogener Aerosole auf den arktischen Klimawandel untersucht werden. In Kooperation mit dem Leibniz-Institut für Troposphärenforschung liegt hierbei der Schwerpunkt auf dem Meridionaltransport der Aerosole (TROPOS) und der Wechselwirkung von Aerosol mit Wolken (LIM).

Mittelgeber: Deutsche Forschungsgemeinschaft (DFG) TRR 172 (AC)³

Arktische Rückkopplungsprozesse in Klimamodellen (E01)
Assessment of Arctic feedback processes in climate models (E01)

Schlagworte: Arktischer Klimawandel, Feedbacks, Modellierung

Projektleiter: Johannes Quaas, Universität Leipzig (johannes.quaas@uni-leipzig.de)

Projektmitarbeiterin: Olivia Linke (olivia.linke@uni-leipzig.de)

Projektbeginn: 1.1.2016
Projektende: 31.12.2023

Beschreibung
In diesem Beitrag zum SFB/Transregio (AC)³ sollen mit Hilfe von globaler Modellierung in Kombination mit verschiedenen Beobachtungen die verschiedenen Klima-Feedback-Mechanismen quantifiziert und in den Klimamodellen evaluiert werden. Spezielles Augenmerk ist hierbei in Kooperation mit der Uni Köln auf dem Wolken-Feedback.

Mittelgeber: Deutsche Forschungsgemeinschaft (DFG) TRR 172 (AC)³

Atmosphären-Modelldaten: Datenqualität, Kurationskriterien und DOI-Branding
Atmospheric model data: data quality, curation criteria, and doi-branding

Projektleiter: Prof. Dr. Johannes Quaas (johannes.quaas@uni-leipzig.de)

Projektmitarbeiter: Dr. Jan Kretzschmar (jan.kretzschmar@uni-leipzig.de)

Projektbeginn: 1.6.2019
Projektende: 31.05.2022

Beschreibung
Der Austausch und die Interpretation von Klimamodelldaten sind weit über die Klimaforschungsgemeinschaft hinaus von Bedeutung, werden jedoch aktuell durch das Fehlen

übergreifender qualitätssichernder Maßnahmen und abgestimmter Kurationskriterien erschwert. In der Meteorologie und Klimaforschung bereits etablierte Datenqualitäts- und Datenkurationsstandards zur Gewährleistung effektiver Teil- und Nachnutzbarkeit der Forschungsdaten finden primär in großen, international koordinierten Modellvergleichsstudien (MIPs, z.B. Coupled Model Intercomparison Project - CMIP) ihre Anwendung. In diesem Vorhaben werden diese auf CMIP fußenden Standards und Konventionen im Austausch mit den Fachcommunities systematisch in weiteren Bereichen der Meteorologie und Klimaforschung angepasst: Zum einen an die Bedürfnisse kleinerer MIPs, für die eine volle CMIP-Adaptierung nicht sinnvoll erscheint und zu aufwändig ist. Zum anderen in der Stadtklimaforschung mit ihren sehr hochauflösenden Daten, einem Forschungsbereich ohne etablierten Datenstandard. Die Ergebnisse werden in der Praxis auf existierende Atmosphärenmodelldaten angewendet (Datenaufbereitung sowie Langzeitarchivierung) und auf ihre universelle Nutzbarkeit hin evaluiert. Die Ergebnisse etablieren zudem auf weitere Bereiche der Klimaforschung anwendbare Blaupausen für Kurationskriterien und Standardisierungen, die eine Reproduzierbarkeit und Prüfbarkeit signifikant erhöhen und darüber hinaus eine interdisziplinäre Nachnutzung von Klimamodelldaten unterstützen. Darüber hinaus wird, um Nachnutzern die Auswahl von Forschungsdaten zu erleichtern, zum einen eine fachspezifische Erweiterung des DataCite Metadatenschemas vorgenommen. Eine zwingend mit einem DOI-Branding verbundene, für Nutzer deutlich sichtbare, anspruchsvollere Qualitätsprüfung für disziplinspezifische Daten und Kurationsprozesse stärkt die Wertigkeit der DataCite DOIs und erhöht das Vertrauen bei der Nachnutzung. Zum anderen wird im Sinne der FAIR-Prinzipien ein maschinenlesbares Fachvokabular auf Basis von DCAT (W3C Data Catalog Vocabulary) bereitgestellt. Eine nachhaltige Anwendung des universellen Datenstandards, der Prozesse zur Kuratierung und Qualitätssicherung sowie auch die Vergabe fachspezifischer DataCite DOI's werden durch die Angebote der beiden beteiligten Infrastrukturdienstleister dauerhaft gesichert und die Etablierung über den Bereich der Meteorologie und Klimaforschung hinaus ermöglicht. Die Verbindung von national und international stark vernetzten Partnern aus der Klimaforschung (Universität Hamburg, Universität Leipzig) mit einem Infrastrukturbetreiber aus der Klimaforschung (DKRZ) sowie der Zentralen Fachbibliothek für Technik und Naturwissenschaften (TIB) im AtMoDat-Konsortium bürgt für eine hochwertige, alle Aspekte dieses Vorhabens abdeckende Kompetenz und eine weitreichende, nachhaltige Aufnahme der Ergebnisse in diesem Forschungsgebiet. AtMoDat ist darüber hinaus fachübergreifend Impulsgeber für Verbesserungen im Forschungsdatenmanagement.

Mittelgeber: BMBF Bundesministerium für Bildung und Forschung, 16QK02B

Besser bestimmes Aerosolforcing für verbesserte Klimaprojektionen (FORCES)
Constrained aerosol forcing for improved climate projections (FORCES)

Projektleiter: Prof. Dr. Johannes Quaas (johannes.quaas@uni-leipzig.de)

Projektmitarbeiter: Dr. Dipu Sudhakar (dipu.sudhakar@uni-leipzig.de)
Enrico Metzner (enrico.metzner@uni-leipzig.de)
Iris Papakonstantinou-Presvelou (iris.presvelou@uni-leipzig.de)

Projektbeginn: 1.10.2019
Projektende: 28.02.2024

Beschreibung
FORCES strebt eine bessere Quantifikation des Klimaantriebs durch Aerosole an, mit dem Ziel, Klimavorhersagen zu verbessern.

Description
FORCES aims at constraining the aerosol-climate forcing in order to improve climate projections.

Mittelgeber: Europäische Union

Besser bestimmte Unsicherheit für multi-dekadische Klimavorhersagen (CONSTRAIN)
Constraining uncertainty of multi decadal climate projections (CONSTRAIN)

Projektleiter: Prof. Dr. Johannes Quaas (johannes.quaas@uni-leipzig.de)
Projektmitarbeiterin: Dr. Karoline Block (karoline.block@uni-leipzig.de)
Olivia Linke (olivia.linke@uni-leipzig.de)

Projektbeginn: 1.6.2019
Projektende: 30.05.2023

Beschreibung
Verschiedene unsichere Aspekte in multi-dekadischen Klimavorhersagen werden in CONSTRAIN besser bestimmt, darunter effektiver Strahlungsantrieb und transiente Klimasensitivität.

Description
Several uncertain aspects for multi-decadal climate projections will be constrained in CONSTRAIN, among which the effective radiative forcing and transient climate sensitivity.

Mittelgeber: Europäische Union

FOR 2820 Teilprojekt: Einfluss von Vulkanen auf Wolken (VolCloud)
FOR 2820 Teilprojekt: Cloud response to Volcanic eruptions (VolCloud)

Projektleiter: Prof. Dr. Johannes Quaas (johannes.quaas@uni-leipzig.de)
Projektmitarbeiterin: Mahnoosh Haghighatnasab (mahnoosh.haghighatnasab@uni-leipzig.de)

Projektbeginn: 1.3.2019
Projektende: 30.11.2022 (verlängert bis 30.11. 2022)

Beschreibung
Wolken spielen eine Schlüsselrolle für die Energiebilanz der Erde. Sie reagieren auf Änderungen in Aerosolen auf verschiedene Weise, und diese Reaktionen sind jeweils einerseits mit großen Unsicherheiten behaftet und andererseits potentiell sehr relevant in ihrer Auswirkung auf Energiebilanz und Klima. (i) Flüssigwasserwolken werden von Aerosol, das als Wolkenkondensationskeim (CCN) dient, verändert. Die Tröpfchenkonzentration wird vergrößert, und dies hat Veränderungen von mikrophysikalischen Wolken- und Niederschlagsprozessen

einerseits, und Wolkendynamik (etwa das Einmischen von trockener Umgebungsluft) andererseits zur Folge. Hierbei ist es vor allem wichtig, die Änderung von Bedeckungsgrad und Flüssigwasserweg der Wolken zu quantifizieren. (ii) Eis- und Mischphasenwolken werden, je nach Eisbildungsmechanismus, durch CCN, aber auch Eiskeime verändert. Veränderungen der komplexen Wolken- und Niederschlagsprozesse sind die Folge. (iii) Die Störung der Energiebilanz bedeutet Änderungen in thermodynamischen Profilen und Zirkulation durch schnelle Anpassungen, auf die Wolken wiederum reagieren. Es ist die Summe aus den ursprünglichen Wolkenänderungen und diesen Anpassungen, aus denen sich die effektive Änderung der Strahlungsbilanz zusammensetzt. (iv) Wird hochreichende Konvektion beeinflusst, können Gewitter sich intensivieren, und der Transport zwischen Troposphäre und Stratosphäre kann verändert werden. Dies hat möglicherweise bedeutende Auswirkungen auf die Zirkulation und das Klima. Diese Fragestellungen sind besonders im Kontext von Vulkanausbrüchen relevant: (a) ein Vulkanausbruch bedeutet eine vergleichsweise gut definierte und gegebenenfalls bedeutende Störung des atmosphärischen Aerosols, aus exogener Quelle. Die Beobachtung der Wolkenreaktion auf einen Vulkanausbruch ist daher eine einzigartige Gelegenheit, um Aerosol-Wolken-Niederschlags- Wechselwirkungen zu untersuchen. (b) Die Reaktion der Wolken beeinflusst die Auswirkung des Vulkanausbruchs auf die Strahlung. Es ist daher essentiell, die Wolkenreaktion angemessen zu quantifizieren, um die Klimawirkung zu beurteilen. VolCloud geht diese Fragen und Herausforderungen an, indem drei verschiedene Typen von Vulkanausbrüchen in der Vergangenheit untersucht werden (eine massive Änderung des troposphärischen Sulfats durch den Holuhraun; eine Eruption, die auch Eiskeime emittiert hat, von Eyjafjallajökull; sowie die größte von Satelliten beobachtete Eruption, Mt. Pinatubo). Hierbei werden Modellsimulationen mit detaillierter Darstellung von Wolken und Aerosol mit Wolkensystem-auflösender Diskretisierung (ICON-NWP-ART, 2 km Auflösung) in Kombination mit Satellitebeobachtung aus passiver und – soweit verfügbar – aktiver Fernerkundung. VolCloud arbeitet eng mit den anderen VolImpact-Projekten zusammen, wobei insbesondere die Möglichkeiten der höheraufgelösten, aber beschränkteren Simulationen einerseits und der gröber aufgelösten, aber globalen Simulationen einerseits ausgewertet werden.

Description

Clouds are a key modulator of the Earth energy budget. They respond to perturbations in aerosol in various ways, and all these pathways are uncertain yet of potentially very large importance when assessing the impact of the aerosol perturbation on the Earth energy budget and on climate. (i) Liquid-water clouds respond to the perturbation in aerosols serving as cloud condensation nuclei (CCN). Cloud droplet number concentration is perturbed, and this entails perturbations to cloud- and precipitation microphysical processes, but also to cloud dynamics responses (e.g. altered entrainment rates of dry air into the clouds). The most relevant question is how cloud fraction and cloud liquid water paths respond to this perturbation. (ii) Ice- and mixed- phase clouds respond to both CCN and ice nucleating particle concentration changes, depending on the ice formation mechanism. Modifications of intricate cloud and precipitation processes follow. (iii) The change in the energy budget leads to alterations in thermodynamic profiles and in atmospheric circulation via rapid adjustments, and clouds respond to these as well. It is the sum of the initial cloud perturbation and these adjustments that composes the effective perturbation of the Earth energy budget. (iv) When deep convective clouds are altered, thunderstorms may become more intense, and transport from the troposphere into the stratosphere may be altered, with strong consequences for circulation and climate. These questions are particularly relevant when considered in the context of volcanic eruptions for two reasons: (a) the volcanic eruption is a relatively well-defined and occasionally strong perturbation to the atmospheric aerosol concentration that is exogenous to the atmosphere system. The observation of the cloud response

to volcanic eruption thus is a unique opportunity to study the aerosol- cloud-precipitation interactions. (b) the cloud response may strongly modulate, and likely enhance, the radiative impact of a volcanic eruption. It is thus crucial to adequately quantify the cloud response, in order to assess the climate response. VolCloud will address these questions and challenges by investigating three different types of past volcanic eruptions (a massive sulfur perturbation to the troposphere, Holuhraun; an eruptive perturbation that also emitted INP, Eyjafjallajökull; and the largest eruption in the satellite era, Mt. Pinatubo) using model simulations with a detailed cloud and aerosol representation, resolving cloud systems (ICON-NWP-ART at 2 km resolution), in combination with satellite observations from passive and – where available – active remote sensing. VolCloud intensely collaborates with the other projects within VolImpact, reaching out to what can be learned from simulations at finer but in extent more limited, and coarser but global scale.

Mittelgeber: DFG Deutsche Forschungsgemeinschaft ,QU 311/23-1

Klimamodell-PArametrisierungen – Revision mit Hilfe von RAdar (PARA)
Climate model PArameterizations informed by RAdar (PARA)

Projektleiter: Prof. Dr. Johannes Quaas (johannes.quaas@uni-leipzig.de)

Projektmitarbeiterin: Sabine Hörnig (sabine.hoernig@uni-leipzig.de)

Projektbeginn: 1.1.2019
Projektende: 30.06.2022

Beschreibung
Die adäquate Darstellung diabatischer Wolken- und Niederschlagsprozesse ist eine besondere Herausforderung für Klimamodelle, da diese räumlich nicht aufgelösten Prozesse mittels subskaliger Parameterisierungen repräsentiert werden. Diese müssten mit Hilfe von Beobachtungen und/oder prozessauflösenden Simulationen erstellt und evaluiert werden. Radarpolarimetrie liefert die am Besten geeingeten Beobachtungen für die Wolken- und Niederschlagsmikrophysik dank der Ableitung mikrophysikalischer Zustandsgrößen und der Prozesserkennung. In der ersten Phase von PROM wird das Projekt PARA die räumliche Heterogenität des Eiswassergehalts sowie die Niederschlagsbildung über de Eisphase betrachten; in der zweiten Phase wird die Betrachtung von Mischphasenprozessen wie Bereifung, und die Rolle der Variabilität der Partikelanzahlkonzentration hinzukommen. PARA betrachtet dabei mit Hilfe von polarimetrischen Radarbeobachtungen und der Evaluierung und Revision der Parametrisierungen im ICON-Klimamodell die vier Prozesse, die für die Bestimmung von aus der Eisphase gebildeten Niederschlag am Boden relevant sind: (i) die Eisbildung und die räumliche Heterogenität des Eiswassergehalts auf bezüglich des ICON-GCM subskaligen Dimensionen, (ii) die Rolle dieser Variabilität für die Schneebildung durch den Aggregationsprozess, (iii) das Schmelzen von Schnee bei Temperaturen über 0°C, und (iv) die Verdunstung von Regen unterhalb der Schmelzschicht.

Description
An adequate representation of moist diabatic processes in clouds and precipitation in climate models is challenging, because these spatially unresolved processes are subject to sub-grid parameterizations, which must be informed by observations and/or models resolving these

processes. Radar polarimetry provides most suitable observations on cloud and precipitation microphysics via microphysical retrievals and process fingerprints. PARA will focus in Phase I of PROM on ice water content heterogeneity and precipitation generation via the ice phase and concentrate on mixed-phase processes including riming and the role of particle number concentration variability in Phase II. PARA will investigate four processes both by polarimetric radar retrievals and the evaluation and revision of their representation in the ICON general circulation model: (i) ice generation and spatial heteorogeneity of ice water content at ICON-GCM sub-grid scales, (ii) the role of both in snow formation like aggregation, (iii) melting of snow falling through the 0°C isotherm, and (iv) evaporation of rain below the melting layer.

Mittelgeber: DFG Deutsche Forschungsgemeinschaft, QU 311/21-1

Wolkentröpfchenanzahlkonzentration aus mit Atmosphärenmodellierung verbesserten Satellitenbeobachtungen für die Analyse von Aerosol-Wolken-Wechselwirkungen (CDNC4aci)
Cloud Droplet Number Concentration – satellite retrievals Advanced by Atmospheric models for Assessing Aerosol-Cloud Interactions (CDNC4aci)

Projektleiter: Prof. Dr. Johannes Quaas (johannes.quaas@uni-leipzig.de)

Projektmitarbeiter: Dr. Tom Goren (tom.goren@uni-leipzig.de)

Projektbeginn: 1.4.2021
Projektende: 31.3.2024

Beschreibung
Die Wechselwirkungen zwischen Aerosolen und Wolken führen zu einem effektiven Strahlungsantrieb, der eine wesentliche Unsicherheit beim Verständnis und Interpretation des beobachteten Klimawandels darstellt. Es werden globale Daten benötigt, um die relevanten Prozesse besser zu quantifizieren, aber eine Schlüsselgröße - die Konzentration der Wolkentröpfchenzahl (CDNC, Nd) - ist in operationellen Produkten nicht verfügbar. Aufbauend auf Vorarbeiten wird CDNC4aci in enger Wechselwirkung zwischen Beobachtungen und Modellen auf zuverlässige Nd-Werte von Satelliten hinarbeiten: Neu verfügbare wolkenauflösende Simulationen ermöglichen die Entwicklung und Verfeinerung der Retrievals. Diese Daten werden umgekehrt dazu verwendet, das Verständnis und die Quantifizierung der Aerosol-Wolken-Wechselwirkungen im Modell und bei der statistischen Analyse zu verbessern. Konkret wird das Projekt multi-angulare und polarimetrische Beobachtungen für bessere Nd-Daten einbeziehen, es wird die Retrievalansätze unter Verwendung einer modellgestützten vertikalen Wolkenschichtung in Abhängigkeit vom Wolkenregime überarbeiten. Das Projekt wird die Informationen über Wolkenprozesse in den Daten mit Hilfe von Modellsensitivitätsanalysen untersuchen, es wird Modell und Daten durch Vorwärtssimulationen vergleichbar machen und die Aerosol-Wolken-Wechselwirkungen in einem globalen Modell, das unter Verwendung der Daten und des Prozessverständnisses verbessert wird, analysieren. Das Ziel ist eine konsistente Quantifizierung des Aerosol-Wolken-Antriebs zwischen Modell und Datenanalyse.

Description
Aerosol-cloud interactions imply an effective radiative forcing that is a key uncertainty when un-

derstanding and interpreting observed climate change. Global data are needed to better quantify the relevant processes, but a key quantity – the cloud droplet number concentration (CDNC, Nd) - is not available from operational products. Building on preliminary work, CDNC4aci will work towards reliable retrievals of Nd from satellites in close observations – model interaction: newly-available cloud-resolving simulations will inform the retrieval development and refinement, and the data, in turn, will be used to improve understanding and quantification of aerosol-cloud interactions in the model and from statistical analysis. Specifically, the project will include multi-angle and polarimetric observations for better Nd data, it will revise retrieval approaches using model-informed cloud vertical stratification conditioned on cloud regime and thoroughly quantify and correct retrieval errors and biases and assess aerosol-cloud interaction processes from data. The project will assess the cloud-process information in the retrieved data using model sensitivity analyses, it will make model and data comparable by forward-simulating measured polarized radiances and retrieval products, and assess aerosol-cloud interactions in a global model evaluated using the data and the process understanding in model-data assessment. The final goal is a consistent quantification of the aerosol-cloud forcing between model and data analysis.

Mittelgeber: DFG Deutsche Forschungsgemeinschaft, QU 311/27-1

Wolkenänderungen durch die Umkehr des Aerosoltrends über China: Beobachtungsdaten – Modell Synergie von regionaler zu großer Skala (Cloudtrend)
Cloudiness change with aerosol trend reversal over China: data-model synergy from regional to large scale (Cloudtrend)

Projektleiter: Prof. Dr. Johannes Quaas (johannes.quaas@uni-leipzig.de)

Projektmitarbeiterin: Dr. Hailing Jia (hailing.jia@uni-leipzig.de)

Projektbeginn: 1.4.2021
Projektende: 31.3.2024

Beschreibung
Die Reaktion von Wolken auf anthropogene Änderungen der Atmosphärenzusammensetzung stellt eine große Unsicherheit bei der Quantifizierung des globalen Klimawandels dar. Ein sehr wichtiger Aspekt dabei ist die Änderung von Wolken durch Aerosolemissionen. In Bezug auf diese Aerosol-Wolken-Wechselwirkungen hat sich in neuen Studien herausgestellt, dass die wesentliche Unbekannte die Änderung der horizontalen Wolkenausdehnung (Bedeckungsgrad) in Anpassung an Wolkentröpfchenkonzentrationsänderungen ist. Cloudtrend wird das Verständnis und die Quantifizierung dieses Problems substantiell verbessern, indem es auf drei Schlüsselideen aufbaut: (i) die stark ansteigenden und dann abnehmenden anthropogenen Aerosolemissionen über China im 21. Jahrhundert bieten eine einzigartige Gelegenheit für die Detection und Attribution von aerosolabhängigen Wolkenänderungen in Beobachtungsdaten, die für diese Periode in hoher Qualität vom Boden und von Satelliten zur Verfügung stehen; (ii) neue Modellier- und Datenanalysewerkzeuge stehen zur Verfügung, einschließlich verbesserter Satellitendaten für Wolkenmikrophysik und Wolkenregimedefinitionen, sowie die CMIP6 Multi-Modell-Daten; und (iii) die Datenanalyse und Klimamodellierung auf großer Skala kann dank neuer Ansätze aus maschinellem Lernen systematisch von den hochaufgelösten regionalen Daten und Modellen lernen. Das Projekt wird durch die Synergie in der Expertise an der Nanjing University

of Information Science and Technology (Schwerpunkt auf den regionalen Referenzdaten und -modellen) und der Universität Leipzig (Schwerpunkt auf der großen Skala) möglich gemacht.

Description
The response of clouds to anthropogenic changes in atmospheric composition constitutes a large uncertainty when quantifying the effective forcing of global climate change. One key element is the response of clouds to aerosol emissions. In these aerosol-cloud interactions, it emerges currently as the key question how cloud horizontal extent, or cloud fraction, changes in adjustment to cloud droplet number concentration changes. Cloudtrend will substantially improve the understanding and quantification for this problem by building on three key ideas: (i) the very strong increasing then decreasing trends in anthropogenic aerosol emissions over China in the 21st Century provide a unique opportunity for a detection and attribution of aerosol-induced cloudiness changes in the high-quality data available from the surface and from satellites; (ii) new modelling and data analysis tools are available, including better satellite retrievals of cloud microphysics and new regime definitions, as well as the new CMIP6 multi-model data; and (iii) the large-scale data analysis and global climate modelling is proposed to systematically learn from the regional, high-quality data and modelling. The project is possible thanks to the synergy between the expertise in the teams at the Nanjing University of Information Science and Technology (regional focus) and the University of Leipzig (large-scale focus).

Mittelgeber: DFG Deutsche Forschungsgemeinschaft, QU 311/28-1

Wechselwirkung zwischen meridionalen Ozean-Wärmetransporten und regionalen Prozessen im Arktischen Ozean (D04)
Interaction of meridional ocean heat transports and regional processes in the Arctic Ocean (D04)

Projektleiter: Prof. Dr. Rüdiger Gerdes, Alfred-Wegener-Institut, Helmholtz-Zentrum für Polar- und Meeresforschung, Prof Dr. Torsten Kanzow, Alfred-Wegener-Institut, Helmholtz-Zentrum für Polar- und Meeresforschung, Dr. Marc Salzmann (marc.salzmann@uni-leipzig.de)

Projektmitarbeiter: Enrico Paul Metzner (enrico.metzner@uni-leipzig.de), Finn Heukamp, Alfred-Wegener-Institut, Helmholtz-Zentrum für Polar- und Meeresforschung

Projektbeginn: 1.1.2020
Projektende: 31.12.2023

Beschreibung
In diesem Teilprojekt sollen die ozeanischen Prozesse besser verstanden werden, welche die Reaktion des arktischen Klimasystems (insbesondere Wärmeflüsse zwischen Ozean und Atmosphäre) auf die Erwärmung der Atmosphäre aufgrund von Treibhausgasen ausmachen. Hierfür sollen regionale und globale Modelle genutzt sowie existierende Ergebnisse von globalen Klimamodellen analysiert werden. Ein Fokus wird auf der Barentssee liegen, wo starke Oberflächen-Wärmeflüsse den Export von Wasser und Meereis an der Meeresoberfläche fördern. Dieser Export wird durch das entsprechende Einströmen atlantischen Wassers kompensiert, welches den positiven Rückkopplungskreislauf schließt. Diese Prozesse können aufgrund ihres Einflusses auf die Schichtung des Ozeans und der Entstehung Wassers hoher Dichte zur weiteren Erwärmung der Arktis beitragen.

Description
This project investigates the oceanic processes which shape the response of the arctic climate system (especially ocean-atmosphere heat fluxes) to greenhouse gas warming using regional and global climate models and analyzing existing model results. A focus will be on the Barents Sea, where strong surface heat fluxes promote the export of water and sea ice at the surface. This export is compensated by inflow of Atlantic water, closing a positive feedback loop. Due to their influence on the ocean stratification and the formation of high density waters these processes can contribute to increased Arctic warming.

Mittelgeber: DFG Projekt Nummer 423239633

FOR 2820 Teilprojekt: Einfluss von Vulkanen auf Wolken (VolCloud)
FOR 2820 Teilprojekt: Cloud response to Volcanic eruptions (VolCloud)

Projektleiter: Prof. Dr. Johannes Quaas (johannes.quaas@uni-leipzig.de)
Projektmitarbeiterin: Charlotte Lange (charlotte.lange@uni-leipzig.de)

Projektbeginn: 1.10.2022
Projektende: 30.9.2025

Beschreibung
Wolken sind eine Schlüsseldeterminante des Energiehaushalts der Erde. Um die Auswirkungen von Vulkanausbrüchen auf das Klima zu verstehen und zu quantifizieren, ist es daher unerlässlich, die Auswirkungen der in die Troposphäre emittierten Aerosole auf Wolken zu quantifizieren, sowie die Reaktion der Wolken auf Zirkulationsänderungen. Allerdings sind Aerosol-Wolken-Wechselwirkungen auf grundlegender Ebene nicht gut quantifiziert. Das Feld, die Aerosol-Wolken-Wechselwirkungen erforscht, wendet sich nun zunehmend Beobachtungen und Simulationen von Wolken zu, die von vulkanischem Aerosol beeinflusst bzw. unbeeinflusst sind, um Wolkenveränderungen zu erkennen und zuzuordnen. Ein Vulkanausbruch ist ein ideales „natürliches Labor“, da es eine wetterunabhängige Aerosolstörung erzeugt. VolCloud hat somit eine zweifache, iterative Rolle innerhalb von VolImpact: Es verschiebt die Grenzen von Wissen darüber, wie Wolken auf Aerosole reagieren, durch Modell- und Datenanalyse der Reaktion von Wolken zu vulkanischem Aerosol, und es nutzt dieses verbesserte Wissen, um dabei zu helfen, den durch Vulkanausbrüche ausgeübten effektiven Strahlungsantrieb insgesamt zu quantifizieren. Spezifische Ziele in Phase II sind (i) zu lernen, wie Grenzschichtwolken in den (Sub-)Tropen auf Aerosole reagieren, indem die mikrophysikalische und die grenzschichtdynamische Antwort an der untersucht werden, u.a. am Beispiel der Kilauea-Eruption 2020; um (ii) die Reaktion von Eiswolken besser zu verstehen und zu quantifizieren und Mischphasenwolken durch Implementierung und Bewertung neuer Parametrisierungen der Eiskeimbildung für vulkanisches Aerosol und Bewertung der Rolle von semi-direkten Effekten; und um (iii) die Gesamtänderung von Wolkenfeldern zu quantifizieren, indem das Projekt zur VolSeamless-Simulation und ihrer Analyse beiträgt. Diese Arbeit wird in enger Interaktion innerhalb von VolImpact durchgeführt, insbesondere mit VolARC und VolPlume; sowie in internationaler Zusammenarbeit insbesondere mit Gruppen in Großbritannien.

Description:
Clouds are a key determinant of the Earth energy budget. In order to understand and quantify the impact of volcanic eruptions on climate, it is thus imperative to quantify the effects aerosols emitted to the troposphere have on clouds, as well as the cloud response to circulation changes. However, aerosol-cloud interactions are not well quantified at a fundamental level. The community researching aerosol-cloud interactions now increasingly turns to observations and simulations of clouds affected and unaffected by volcanic aerosol to detect and attribute changes. A volcanic eruption is an ideal “natural laboratory”, since it generates an aerosol perturbation that is independent of weather conditions. VolCloud thus has a two-fold, iterative role within VolImpact: it pushes the limits of knowledge on how clouds respond to aerosols by model and data analysis of the response of clouds to volcanic aerosol, and it makes use of this improved knowledge to help quantify the overall effective radiative forcing exerted by volcanic eruptions. Specific targets in phase II are to (i) learn about how boundary-layer clouds in the (sub-)tropics respond to aerosol by studying the microphysical and the boundary-layer-dynamics response at the example of the Kilauea eruption 2020; to (ii) better understand and quantify the response of ice and mixed-phase clouds by implementing and evaluating new ice nucleation parameterisations for volcanic aerosol, and assessing the role of semi-direct effects; and to (iii) quantify the overall cloud response by contributing to the VolSeamless simulation and its analysis. This work is performed in close interaction within VolImpact in the common research projects, and specific cross-project collaboration especially with VolARC and VolPlume; as well as in international collaboration in particular with groups in the UK.

Mittelgeber: DFG Deutsche Forschungsgemeinschaft ,QU 311/23-2

Junior-Professorin Dr. Heike Kalesse-Los

Fernerkundung; Heike Kalesse-Los
AG Fernerkundung der Atmosphäre und das Arktische Klimasystem

---

Bodengebundene Fernerkundung der Atmosphäre zur Verbesserung der Charakterisierung mikrophysikalischer Wolkeneigenschaften sowie der Leistungsprognose erneuerbarer Energien

Ground-based remote sensing of the atmosphere for improving the characterization of microphysical cloud properties and for improving the load prediction of renewable energies

Schlagworte: bodengebundene Fernerkundung, erneuerbare Energien, Wolkenretrieval, DACAPO-PESO, EUREC4A

Projektleiter: H. Kalesse-Los (heike.kalesse@uni-leipzig.de), A. Ehrlich (a.ehrlich@uni-leipzig.de), M. Schäfer (michael.schaefer@uni-leipzig.de), M. Wendisch (m.wendisch@uni-leipzig.de)

Projektmitarbeiter: AP1: M. Lochmann (moritz.lochmann@uni-leipzig.de), AP2: W. Schimmel (willi.schimmel@uni-leipzig.de), AP3: Johannes Stapf (johannes.stapf@uni-leipzig.de) und Teresa Vogl (teresa.vogl@uni-leipzig.de)

Projektbeginn: 1.9.2018
Projektende: 28.2.2022

Beschreibung
Die bodengebundene Fernerkundung der Atmosphäre dient sowohl der Grundlagenforschung von Wolken und Niederschlag, als auch im operationellen Dienst der Wettervorhersage als ein wichtiger Baustein für die Leistungsprognose erneuerbarer Energien. Innerhalb dieses Projekts gibt es zwei Hauptzielstellungen: Zum einen wird analysiert werden, wie künstliche neuronale Netze (KNN) zur Leistungsprognose von Photovoltaik- und Windkraftanlagen optimiert werden können, wenn zusätzliche Daten von Wetterstationen und bodengebundenen Fernerkundungsmessungen implementiert werden. Zum anderen sollen in zwei weiteren Teilprojekten für Wolkenbeobachtungen Ableitungsalgorithmen (Retrievals) weiterentwickelt werden, um die Bestimmung von Wolkeneigenschaften zu verbessern und zu erweitern. Dabei stehen Messgerätesynergien zur Ableitung der Wolkentröpfchenkonzentration sowie die Entwicklung anwendungsspezifischer KNN zur Charakterisierung der Verteilung von Flüssigwasser in Mischphasenwolken im Vordergrund.

Das Projekt ist in drei Arbeitspakete unterteilt:
AP1: Test des Einflusses zusätzlicher Messdaten von Wetterstationen und aus der bodengebundenen Fernerkundung auf die Leistungsprognose von PV- und Windkraft-Anlagen mittels künstlicher Neuronaler Netze (KNN)

AP2: Entwicklung eines auf Wolkenradar- und Lidar basierendem KNN zur Detektion von Flüssigwasser in Wolken

AP3: Entwicklung einer auf synergistischen Fernerkundungsmessungen basierenden Methode zur Ableitung der Wolkentröpfchenkonzentration

Description
Ground-based remote sensing of the atmosphere serves both, the basic research of clouds and precipitation, and in the operational service of weather forecasting as an important building block for the power prognosis of renewable energies. Within this project there are two main objectives: Firstly, it will be analysed how artificial neural networks (ANN) can be optimized for power forecasting of Photovoltaics (PV) and wind turbines, if additional data from weather stations and ground-based remote sensing measurements are implemented. On the other hand, in two further subprojects for cloud observations, retrieval algorithms will be developed to improve and extend the determination of cloud properties. The focus will be on instrument synergies for the derivation of cloud droplet concentrations and the development of application-specific ANN for the characterization of the distribution of liquid water in mixed-phase clouds.

The project is divided into three work packages:
AP1: Testing the influence of additional measurement data from weather stations and ground-based remote sensing on the power prognosis of PV and wind power plants using artificial neural networks (ANN)
AP2: Development of a cloud radar and lidar based ANN for detection of liquid water in clouds
AP3: Development of a cloud droplet concentration retrieval based on synergistic remote sensing observations

Mittelgeber: ESF - Sächsische Aufbaubank (SAB), Antragsnummer: 100339509

PICNICC - Durch CCN und INP beeinflusste Polarimetrie in Zypern und Chile – Abschätzung von hemisphärischen Kontrasten in radarpolarimetrischen Größen und deren Beziehung zu Unterschieden in der Aerosolbelastung
Polarimetry Influenced by CCN aNd INP in Cyprus and Chile (PICNICC):
An assessment of hemispheric cloud polarimetric contrasts and its relation to differences in aerosol load

Schlagworte: Radarpolarimetrie, DACAPO-PESO, Wolkenmikrophysik, Aerosol-Wolken-Wechselwirkung

Projektleiter: H. Kalesse-Los (heike.kalesse@uni-leipzig.de)
Dr. P. Seifert, Leibniz Institut für Troposphärenforschung (TROPOS)

Projektmitarbeiter: Prof. J. Quaas (johannes.quaas@uni-leipzig.de)
Teresa Vogl (teresa.vogl@uni-leipzig.de), A. Teissiere (TROPOS)

Projektbeginn: 1.11.2018
Projektende: 31.12.2023

Beschreibung
Das Verständnis von mikrophysikalischen Wachstumsprozessen in Mischphasenwolken wie Aggregation und Bereifung beruht auf einer gründlichen Charakterisierung der in der Wolke vorhandenen Flüssigphase. In dieser Studie wird eine einzigartige Messmöglichkeit mit einer erweiterten Fernerkundungsinstrumentensuite genutzt, die polarimetrische Radarbeobachtungen bei mehreren Wellenlängen auf der Nord- und Südhalbkugel beinhaltet, um die Millimeterwellenlängen-Radarpolarimetrieforschung für mikrophysikalische Prozessstudien voranzubringen. Die übergeordnete Hypothese, die in diesem Projekt untersucht wird, ist, dass Mischphasen-Wolkenprozesse anfällig für Aerosolstörungen sind. Wir postulieren, dass:
A) Die Aggregation wird bei hohen Aerosolbelastungen und damit verbundenen höheren INP (Ice Nucleating Particle)-Konzentrationen häufiger erfolgen, da höhere Eiskristallkonzentrationen die Aggregation begünstigen.
B) Bereifung von Eiskristallen wird häufiger auftreten, wenn aufgrund einer Knappheit von INP anhaltende unterkühlte Flüssigkeitsschichten auftreten.
Um diese Hypothesen anzugehen, wird die Häufigkeit des Auftretens von Aggregation und Bereifung in mehrjährigen Datensätzen charakterisiert, die bei Feldexperimenten in der Aerosol-Lasten-Atmosphäre über Limassol, Zypern und der unberührten Region Punta Arenas, Chile, erhalten wurden und werden. Die beobachtete Reaktion von Mischphasen-Wolkenprozessen auf Aerosolstörungen wird im Zusammenhang mit einer Modellsensitivitätsstudie von Simulationen mit einer wolkensystemauflösenden (1 km) Version des ICON-NWP für die gesamten Beobachtungszeiträume für regionale Bereiche um die Beobachtungsstandorte in Zypern und Chile gestellt, die von Radar-Fortsimulationen begleitet werden.

Description
Understanding mixed-phase cloud processes such as aggregation and riming relies on a thorough characterization of the liquid phase present in the cloud. For this study we propose to use a unique measurement opportunity with an extended remote-sensing instrument suite including triple-frequency polarimetric radar observations on the Northern and Southern hemisphere to bring forward millimeter wavelength radar polarimetry research for microphysical process studies. The

overarching hypothesis that we would like to study within this project is that mixed-phase cloud processes are susceptible to aerosol perturbations. We postulate that
A) Aggregation will be more frequent for high aerosol loads and associated higher ice nucleating particle (INP) concentrations because higher ice crystal concentrations favor aggregation.
B) Riming will be more frequent where sustained supercooled liquid layers occur due to a scarcity of INP.
To address these hypotheses, we will characterize the frequency of occurrence of aggregation and riming in multi-year datasets obtained during institutional-funded field experiments in the aerosol-burden atmosphere above Limassol, Cyprus and the pristine region of Punta Arenas, Chile. For that purpose, we will make slanted linear depolarization (SLDR) polarimetric observations with a Ka-band radar a versatile technique for classification of hydrometeors in mixed-phase clouds.
The observed response of mixed-phase cloud processes to aerosol perturbations will be put in context to a model sensitivity study of simulations with a cloud-system-resolving (1 km) version of the ICON-NWP for the entire observation periods for regional domains around the observations sites in Cyprus and Chile that are accompanied by radar forward simulations.

Mittelgeber: DFG KA 4162/2-1

Einfluss von Wasserrinnen im Meereis und Polynyas auf arktische Wolkeneigenschaften – B07
(Influence of sea ice leads or polynyas on Arctic cloud properties – B07)

Schlagworte: Arktische Verstärkung, Arktische Wolken, bodengebundene Fernerkundung von Wolken

Projektleiter: H. Kalesse-Los (heike.kalesse@uni-leipzig.de)

Projektmitarbeiter: Pablo Saavedra-Garfias (pablo.saavedra@uni-leipzig.de)

Projektbeginn: 01.01.2020
Projektende: 31.12.2023

Beschreibung
Die winterliche Meereisbedeckung ist charakterisiert durch verschiedenste Brüche unterschiedlichsten Levels. Wasserrinnen und Polynyas führen zu erheblichen Wärme- und Feuchteflüssen vom relativ warmen Ozean zur kalten Atmosphäre. Damit beeinflussen sie die Struktur der atmosphärischen Grenzschicht, Wolkenbedeckung und das Energiebudget an der Oberfläche und ebenfalls den chemischen Austausch zwischen Atmosphäre und Ozean. Um den Einfluss von Meereisrinnen und Polynyas auf Wolken zu quantifizieren, werden mikro- und makrophysikalische Eigenschaften von bodennahen Wolken während auflandigen Winden in Anwesenheit von Meereisrinnen oder Polynyas verglichen mit Wolken während auflandigen Wind über einer geschlossenen Eisdecke.

Description
The wintertime Arctic sea ice area is characterised by different degrees of fracturing. Leads and polynyas result in a substantial heat and moisture flux from the relatively warm ocean to the cold atmosphere. They thus alter the atmospheric boundary layer structure, cloud cover, and the surface energy budget and also affect atmosphere-ocean chemical exchanges. To quantify the influence of leads or polynyas on clouds, the micro- and macrophysical properties of surface-

coupled clouds during onshore winds in the presence of leads or polynyas will be compared to clouds observed during onshore winds in closed sea-ice conditions.

Mittelgeber: Projektnummer 268020496 innerhalb von TRR 172 „Arktische Verstärkung (AC)^3“

Ein neuartiger Retrievalansatz zur Ableitung troposphärischer Temperatur- und Feuchteprofile unter allen Wetterbedingungen für eine verbesserte Quantifizierung von Verdunstungsraten
(A novel synergistic retrieval approach to enable tropospheric temperature and humidity profiling under all weather conditions for an improved quantification of evaporation rates)

Schlagworte: Instrumentensynergie, bodengebundene Fernerkundung, Niederschlag, Neuronale Netze, optimale Schätzung, Wasserdampfprofile, Temperaturprofile, Verdunstungsraten, Abkühlungsraten

Projektleiter: A. Foth (andreas.foth@uni-leipzig.de)
Projektmitarbeiter: A. Foth (andreas.foth@uni-leipzig.de)

Projektbeginn: 1.4.2020
Projektende: 20.06.2024

Beschreibung
Die ständige Weiterentwicklung und Verbesserung der Wetter- und Klimamodelle stellt die Fernerkundung der Atmosphäre vor große Herausforderungen. Für die Evaluierung der Modelle werden immer besser aufgelöste Messungen und Methoden benötigt. Herkömmliche Ansätze scheitern hier vor allem an fehlenden kontinuierlichen Beobachtungen der Temperatur und Feuchte bei allen Wetterbedingungen und insbesondere bei Regen. Ein Windprofiler ist allerdings auch bei solchen Bedingungen in der Lage Vertikalinformationen der Temperatur- und Feuchtegradienten zu messen. Der hier vorgeschlagene neuartige Ansatz aus einer Synergie aus Windprofiler (inklusive Radio Acoustic Sounding System), Ramanlidar, Mikrowellenradiometer und Wolkenradar ermöglicht eine automatisierte und kontinuierliche Erstellung von Temperatur- und Feuchteprofilen sogar bei Niederschlägen. Langzeitbeobachtungen an Meteorologischen Observatorium in Lindenberg werden genutzt, um aussagekräfige Statistiken über die Verdunstungs- und Abkühlungsraten zu erstellen. Die Ergebnisse werden für verschiedene Bedingungen wie stratiformen und konvektiven Niederschlag und für verschiedenen Jahreszeiten evaluiert. Dies wird den Modellieren helfen, die Parametrisierungen der Verdunstungsraten in kleinskaligen Modellen zu evaluieren.

Description
Steady improvements of weather and climate models are challengeing for remote sensing of the atmosphere. For the evaluation of the models highly resolved measurements and methods are necessary. Usual approaches fail due to the lack of continuous observation of temperature and humidity profiles during all weather conditions, especially during precipitation. A wind profiling radar enables the measurement vertical profiles of temperature and humidity gradients. The novel approach based on synergy between and profiling radar (with Radio Acoustic Sounding System), Raman lidar, microwave radiometer, and cloud radar enables an automated and continuous observation of temperature and humidity profiles even during precipitation. The used variational approach (optimal estimation) provides a robust tool for the combination of different instruments

including the uncertainties of the single systems. Longterm observation at the meteorological observatory Lindenberg will be used to estimate robust statistics about evaporation and cooling rates. The results will be evaluated for different conditions as stratiform or convective precipitation or for different seasons. The outcome will help modellers to evaluate the parametrizations of evaporation rates in small-scale models.

Mittelgeber: Deutsche Forschungsgemeinschaft (DFG FO 1285/2-1)

Verbesserung der Leistungsprognose von Windkraftanlagen zur Unterstützung der Energiewende
Improvement of load prediction of wind turbines for support of the green energy transition

Schlagworte: bodengebundene Fernerkundung, erneuerbare Energien, Southern Ocean Radiation Bias, DACAPO-PESO, EUREC4A

Projektleiter: H. Kalesse-Los (heike.kalesse@uni-leipzig.de), A. Ehrlich (a.ehrlich@uni-leipzig.de), M. Schäfer (michael.schaefer@uni-leipzig.de), M. Wendisch (m.wendisch@uni-leipzig.de)

Projektmitarbeiter: AP1: M. Lochmann (moritz.lochmann@uni-leipzig.de), AP2: W. Schimmel (willi.schimmel@uni-leipzig.de), AP3: Jonas Witthuhn (jonas.witthuhn@uni-leipzig.de), AP4: Elena Ruiz-Donoso (elena.ruiz_donoso@uni-leipzig.de)

Projektbeginn: 1.3.2022
Projektende: 31.12.2022

Beschreibung: Es lassen sich zwei Hauptziele aufzeigen, welche beide auf bodengebundenen Fernerkundungsdaten der Atmosphäre basieren: Zum einen wird analysiert wie künstliche neuronale Netze (KNN) zur Leistungsprognose von Windkraftanlagen optimiert werden können, wenn zusätzliche Daten von bodengebundenen Fernerkundungsmessungen implementiert werden. Zum anderen werden Ableitungsalgorithmen (Retrievals) für Wolkenbeobachtungen neu- und weiterentwickelt, um die Bestimmung von Wolkeneigenschaften zu verbessern, zu erweitern und den Wolkenstrahlungseffekt sowie die Niederschlagsverdunstung zu quantifizieren. Selbst erhobene Messdaten im westlichen tropischen Atlantik sowie an der Südspitze Südamerikas bilden die Datenbasis.

Description: Two main objectives can be identified, both based on ground-based remote sensing data of the atmosphere: On the one hand, it is analysed how artificial neural networks (ANN) can be optimised for the power prognosis of wind turbines if additional data from ground-based remote sensing measurements are implemented. On the other hand, retrieval algorithms for cloud observations are being developed and refined in order to improve and expand the determination of cloud properties and to quantify the cloud radiation effect and precipitation evaporation for field data obtained in the tropical Western Atlantic and the Southern Ocean region.

Mittelgeber: ESF - Sächsische Aufbaubank (SAB), Antragsnummer: 100602743

CORSIPP: Charakterisierung von orographisch beeinflusster Bereifung und sekundärer Eisproduktion und deren Auswirkungen auf Niederschlagsraten mittels Radarpolarimetrie und Dopplerspektren
CORSIPP: Characterization of orography-influenced riming and secondary ice production and their effects on precipitation rates using radar polarimetry and Doppler spectra

Schlagworte: Mischphasenwolken; bodengebunde Fernerkundung; Doppler-Wolkenradar und Radar-Polarimetrie; Bereifung und SekundäreEispartikelbildung; Niederschlagsbildung in komplexem Gelände;Bayes'sches Machine Learning Verfahren; Modellierung von Radarbeobachtungen

Keywords: mixed-phase clouds; ground-based remote sensing; Doppler cloud radar and radar polarimetry; riming and secondary ice production; precipitation formation in complex terrain; Bayesian machine learning retrieval techniques; Modeling radar observations

Projektleiter: Heike Kalesse-Los (heike.kalesse@uni-leipzig.de), Maximilian Maahn (maximilian.maahn@uni-leipzig.de)

Projektmitarbeiter: Anton Kötsche (anton.kötsche@uni-leipzig.de), Veronika Ettrichrätz (ab März 2023)

Projektbeginn: 1.1.2023
Projektende: 31.5.2025

Beschreibung: Niederschlag ist eine wichtige Komponente des hydrologischen Kreislaufs. Um zu verstehen, wie sich der Wasserhaushalt in einemsich erwärmenden Klima verändert, ist ein umfassendes Verständnisder Niederschlagsbildungsprozesse erforderlich. In den mittleren Breiten wird der meiste Niederschlag unter Beteiligung der Eisphase in Mischphasenwolken erzeugt, aber die genauen Interaktionen zwischen Eis, flüssigem Wasser, Wolkendynamik, orografischem Antrieb und Aerosolpartikeln während der Eis-, Schnee- und Regenbildung sind nicht gut verstanden. Dies gilt insbesondere für Bereifungs- und Sekundäre Eisproduktion (SIP) Prozesse, die mit den größten quantitative Unsicherheiten in Bezug auf die Schneefallbildung verbunden sind. Die Lücken in unserem Verständnis von SIP- und Bereifungsprozesse zu schließen, ist vor allem für Gebirgsregionen entscheidend, die besonders anfällig für Änderungen des Niederschlags und des Wasserhaushalts, wie z.B. des Verhältnisses zwischen Regen und Schneefall, sind. In diesem Antrag wird ein Forschungsprojekt vorgeschlagen, das sich dem Verständnis von Bereifungs- und SIP-Prozessen in komplexem Terrain widmet. Dazu betreiben wir ein innovatives, simultan sendendes und simultan empfangendes (STSR), scannendes W-Band- Wolkenradar zusammen mit einer neuartigen In-situ- Schneefallkamera eine ganze Wintersaison lang in den Rocky Mountains von Colorado, USA betreiben. Die Instrumente sind Teil der Atmospheric Radiation Measurement (ARM) Surface Atmosphere Integrated Field Laboratory (SAIL) Kampagne sein, bei der ein Ka-Band und ein X-Band Radar eingesetzt werden. Durch die Kombination von spektralen polarimetrischen und Multifrequenz- Doppler-Radarbeobachtungen mit empirischen und Bayes'schen Machine Learning Verfahren werden wir Bereifungs- und SIP Ereignisse identifizieren und deren Einfluss auf die Schneefallrate quantifizieren. Dies erfordert die Erweiterung des Passive and Active Microwave radiative TRAnsfer Modells (PAMTRA) mit zusätzlichen polarimetrischen Variablen und modernsten Berechnungen von Streueigenschaften. Durch die Nutzung der umfangreichen kollokierten Messungen während SAIL wird es ermöglicht,

die beobachteten Prozessraten mit Umweltbedingungen wie Temperatur, Luftfeuchtigkeit und Flüssigwasserpfad sowie mit der Wolkendynamik in Beziehung zu setzen. Darüber hinaus werden wir einen besonderen Fokus auf den Einfluss von vertikalen Luftbewegungen legen, die unter orographischen Bedingungen häufig auftreten. Zusammengenommen wird das vorgeschlagene Projekt unser Verständnis von Bereifungs- und SIP-Prozessen in komplexem Gelände verbessern.

Description: Precipitation is a major component of the hydrological cycle. A comprehensive understanding of the precipitation formation processes is required to understand how the water budget is changing in a warming climate. In mid-latitudes, most precipitation is generated through the ice phase in mixed-phase clouds, but the exact pathways through which ice, liquid water, cloud dynamics, orographic forcing, and aerosol particles are interacting during ice, snow and rain formation are not well understood. This is particularly true for riming and secondary ice production (SIP) processes that are likely related to the largest uncertainties with respect to quantitative snowfall formation. Filling the gaps in our understanding of SIP and riming is especially crucial for mountainous regions that are particularly vulnerable to changes in precipitation and the water budget such as the ratio between rain and snowfall. Here, we propose a research project dedicated to understanding riming and SIP processes in complex terrain. For this, we are operating an innovative simultaneous transmission- simultaneous-reception (STSR) scanning W-band cloud radar together with a novel in situ snowfall camera for one entire winter season in the Colorado Rocky Mountain. The instruments are part of the Atmospheric Radiation Measurement (ARM) Surface Atmosphere Integrated Field Laboratory (SAIL) campaign where a Ka-band and a X-band radar will be deployed. Combining spectral polarimetric and multi frequency Doppler radar observations with empirical and Bayesian machine learning retrieval techniques, we will identify riming and SIP events and quantify their impact on snowfall rates. This goal requires extending the Passive and Active Microwave radiative TRAnsfer model (PAMTRA) with additional polarimetric variables and state of the art scattering capabilities. Finally, using the extensive collocated measurements of SAIL will allow us to relate the observed process rates to environmental conditions such as temperature, humidity and liquid water path as well as cloud dynamics. In addition, we will put a special focus on the impact of vertical air motions that appear frequently in orographic conditions.

Mittelgeber: Deutsche Forschungsgemeinschaft (DFG KA 4162/2-2)

Aerosole und Wolken, Matthias Tesche
Aerosols and Clouds

Partikel in Aerosol-Wolken Wechselwirkungen: Schichtung, Konzentration und Wolkenlebenszyklus
Particles in Aerosol Cloud Interactions: stratification, CCN/INP concentrations, and Cloud lifecycle (PACIFIC)

Schlagworte: Aerosol-Wolken-Wechselwirkungen, Satellitenfernerkundung, Wolkenverfolgung, Wolken- und Eiskeime

Projektleiter: Dr. Matthias Tesche (matthias.tesche@uni-leipzig.de)

Projektmitarbeiter: Dr. Torsten Seelig, Dr. Diego Villanueva, Fani Alexandri, Goutam Choudhury, Sabine Doktorowski, Felix Müller

Projektbeginn: 01.01.2019
Projektende: 31.12.2022

Beschreibung
Aerosolpartikel sind von herausragender Bedeutung für die Bildung von Wolken, da sie als Wolkenkondensationskerne in Flüssigwasserwolken and als Eiskeime in eisenthaltenden Wolken wirken. Veränderungen der Aerosolkonzentration in der Atmosphäre beeinflussen die Reflektivität, die Entwicklung, die Wasserphase, die Lebenszeit und die Regenrate von Wolken. Diese Prozesse werden als Aerosol-Wolken-Wechselwirkungen bezeichnet. Obwohl ihr Einfluss auf das Klima der Erde seit Jahrzenten einen Schwerpunkt der Atmosphärenforschung bildet, ist unser derzeitiger Wissensstand, so wie er im letzten Bericht des Weltklimarates zusammengefasst wurde, dass Aerosol-Wolken-Wechselwirkungen die größte Unsicherheit zu unserem Verständnis des Klimawandels beiträgt.
PACIFIC wird unser Verständnis von Aerosol-Wolken-Wechselwirkungen durch zwei Innovationen verbessern: (1) die Charakterisierung der für diese Prozesse relevanten Aerosolpartikel und (2) die Untersuchung der zeitlichen Veränderung der Eigenschaften von Wolken im Verlauf ihres Lebenszyklus. Untersuchungen von Aerosol-Wolken-Wechselwirkungen mit Geräten auf polarumlaufenden Satelliten sind auf Wolkenbeobachtungen zu festen Zeiten beschränkt. Die für solche Studien benötigte Information der Anzahl vorhandener Wolkenkondensationskerne wird derzeit aus säulenintegrierten optischen Aerosoleigenschaften abgeschätzt. Eine ähnliche Methodik zur Abschätzung der Konzentration von Eiskeimen existiert nicht, da deren Eigenschaften von der Art und Größe der Partikel abhängen. Daher sind zur Zeit keinen Studien von Aerosol-Wolken-Wechselwirkungen auf eisenthaltende Wolken basierend auf Fernerkundungsmessungen möglich. Die quantitative Abschätzung der Bedeutung von Aerosolen in Aerosol-Wolken-Wechselwirkungen verlangt, dass Informationen über die räumliche Verteilung von Wolkenkondensationskernen und Eiskeimen vorhanden sind. Das Projekt strebt an bisher nicht erhältliche Informationen über die Konzentration von Wolkenkondensationskernen und Eiskeimen aus weltraumgetragenen Lidarmessungen zu erlangen. Dessweiteren wird die Entwicklung von Wolken vor und nach der Punktbeobachtung mir polarumlaufenden Geräten dadurch charakterisiert, dass diese Wolken in zeitlich aufgelösten Beobachtungen von geostationären Geräten verfolgt werden. Die neuartige Information wird dann zum Studium der Effekte von Wolkenkondensationskernen und Eiskeimen auf die Helligkeit, den Flüssig- und Eiswassergehalt, die Tropfen- und Eiskristallgröße, die Entwicklung, die Wasserphase und die Regenrate von Wolken in verschiedenen Wolkenregimen verwendet. Besonderes Augenmerk wird dabei auf eine umfassende Berücksichtigung der meteorologischen Rahmenbedingungen gelegt werden. Die Ergebnisse von PACIFIC sind von Bedeutung für die Untersuchung und Verbesserung des Verhaltens von Klimamodellen.

Description:
Atmospheric aerosol particles are of great importance for cloud formation in the atmosphere because they are needed to act as cloud condensation nuclei (CCN) in liquid-water clouds and as ice nucleating particles (INP) in ice-containing clouds. Changes in aerosol concentration affect the albedo, development, phase, lifetime and rain rate of clouds. These aerosol-cloud interactions (ACI) and the resulting climate effects have been in the focus of atmospheric research for several

decades. Nevertheless, the IPCC still concludes that ACI cause the largest uncertainty in assessing climate change as they are understood only with medium confidence.
PACIFIC will improve our understanding of ACI by enhancing the representation of the aerosols relevant for cloud processes and by quantifying temporal changes in cloud properties throughout the cloud life cycle. ACI studies using polar-orbiting sensors are limited to snap-shot observations of clouds. CCN concentrations for assessing ACI are currently estimated from column- integrated optical aerosol parameters. There is no such proxy of INP concentrations for remote-sensing studies of aerosol effects on cold clouds as INP activity depends on aerosol type and size. Quantifying the role of aerosols in ACI requires knowledge of the spatial and vertical distribution of CCN and INP. The project aims to obtain unprecedented insight in CCN and INP concentrations from spaceborne lidar data. In addition, the development of clouds before and after the snap-shot view of polar-orbiting sensors is characterised by tracking those clouds in time-resolved geostationary observations. This novel information will be used to study the effects of CCN and INP on the albedo, liquid and ice water content, droplet and crystal size, development, phase and rain rate of clouds within different regimes carefully accounting for the meteorological background. The findings of PACIFIC are crucial for assessing and improving the performance of climate models.

Mittelgeber: Bundesministerium für Bildung und Forschung (BMBF) und Deutscher Akademischer Austauschdienst (DAAD), MOPGA-GRI Senior Research Grant PACIFIC (57429422)

MAMiP – Mehrschichtige Arktische Mischphasenwolken: Beobachtungen
Multilayer Arctic Mixed-Phased Clouds: Observations (MAMiP:O)

Projektleiter: Dr. Matthias Tesche (matthias.tesche@uni-leipzig.de)

Projektmitarbeiterin: Dr. Peggy Achtert

Projektbeginn: 01.07.2021
Projektende: 30.06.2024

Beschreibung
Wolken spielen eine zentrale Rolle in der Kopplung der Atmosphäre mit der Erdoberfläche. Diese Verbindung wird durch den direkten Strahlungstransport im solaren und terrestrischen Wellenlängenbereich sowie den Austausch latenter Energie in der Form von Feuchteflüssen und Niederschlag hergestellt. Im Gegensatz zu anderen Orten auf der Erde können Wolken in der Arktis mit ihrer im Vergleich zur Erdoberfläche oft wärmeren Wolkenoberkante eine erwärmende Wirkung auf der Erdoberfläche ausüben. Der Fokus in der Untersuchung arktischer Wolken lag bisher auf sogenannten Einschichtwolken, welche sich in der Regel am Oberrand der planetaren Grenzschicht bilden. Wolken, die in einer anderen Höhe oder in mehreren Höhen gleichzeitig auftreten (Mehrschichtwolken), könnten allerdings einen Einfluss auf die Energiebilanz der Erdoberfläche ausüben, der sich von dem der umfangreich untersuchten Einschichtwolken unterscheidet. Dies hat mehrere Gründe: (i) den komplexen Strahlungstransport im Vergleich zu Einschichtwolken, (ii) der Einfluss oberer Wolken auf die diabatische Abkühlung darunter liegender Wolken und (iii) Eiskristalle, die aus oberen in die unteren Wolken fallen, können durch Eisimpfung die Wasserphase der unteren Wolken verändern und damit die Bildung von Mischphasenwolken im Temperaturbereich des heterogenen Gefrierens ermöglichen.

MAMiP:O strebt an die Lücken in unserem wissenschaftlichen Verständnis arktischer Mehrschichtwolken durch die systematische Auswertung von Fernerkundungsmessdaten zu schließen. Folgende Fragen sollen beantwortet werden:
1. Wie häufig treten Mehrschichtwolken im Vergleich zu Einschichtwolken auf?
2. Kann das Auftreten arktischer Einschicht- und Mehrschichtwolken aus aktiven und passiven Satellitenbeobachtungen abgeleitet werden?
3. Wie oft tritt Eiskristallimpfung in arktischen Mischphasenwolkensystemen auf?
4. Welche Faktoren bestimmen die Eiskristallimpfung? Lösen sich geimpfte Wolken auf oder verdicken sie sich?

Description:
Arctic clouds with their warm cloud tops (compared to the surface) can have a warming effect on the atmosphere. So far, studies of Arctic clouds have focussed on single-layer clouds, which form at boundary layer top. The radiative effect of clouds that occur at multiple heights simultaneously (multi-layer clouds) can be very different from that of single-layer clouds. This is because of (i) more complex radiative transport, (ii) adiabatic cooling of lower clouds, and (iii) glaciation of lower clouds as a result of ice-crystal seeding from upper cloud layers.
MAMiP will address gaps in our scientific understanding of Arctic multi-layer clouds through four questions:
1. What is the occurrence rate of Arctic multi-layer clouds compared to single-layer clouds?
2. What is the occurrence rate of ice-crystal seeding in Arctic multi-layer clouds?
3. Can simulations of Arctic multi-layer clouds with cloud-resolving models reproduce observations and provide insight into the dominating processes?
4. Which factors determine ice-crystal seeding? What happens to seeded clouds?

MAMiP:O will analyse observations beyond the MOSAiC data set. In MAMiP:M, the observed cases will be simulated with a cloud-resolving model to investigate the connection between radiative and microphysical processes, the predictability of multi-layer clouds, and their effect on the radiative budget at the surface.

Mittelgeber: Bundesministerium für Bildung und Forschung (BMBF), Förderkennzeichen 03F0891A

Maximilian Maahn
AG drOPS - clouD and pRecipitation Observations for Process Studies

---

Charakterisierung der räumlichen Variabilität von Eiswassergehalt in und unter Mischphasenwolken (B08)
Characterising the spatial variability of ice water content in and below mixed-phase clouds (B08)

Schlagworte: Arktischer Klimawandel, Fernerkundung, Mischphasenwolken

Projektleiter: Maximilian Maahn, Universität Leipzig (maximilian.maahn@uni-leipzig.de)

Projektmitarbeiterin: Nina Maherndl (nina.maherndl@uni-leipzig.de)

Projektbeginn: 1.1.2021
Projektende: 31.12.2023

Beschreibung
Die Prozesse, die die räumliche Variabilität des Eiswassergehalts (IWG) in Mischphasenwolken (MPW) bestimmen, sind nicht ausreichend erforscht. Deswegen wird ein Forschungsprojekt vorgeschlagen, welches sich explizit dem Verständnis und der Quantifizierung dieser Prozesse widmet. Es ist zwar eine Herausforderung, diese MPW Prozesse direkt zu beobachten, jedoch können Fingerabdrücke der dominierenden MPW Prozesse in verbesserten Flugzeugbeobachtungen von IWG und Schneefallrate (SR) identifiziert werden. Dafür werden Beobachtungen verwendet, die während der ACLOUD Kampagne 2017 sowie weiteren (AC)3 Flugzeug Kampagnen gemacht wurden, bzw. die bei der für 2021 geplanten HALO-(AC)3 Kampagne gemacht werden. Bei ACLOUD und HALO-(AC)3 flogen bzw. fliegen mindestens zwei Flugzeuge in einer Tandemformation wodurch kollokierte in situ und Fernerkundungsmessungen zur Verfügung stehen. Auf Basis dieser seltenen Tandemdatensätze wird ein nahtloses Umkehr Verfahren (engl. Retrieval) entwickelt, welches auf der Bayesschen Optimal Estimation Theorie basiert: Die flugzeuggebundenen Fernerkundungs- und in situ Daten werden kombiniert, um die in situ Daten nicht nur für die Datenpunkte zu verwenden, an denen sie gemessen wurden, sondern für alle vom Radar erfassten Wolkenbereiche. Dafür wird ihr Gewicht im Umkehr Verfahren proportional zum Abstand zwischen Radar und in situ Messung unter Berücksichtigung der Autokorrelationslängen der gemessenen Parameter gewählt. Dadurch kann berücksichtigt werden, wie sich der Informationsgehalt der in situ Messungen mit zunehmendem Abstand verringert. So können alle verfügbaren Informationen kombiniert werden und die vertikale und horizontale Variabilität von IWG und SR in und unter Wolken kann mit hoher räumlicher Auflösung bestmöglich bestimmt werden. Basierend auf den verbesserten Beobachtungsverfahren wird die beobachtete IWG Variabilität mit andern Mikro- und Makrophysikalischen Wolkeneigenschaften (z.B. dominierender Eispartikelwachstumsprozess, Wolkentyp, Flüssigwassergehalt, Wolkendicke, Variabilität von Wolkenphase an der Wolkenoberseite, turbulente Koppelung mit der Oberfläche) verknüpft. Ein besonderer Fokus wird auf die vertikale IWG Variabilität und den daraus resultierenden Einfluss auf die Massenflüsse von Eiskristallen gelegt. Dafür kann man nicht nur auf die umfangreichen Flugzeugmessungen zurückgreifen, sondern auch auf die bodengebundenen Beobachtungen in Ny-Ålesund und von der PASCAL Kampagne. Dadurch werden nicht nur die Prozesse identifiziert, die für die Quellen und Senken von IWG in der Atmosphäre am wichtigsten sind, sondern auch auf welchen räumlichen Skalen diese Prozesse aktiv sind. Simulationen mit dem ICON-LEM Atmosphärenmodel werden analysiert, um Unterschiede in der Darstellung von IWG zu identifizieren. Durch Anwendung der gleichen mikro- und makrophysikalischen Wolkenklassifikationen wie bei den Beobachtungen werden die Modellparametrisierungen identifiziert, die verbessert werden müssen.

Description
The processes determining spatial variability of ice water content (IWC) in mixed-phase clouds (MPCs) are not sufficiently understood. Therefore, we propose a project targeted at understanding and quantifying these processes. While it is challenging to observe MPC processes directly, we will advance techniques for quantifying IWC and snowfall rate (SR) with low uncertainty from airborne radar measurements so that we are able to observe fingerprints of the dominating processes. We will use data collected during the (AC)3 aircraft campaigns with a particular focus on the ACLOUD

campaign performed in 2017, and the upcoming HALO-(AC)3 campaign planned within the current phase of (AC)3. For these campaigns, at least two closely collocated aircraft are flying in formation for obtaining collocated in situ and remote sensing observations. We will use these rare data collected during tandem flights to develop a seamless Bayesian Optimal Estimation retrieval for obtaining IWC and SR from combined radar and in situ measurements along a flight track 'curtain'. We will develop a novel retrieval approach where the in situ data are exploited not only for the observation point where they were obtained, but for the whole curtain by scaling their weight proportional to the autocorrelation lengths of the microphysical properties. By this, we can consider how the information content of the in situ instruments is reduced with increasing distance between in situ and remote sensing observation volume. Such a retrieval can combine all available information from radar and in situ observations and will close an important gap in our ability to observe the vertical and horizontal spatial variability of IWC in clouds with high accuracy and high spatial resolution. Based on the improved observations, we will link the observed IWC variability to other microphysical and macrophysical cloud properties (among others, dominating particle growth process, cloud type, liquid water content, cloud depth, cloud top phase variability, surface coupling). A particular emphasis will be put on vertical IWC variability and the resulting impact on precipitation mass fluxes. For this, we can rely on the extensive supporting aircraft data sets, but also on ground-based observations in Ny-Ålesund and during the PASCAL campaign. By this, we will identify the processes most relevant for IWC sources and sinks as well as the spatial scales on which these processes are active. Model simulations using ICON-LEM will be analysed for quantifying differences in the representation of IWC. By comparing to the same microphysical and macrophysical cloud classifications used for the observations, we will identify which model MPCs parameterisations need to be improved.

Mittelgeber: Deutsche Forschungsgemeinschaft (DFG) TRR 172 $(AC)^3$

Characterization of orography-influenced riming and secondary ice production and their effects on precipitation rates using radar polarimetry and Doppler spectra (CORSIPP)
Charakterisierung von orographisch beeinflusster Bereifung und sekundärer Eisproduktion und deren Auswirkungen auf Niederschlagsraten mittels Radarpolarimetrie und Dopplerspektren (CORSIPP)

Schlagworte: Fernerkundung, In Situ Beobachtungen, Mischphasenwolken, Bereifung, Secondary Ice Formation

Projektleiter: Maximilian Maahn, Universität Leipzig (maximilian.maahn@uni-leipzig.de)

Projektmitarbeiterin: Isabelle Steinke (isabelle.steinke@uni-leipzig.de)

Projektbeginn: 15.06.2022
Projektende: 14.08.2025

Beschreibung
Niederschlag ist eine wichtige Komponente des hydrologischen Kreislaufs. Um zu verstehen, wie sich der Wasserhaushalt in einem sich erwärmenden Klima verändert, ist ein umfassendes Verständnis der Niederschlagsbildungsprozesse erforderlich. In den mittleren Breiten wird der meiste Niederschlag unter Beteiligung der Eisphase in Mischphasenwolken erzeugt, aber die genauen Interaktionen zwischen Eis, flüssigem Wasser, Wolkendynamik, orografischem Antrieb und Aerosolpartikeln während der Eis-, Schnee- und Regenbildung sind nicht gut verstanden. Dies

gilt insbesondere für Bereifungs- und Sekundäre Eisproduktion (SIP) Prozesse, die mit den größten quantitative Unsicherheiten in Bezug auf die Schneefallbildung verbunden sind. Die Lücken in unserem Verständnis von SIP- und Bereifungsprozesse zu schließen, ist vor allem für Gebirgsregionen entscheidend, die besonders anfällig für Änderungen des Niederschlags und des Wasserhaushalts, wie z.B. des Verhältnisses zwischen Regen und Schneefall, sind. In diesem Antrag wird ein Forschungsprojekt vorgeschlagen, das sich dem Verständnis von Bereifungs- und SIP-Prozessen in komplexem Terrain widmet. Dazu werden wir ein innovatives, simultan sendendes und simultan empfangendes (STSR), scannendes W-Band-Wolkenradar zusammen mit einer neuartigen In-situ-Schneefallkamera eine ganze Wintersaison lang in den Rocky Mountains von Colorado, USA betreiben. Die Instrumente werden Teil der Atmospheric Radiation Measurement (ARM) Surface Atmosphere Integrated Field Laboratory (SAIL) Kampagne sein, bei der ein Ka-Band und ein X-Band Radar eingesetzt werden. Durch die Kombination von spektralen polarimetrischen und Multifrequenz-Doppler-Radarbeobachtungen mit empirischen und Bayes'schen Machine Learning Verfahren werden wir Bereifungs- und SIP-Ereignisse identifizieren und deren Einfluss auf die Schneefallrate quantifizieren. Dies erfordert die Erweiterung des Passive and Active Microwave radiative TRAnsfer Modells (PAMTRA) mit zusätzlichen polarimetrischen Variablen und modernsten Berechnungen von Streueigenschaften. Durch die Nutzung der umfangreichen kollokierten Messungen während SAIL wird es ermöglicht, die beobachteten Prozessraten mit Umweltbedingungen wie Temperatur, Luftfeuchtigkeit und Flüssigwasserpfad sowie mit der Wolkendynamik in Beziehung zu setzen. Darüber hinaus werden wir einen besonderen Fokus auf den Einfluss von vertikalen Luftbewegungen legen, die unter orographischen Bedingungen häufig auftreten. Zusammengenommen wird das vorgeschlagene Projekt unser Verständnis von Bereifungs- und SIP-Prozessen in komplexem Gelände verbessern.

Becker	**Sebastian**	**Ehrlich, A.**, **Jäkel, E.**, Carlsen, T., **Schäfer, M.**, and **Wendisch, M.**	Airborne measurements of directional reflectivity over the Arctic marginal sea ice zone	doi:10.5194/amt-15-2939-2022 Atmos. Meas. Tech., 15, 2939–2953 (2022)
Braga	Ramon C.	Rosenfeld, D., Andreae, M. O., Pöhlker, C., Pöschl, U., Voigt, C., Weinzierl, B., **Wendisch, M.**, Pöhlker, M. L., and Harrison, D.	Detrainment dominates CCN concentrations around non-precipitating convective clouds over the amazon	doi:10.1029/2022gl100411 Geophys. Res. Lett., 49 (2022)
Geerts	Bart	Giangrande, S. E., McFarquhar, G. M., Xue, L., Abel, S. J., Comstock, J. M., Crewell, S., DeMott, P. J., Ebell, K., Field, P., Hill, T. C. J., Hunzinger, A., Jensen, M. P., Johnson, K. L., Juliano, T. W., Kollias, P., Kosovic, B., Lackner, C., Luke, E., Lüpkes, C., Matthews, A. A., Neggers, R., Ovchinnikov, M., Powers, H., Shupe, M. D., Spengler, T., Swanson, B. E., Tjernström, M., Theisen, A. K., Wales, N. A., Wang, Y., **Wendisch, M.**, and Wu, P.	The COMBLE campaign: a study of marine boundary layer clouds in Arctic cold-air outbreaks	doi:10.1175/bams-d-21-0044.1 Bull. Amer. Meteorol. Soc., 103, E1371–E1389 (2022)
Lonardi	**Michael**	Pilz, C., Akansu, E. F., Dahlke, S., Egerer, U., **Ehrlich, A.**, Griesche, H., Heymsfield, A. J., **Kirbus, B.**, Schmitt, C. G., Shupe, M. D., Siebert, H., Wehner, B., and **Wendisch, M.**	Tethered balloon-borne profile measurements of atmospheric properties in the cloudy atmospheric boundary layer over the Arctic sea ice during MOSAiC: overview and first results	doi:10.1525/elementa.2021.000120 Elem. Sci. Anth., 10 (2022)

Luebke	**Anna E.**	**Ehrlich, A.**, **Schäfer, M.**, Wolf, K., and **Wendisch, M.**	An assessment of macrophysical and microphysical cloud properties driving radiative forcing of shallow trade-wind clouds	doi:10.5194/acp-22-2727-2022 Atmos. Chem. Phys., 22, 2727–2744 (2022)
Mahecha	Miguel D.	Bastos, A., Bohn, F. J., Eisenhauer, N., Feilhauer, H., Hartmann, H., Hickler, T., **Kalesse-Los, H.**, Migliavacca, M., Otto, F. E. L., Peng, J., **Quaas, J.**, Tegen, I., Weigelt, A., **Wendisch, M.**, and Wirth, C.	Biodiversity loss and climate extremes — study the feedbacks	doi:10.1038/d41586-022-04152-y Nature, 612, 30–32 (2022)
Mech	Mario	**Ehrlich, A.**, Herber, A., Lüpkes, C., **Wendisch, M.**, **Becker, S.**, Boose, Y., Chechin, D., Crewell, S., Dupuy, R., Gourbeyre, C., Hartmann, J., **Jäkel, E.**, Jourdan, O., Kliesch, L., **Klingebiel, M.**, Kulla, B. S., Mioche, G., Moser, M., Risse, N., **Ruiz-Donoso, E.**, **Schäfer, M.**, **Stapf, J.**, and Voigt, C.	MOSAiC-ACA and AFLUX - Arctic airborne campaigns characterizing the exit area of MOSAiC	doi:10.1038/s41597-022-01900-7 Sci. Data, 9 (2022)
Nicolaus	Marcel	Perovich, D. K., Spreen, G., Granskog, M. A., Albedyll, L. v., Angelopoulos, M., Anhaus, P., Arndt, S., Belter, H. J., Bessonov, V., Birnbaum, G., Brauchle, J., Calmer, R., Cardellach, E., Cheng, B., Clemens-Sewall, D., Dadic, R., Damm,	Overview of the MOSAiC expedition: snow and sea ice	doi:10.1525/elementa.2021.000046 Elem. Sci. Anth., 10 (2022)

		E., Boer, G. d., Demir, O., Dethloff, K., Divine, D. V., Fong, A. A., Fons, S., Frey, M. M., Fuchs, N., ó, C., Gerland, S., Goessling, H. F., Gradinger, R., Haapala, J., Haas, C., Hamilton, J., Hannula, H., Hendricks, S., Herber, A., Heuzé, C., Hoppmann, M., ø, K. V., Huntemann, M., Hutchings, J. K., Hwang, B., Itkin, P., Jacobi, H., Jaggi, M., Jutila, A., Kaleschke, L., Katlein, C., Kolabutin, N., Krampe, D., Kristensen, S. S., Krumpen, T., Kurtz, N., Lampert, A., Lange, B. A., Lei, R., Light, B., Linhardt, F., Liston, G. E., Loose, B., Macfarlane, A. R., Mahmud, M., Matero, I. O., Maus, S., Morgenstern, A., Naderpour, R., Nandan, V., Niubom, A., Oggier, M., Oppelt, N., Pätzold, F., Perron, C., Petrovsky, T., Pirazzini, R., Polashenski, C., Rabe, B., Raphael, I. A., Regnery, J., Rex, M., Ricker, R., Riemann-Campe, K., Rinke, A., Rohde, J., Salganik, E., Scharien, R. K., Schiller, M., Schneebeli, M., Semmling, M., Shimanchuk, E., Shupe, M. D., Smith, M. M., Smolyanitsky, V., Sokolov, V., Stanton, T., Stroeve, J., Thielke, L., Timofeeva, A., Tonboe, R. T., Tavri, A., Tsamados, M., Wagner, D. N., Watkins, D., Webster, M., and **Wendisch, M.**		

Rabe	Benjamin	Heuzé, C., Regnery, J., Aksenov, Y., Allerholt, J., Athanase, M., Bai, Y., Basque, C., Bauch, D., Baumann, T. M., Chen, D., Cole, S. T., Craw, L., Davies, A., Damm, E., Dethloff, K., Divine, D. V., Doglioni, F., Ebert, F., Fang, Y., Fer, I., Fong, A. A., Gradinger, R., Granskog, M. A., Graupner, R., Haas, C., He, H., He, Y., Hoppmann, M., Janout, M., Kadko, D., Kanzow, T., Karam, S., Kawaguchi, Y., Koenig, Z., Kong, B., Krishfield, R. A., Krumpen, T., Kuhlmey, D., Kuznetsov, I., Lan, M., Laukert, G., Lei, R., Li, T., Torres-Valdés, S., Lin, L., Lin, L., Liu, H., Liu, N., Loose, B., Ma, X., McKay, R., Mallet, M., Mallett, R. D. C., Maslowski, W., Mertens, C., Mohrholz, V., Muilwijk, M., Nicolaus, M., O'Brien, J. K., Perovich, D., Ren, J., Rex, M., Ribeiro, N., Rinke, A., Schaffer, J., Schuffenhauer, I., Schulz, K., Shupe, M. D., Shaw, W., Sokolov, V., Sommerfeld, A., Spreen, G., Stanton, T., Stephens, M., Su, J., Sukhikh, N., Sundfjord, A., Thomisch, K., Tippenhauer, S., Toole, J. M., Vredenborg, M., Walter, M., Wang, H., Wang, L., Wang, Y., **Wendisch, M.**, Zhao, J., Zhou, M., and Zhu, J.	Overview of the MOSAiC expedition: physical oceanography	doi:10.1525/elementa.2021.00062 Elem. Sci. Anth., 10 (2022)

Schäfer	**Michael**	Wolf, K., **Ehrlich, A.**, Hallbauer, C., a, E., Jansen, F., Luebke, A. E., u, J., o, J., o, T., Stevens, B., and **Wendisch, M.**	VELOX – a new thermal infrared imager for airborne remote sensing of cloud and surface properties	doi:10.5194/amt-15-1491-2022 Atmos. Meas. Tech., 15, 1491–1509 (2022)
Shrivastava	Manish	Rasool, Q. Z., Zhao, B., Octaviani, M., Zaveri, R. A., Zelenyuk, A., Gaudet, B., Liu, Y., Shilling, J. E., Schneider, J., Schulz, C., Zöger, M., Martin, S. T., Ye, J., Guenther, A., Souza, R. F., **Wendisch, M.**, and Pöschl, U.	Tight coupling of surface and in-plant biochemistry and convection governs key fine particulate components over the amazon rainforest	doi:10.1021/acsearthspacechem.1c00356 ACS Earth Space Chem., 6, 380–390 (2022)
Shupe	Matthew D.	Rex, M., Blomquist, B., Persson, P. O. G., Schmale, J., Uttal, T., Althausen, D., Angot, ; Archer, S., Bariteau, L., Beck, I., Bilberry, J., Bucci, S., Buck, C., Boyer, M., Brasseur, Z., Brooks, I. M., Calmer, R., Cassano, J., Castro, V., Chu, D., Costa, D., Cox, C. J., Creamean, J., Crewell, S., Dahlke, S., Damm, E., Boer, G. d., Deckelmann, H., Dethloff, K., Dütsch, M., Ebell, K., **Ehrlich, A.**, Ellis, J., Engelmann, R., Fong, A. A., Frey, M. M., Gallagher, M. R., Ganzeveld, L., Gradinger, R., Graeser, J., Greenamyer, V., Griesche, H., Griffiths, S., Hamilton, J., Heinemann, G., Helmig, D., Herber, A., Heuzé, C., Hofer, J., Houchens, T., Howard, D., Inoue, J., Jacobi, H., Jaiser, R., Jokinen, T., Jourdan, O., Jozef, G., King, W., Kirchgaessner, A.,	Overview of the MOSAiC expedition: atmosphere	doi:10.1525/elementa.2021.00060 Elem. Sci. Anth., 10 (2022)

		Klingebiel, M., Krassovski, M., Krumpen, T., Lampert, A., Landing, W., Laurila, T., Lawrence, D., **Lonardi, M.**, Loose, B., Lüpkes, C., **Maahn, M.**, Macke, A., Maslowski, W., Marsay, C., Maturilli, M., Mech, M., Morris, S., Moser, M., Nicolaus, M., Ortega, P., Osborn, J., Pätzold, F., Perovich, D. K., Petäjä, T., Pilz, C., Pirazzini, R., Posman, K., Powers, H., Pratt, K. A., ß, A., Quéléver, L., Radenz, M., Rabe, B., Rinke, A., Sachs, T., Schulz, A., Siebert, H., Silva, T., Solomon, A., Sommerfeld, A., Spreen, G., Stephens, M., Stohl, A., Svensson, G., Uin, J., Viegas, J., Voigt, C., Gathen, P. v. d., Wehner, B., Welker, J. M., **Wendisch, M.**, Werner, M., Xie, Z., and Yue, F.		
Wendisch	**Manfred**	**Brückner, M.**, Crewell, S., **Ehrlich, A.**, Notholt, J., Lüpkes, C., Macke, A., Burrows, J. P., Rinke, A., **Quaas, J.**, Maturilli, M., Schemann, V., Shupe, M. D., Akansu, E. F., Barrientos-Velasco, C., Bärfuss, K., Blechschmidt, A., **Block, K.**, Bougoudis, I., Bozem, H., Böckmann, C., Bracher, A., Bresson, H., Bretschneider, L., Buschmann, M., Chechin, D. G., Chylik, J., Dahlke, S., Deneke, H., Dethloff, K., **Donth, T.**, Dorn, W., Dupuy, R., Ebell, K., Egerer, U., Engelmann, R., Eppers, O.,	Atmospheric and surface processes, and feedback mechanisms determining arctic amplification: a review of first results and prospects of the $(AC)^3$ project	doi:10.1175/bams-d-21-0218.1 Bull. Amer. Meteorol. Soc. (2022)

		Gerdes, R., Gierens, R., Gorodetskaya, I. V., **Gottschalk, M.**, Griesche, H., Gryanik, V. M., Handorf, D., Harm-Altstädter, B., Hartmann, J., Hartmann, M., Heinold, B., Herber, A., Herrmann, H., Heygster, G., Höschel, I., Hofmann, Z., Hölemann, J., Hünerbein, A., Jafariserajehlou, S., **Jäkel, E.**, **Jacobi, C.**, Janout, M., Jansen, F., Jourdan, O., Jurányi, Z., **Kalesse-Los, H.**, Kanzow, T., Käthner, R., Kliesch, L. L., **Klingebiel, M.**, Knudsen, E. M., Kovács, T., Körtke, W., Krampe, D., **Kretzschmar, J.**, Kreyling, D., Kulla, B., Kunkel, D., Lampert, A., Lauer, M., Lelli, L., Lerber, A. v., **Linke, O.**, Löhnert, U., **Lonardi, M.**, Losa, S. N., Losch, M., **Maahn, M.**, Mech, M., Mei, L., Mertes, S., **Metzner, E.**, **Mewes, D.**, Michaelis, J., Mioche, G., Moser, M., Nakoudi, K., Neggers, R., Neuber, R., Nomokonova, T., Oelker, J., **Papakonstantinou-Presvelou, I.**, Pätzold, F., Pefanis, V., Pohl, C., Pinxteren, M. v., Radovan, A., Rhein, M., Rex, M., Richter, A., Risse, N., Ritter, C., Rostosky, P., Rozanov, V. V., **Ruiz Donoso, E.**, Saavedra-Garfias, P., **Salzmann, M.**, Schacht, J., **Schäfer, M.**, Schneider, J., Schnierstein, N., Seifert, P., Seo, S., Siebert, H., Soppa, M. A., Spreen, G., Stachlewska, I. S., **Stapf, J.**, Stratmann, F.,		

		Tegen, I., Viceto, C., Voigt, C., Vountas, M., Walbröl, A., Walter, M., Wehner, B., Wex, H., Willmes, S., Zanatta, M., and Zeppenfeld, S.		
Charuvil Asokan	Harikrishnan	Chau, J. L., Marino, R., Vierinen, J., Vargas, F., Urco, J. M., Clahsen, M., and **Jacobi, Ch.**	Frequency spectra of horizontal winds in the mesosphere and lower thermosphere region from multistatic specular meteor radar observations during the SIMONe 2018 campaign	doi:10.1186/s40623-022-01620-7 Earth Planets Space, 74 (2022)
Jaen	Juliana	Renkwitz, T., Chau, J. L., He, M., Hoffmann, P., Yamazaki, Y., **Jacobi, Ch.**, Tsutsumi, M., Matthias, V., and Hall, C.	Long-term studies of mesosphere and lower-thermosphere summer length definitions based on mean zonal wind features observed for more than one solar cycle at middle and high latitudes in the northern hemisphere	doi:10.5194/angeo-40-23-2022 Ann. Geophys., 40, 23–35 (2022)
Karami	**Khalil**	**Mehrdad, S.**, and **Jacobi, Ch.**	Response of the resolved planetary wave activity and amplitude to turned off gravity waves in the UA-ICON general circulation model	doi:10.1016/j.jastp.2022.105967 J. Atmos. Sol. Terr. Phys., 241, 105967 (2022)

Sarkhel	Sumanta	Stober, G., Chau, J. L., Smith, S. M., **Jacobi, Ch.**, Mondal, S., Mlynczak, M. G., and Russell III, J. M.	A case study of a ducted gravity wave event over northern germany using simultaneous airglow imaging and wind-field observations	doi:10.5194/angeo-40-179-2022 Ann. Geophys., 40, 179–190 (2022)
Stober	Gunter	Liu, A., Kozlovsky, A., Qiao, Z., **Kuchar, A.**, **Jacobi, Ch.**, Meek, C., Janches, D., Liu, G., Tsutsumi, M., Gulbrandsen, ; Nozawa, S., Lester, M., Belova, E., Kero, J., and Mitchell, N.	Meteor radar vertical wind observation biases and mathematical debiasing strategies including the 3dvar+DIV algorithm	doi:10.5194/amt-15-5769-2022 Atmos. Meas. Tech., 15, 5769–5792 (2022)
Satterfield	Elizabeth A.	Waller, J. A., Kuhl, D. D., Hodyss, D., Hoppel, K. W., Eckermann, S. D., McCormack, J. P., Ma, J., Fritts, D. C., Iimura, H., Stober, G., Meek, C. E., Hall, C., **Jacobi, Ch.**, Latteck, R., Mitchell, N. J., Espy, P. J., Li, G., Brown, P., Yi, W., Li, N., Batista, P., Reid, I. M., Sunkara, E., Moffat-Griffin, T., Murphy, D. J., Tsutsumi, M., and Marino, J.	Statistical parameter estimation for observation error modelling: application to meteor radars	doi:10.1007/978-3-030-77722-7_8 In: Park, S., and Xu, L. (Hrsg.) Data Assimilation for Atmospheric, Oceanic and Hydrologic Applications (Vol. IV), 185–213 (2022)
Vaishnav	**Rajesh**	**Jacobi, Ch.**, Berdermann, J., Schmölter, E., and Codrescu, M.	Delayed ionospheric response to solar extreme ultraviolet radiation variations: a modeling approach	doi:10.1016/j.asr.2021.12.041 Adv. Space Res., 69, 2460–2476 (2022)
Arola	Antti	Lipponen, A., Kolmonen, P., Virtanen, T. H., Bellouin, N., Grosvenor, D. P., Gryspeerdt, E., **Quaas, J.**, and Kokkola, H.	Aerosol effects on clouds are concealed by natural cloud heterogeneity and satellite retrieval errors	doi:10.1038/s41467-022-34948-5 Nat. Commun., 13 (2022)

Caldas-Alvarez	Alberto	Augenstein, M., Ayzel, G., Barfus, K., **Cherian, R.**, Dillenardt, L., Fauer, F., Feldmann, H., Heistermann, M., Karwat, A., Kaspar, F., Kreibich, H., Lucio-Eceiza, E. E., Meredith, E. P., Mohr, S., Niermann, D., Pfahl, S., Ruff, F., Rust, H. W., Schoppa, L., Schwitalla, T., Steidl, S., Thieken, A. H., Tradowsky, J. S., Wulfmeyer, V., and **Quaas, J.**	Meteorological, impact and climate perspectives of the 29 june 2017 heavy precipitation event in the berlin metropolitan area	doi:10.5194/nhess-22-3701-2022 Nat. Hazards Earth Syst. Sci., 22, 3701–3724 (2022)
Christensen	Matthew W.	Gettelman, A., Cermak, J., Dagan, G., Diamond, M., Douglas, A., Feingold, G., Glassmeier, F., **Goren, T.**, Grosvenor, D. P., Gryspeerdt, E., Kahn, R., Li, Z., Ma, P., Malavelle, F., McCoy, I. L., McCoy, D. T., McFarquhar, G., Mülmenstädt, J., Pal, S., Possner, A., Povey, A., **Quaas, J.**, Rosenfeld, D., Schmidt, A., Schrödner, R., Sorooshian, A., Stier, P., Toll, V., Watson-Parris, D., Wood, R., Yang, M., and Yuan, T.	Opportunistic experiments to constrain aerosol effective radiative forcing	doi:10.5194/acp-22-641-2022 Atmos. Chem. Phys., 22, 641–674 (2022)
Dipu	**Sudhakar**	Schwarz, M., Ekman, A. M. L., Gryspeerdt, E., **Goren, T.**, Sourdeval, O., **Mülmenstädt, J.**, and **Quaas, J.**	Exploring satellite-derived relationships between cloud droplet number concentration and liquid water path using a large-domain large-eddy simulation	doi:10.16993/tellusb.27 Tellus B: Chem. Phys. Meteorol., 74, 176 (2022)

Ganske	Anette	Heil, A., Lammert, A., **Kretzschmar, J.**, and **Quaas, J.**	Publication of atmospheric model data using the ATMODAT standard	doi:10.1127/metz/2022/1118 Meteorol. Zeitschrift, 31, 493–504 (2022)
Goren	**Tom**	Feingold, G., Gryspeerdt, E., Kazil, J., **Kretzschmar, J.**, **Jia, H.**, and **Quaas, J.**	Projecting stratocumulus transitions on the albedo—cloud fraction relationship reveals linearity of albedo to droplet concentrations	doi:10.1029/2022gl101169 Geophys. Res. Lett., 49 (2022)
Haghighatnasab	**Mahnoosh**	**Kretzschmar, J.**, **Block, K.**, and **Quaas, J.**	Impact of holuhraun volcano aerosols on clouds in cloud-system-resolving simulations	doi:10.5194/acp-22-8457-2022 Atmos. Chem. Phys., 22, 8457–8472 (2022)
Jia	**Hailing**	**Quaas, J.**, Gryspeerdt, E., Böhm, C., and Sourdeval, O.	Addressing the difficulties in quantifying droplet number response to aerosol from satellite observations	doi:10.5194/acp-22-7353-2022 Atmos. Chem. Phys., 22, 7353–7372 (2022)
Krüger	Ovid O.	Holanda, B. A., Chowdhury, S., Pozzer, A., Walter, D., Pöhlker, C., Hernández, M. D. A., Burrows, J. P., Voigt, C., Lelieveld, J., **Quaas, J.**, Pöschl, U., and Pöhlker, M. L.	Black carbon aerosol reductions during COVID-19 confinement quantified by aircraft measurements over europe	doi:10.5194/acp-22-8683-2022 Atmos. Chem. Phys., 22, 8683–8699 (2022)

Linke	**Olivia**	**Quaas, J.**	The impact of CO2-driven climate change on the arctic atmospheric energy budget in CMIP6 climate model simulations	doi:10.16993/tellusa.29 Tellus A: Dyn. Meteorol. Oceanogr., 74, 106–118 (2022)
Ma	Po-Lun	Harrop, B. E., Larson, V. E., Neale, R. B., Gettelman, A., Morrison, H., Wang, H., Zhang, K., Klein, S. A., Zelinka, M. D., Zhang, Y., Qian, Y., Yoon, J., Jones, C. R., Huang, M., Tai, S., Singh, B., Bogenschutz, P. A., Zheng, X., Lin, W., **Quaas, J.**, Chepfer, ; Brunke, M. A., Zeng, X., Mülmenstädt, J., Hagos, S., Zhang, Z., Song, H., Liu, X., Pritchard, M. S., Wan, H., Wang, J., Tang, Q., Caldwell, P. M., Fan, J., Berg, L. K., Fast, J. D., Taylor, M. A., Golaz, J., Xie, S., Rasch, P. J., and Leung, L. R.	Better calibration of cloud parameterizations and subgrid effects increases the fidelity of the E3SM atmosphere model version 1	doi:10.5194/gmd-15-2881-2022 Geosci. Model Dev., 15, 2881–2916 (2022)
Marjani	**Sajedeh**	**Tesche, M.**, Bräuer, P., Sourdeval, O., and **Quaas, J.**	Satellite observations of the impact of individual aircraft on ice crystal number in thin cirrus clouds	doi:10.1029/2021gl096173 Geophys. Res. Lett., 49 (2022)
Myhre	Gunnar	Samset, ; Forster, P. M., Hodnebrog, ; Sandstad, M., Mohr, C. W., Sillmann, J., Stjern, C. W., Andrews, T., Boucher, O., Faluvegi, G., Iversen, T., Lamarque, J., Kasoar, M., å, A., Kramer, R., Liu, L.,	Scientific data from precipitation driver response model intercomparison project	doi:10.1038/s41597-022-01194-9 Sci. Data, 9 (2022)

		Mülmenstädt, J., Olivié, D., **Quaas, J.**, Richardson, T. B., Shawki, D., Shindell, D., Smith, C., Stier, P., Tang, T., Takemura, T., Voulgarakis, A., and Watson-Parris, D.		
Papakonstantinou-Presvelou	**Iris**	Sourdeval, O., and **Quaas, J.**	Strong ocean/sea-ice contrasts observed in satellite-derived ice crystal number concentrations in arctic ice boundary-layer clouds	doi:10.1029/2022gl098207 Geophys. Res. Lett., 49 (2022)
Quaas	**Johannes**	**Jia, H.**, Smith, C., Albright, A. L., Aas, W., Bellouin, N., Boucher, O., Doutriaux-Boucher, M., Forster, P. M., Grosvenor, D., Jenkins, S., Klimont, Z., Loeb, N. G., Ma, X., Naik, V., Paulot, F., Stier, P., Wild, M., Myhre, G., and Schulz, M.	Robust evidence for reversal of the trend in aerosol effective climate forcing	doi:10.5194/acp-22-12221-2022 Atmos. Chem. Phys., 22, 12221–12239 (2022)
Quaas	**Johannes**	Gryspeerdt, E.	Aerosol-cloud interactions in liquid clouds	doi:10.1016/b978-0-12-819766-0.00019-5 In: Aerosols and Climate, 489–544 (2022)
Salzmann	**Marc**	Ferrachat, S., Tully, C., Münch, S., Watson-Parris, D., Neubauer, D., Drian, C. S., Rast, S., Heinold, B., Crueger, T., Brokopf, R., **Mülmenstädt, J.**, **Quaas, J.**, Wan, H., Zhang, K., Lohmann, U., Stier, P., and Tegen, I.	The global atmosphere-aerosol model ICON-a-HAM2.3–initial model evaluation and effects of radiation balance tuning on aerosol optical thickness	doi:10.1029/2021ms002699 Journal of Advances in Modeling Earth Systems, 14 (2022)

Kalesse-Los	**Heike**	Kötsche, A., **Foth, A.**, **Röttenbacher, J.**, **Vogl, T.**, and **Witthuhn, J.**	The virga-sniffer – a new tool to identify precipitation evaporation using ground-based remote-sensing observations	doi:10.5194/amt-2022-252 Atmos. Meas. Tech. Discuss. [preprint], in review (2022)
Kalesse-Los	**Heike**	**Schimmel, W.**, Luke, E., and Seifert, P.	Evaluating cloud liquid detection against Cloudnet using cloud radar doppler spectra in a pre-trained artificial neural network	doi:10.5194/amt-15-279-2022 Atmos. Meas. Tech., 15, 279–295 (2022)
Vogl	**Teresa**	**Maahn, M.**, Kneifel, S., **Schimmel, W.**, Moisseev, D., and **Kalesse-Los, H.**	Using artificial neural networks to predict riming from doppler cloud radar observations	doi:10.5194/amt-15-365-2022 Atmos. Meas. Tech., 15, 365–381 (2022)
Schimmel	**Willi**	**Kalesse-Los, H.**, **Maahn, M.**, **Vogl, T.**, **Foth, A.**, **Saavedra Garfias, P.**, and Seifert, P.	Identifying cloud droplets beyond lidar attenuation from vertically pointing cloud radar observations using artificial neural networks	doi:10.5194/amt-15-5343-2022 Atmos. Meas. Tech., 15, 5343–5366 (2022)
Bräuer	**Peter**	**Tesche, M.**	TrackMatcher – a tool for finding intercepts in tracks of geographical positions	doi:10.5194/gmd-15-7557-2022 Geosci. Model Dev., 15, 7557–7572 (2022)
Choudhury	**Goutam**	**Tesche, M.**	Assessment of CALIOP-derived CCN concentrations by in situ surface measurements	doi:10.3390/rs14143342 Remote Sens., 14, 3342 (2022)

Choudhury	**Goutam**	**Tesche, M.**	Estimating cloud condensation nuclei concentrations from CALIPSO lidar measurements	doi:10.5194/amt-15-639-2022 Atmos. Meas. Tech., 15, 639–654 (2022)
Shin	Juseon	Sim, J., Dehkhoda, N., Joo, S., Kim, T., Kim, G., Müller, D., **Tesche, M.**, Shin, S., Shin, D., and Noh, Y.	Long-Term variation study of fine-mode particle size and regional characteristics using AERONET data	doi:10.3390/rs14184429 Remote Sens., 14, 4429 (2022)
Tesche	**Matthias**	Noel, V.	Locations for the best lidar view of mid-level and high clouds	doi:10.5194/amt-15-4225-2022 Atmos. Meas. Tech., 15, 4225–4240 (2022)
Villanueva	Diego	Possner, A., Neubauer, D., Gasparini, B., Lohmann, U., and **Tesche, M.**	Mixed-phase regime cloud thinning could help restore sea ice	doi:10.1088/1748-9326/aca16d Environ. Res. Lett., 17, 114057 (2022)

Gremium Mitgliedschaft

Prof. Dr. Manfred Wendisch

Seit 2010	Koordinator des DFG-SPP (Schwerpunktprogramm) 1294 zu HALO (High Altitude and Long Range Research Aircraft), gemeinsam mit Prof. J. Curtius (Uni Frankfurt am Main) und Mirko Scheinert (TU Dresden)
Seit 2011	Ordentliches Mitglied der Sächsischen Akademie der Wissenschaften
Seit 2012	Gewähltes Mitglied im IRC (Internationale Strahlungskommission) innerhalb von IAMAS
Seit 2012	Vize-Sprecher der „Leibniz-Graduate School on Clouds, Aerosols, and Radiation (LGS-CAR)“
Seit 2015	Mitglied des Wissenschaftlichen Beirats des Deutschen Wetterdienstes (DWD)
Seit 2015	Mitglied des Programmrates des „Hans-Ertel-Zentrum für Wetterforschung (HErZ)“ des DWD
Seit 2016	Mitglied des Präsidiums der Sächsischen Akademie der Wissenschaften
Seit 2016	Stellvertretender Vorsitzender des Wissenschaftlichen Lenkungsausschuss (WLA) für HALO (High Altitude and Long Range Research Aircraft)
Seit 2016	Sprecher des Sonderforschungsbereiches SFB-Transregio 172: “Arktische Verstärkung: Klimarelevante Atmosphären- und Oberflächenprozesse, und Rückkopplungsmechanismen (AC)^3”
Seit 2016	Koordinator des YOPP (Year of Polar Prediction) Task Teams zu Flugzeuggetragenen Messplattformen
Seit 2017	Mitglied des Projekt-Kommittees für MOSAiC (**M**ultidisciplinary drifting **O**bservatory for the **S**tudy of **A**rct**i**c **C**limate), Team Koordinator für Flugzeugoperation
Seit 2017	Mitglied DFG-Senatskommission für Erdsystemforschung
Seit 2019	Mitglied der International Commission on Atmospheric Chemistry and Global Pollution, ICACGP, of the International Association of Meteorology and Atmospheric Science IAMAS. http://www.icacgp.org
Seit 2020	Mitglied des deutschen Nationalkomitees SCAR/IASC (Scientific Committee on Arctic Research / International Arctic Science Committee)
Seit 2020	Mitglied des Kuratoriums des Alfred-Wegener-Instituts, Helmholtz-Zentrum für Polar- und Meeresforschung (AWI)
Seit 2020	Mitglied im DFG Fachkollegium 313 «Atmosphären- und Klimaforschung» für das Fach 313-01 «Physik und Chemie der Atmosphäre», Stellvertretender Sprecher
Seit 2020	Vorsitzender des Wissenschaftlichen Beirats des Deutschen Wetterdienstes (DWD)
Seit 2020	Vize-Präsident IRC (Internationale Strahlungskommission) innerhalb von IAMAS
Seit 2021	Gewähltes Mitglied im Senat der Universität Leipzig
Seit 2022	Sprecher im DFG Fachkollegiums 313 «Atmosphären- und Klimaforschung» für das Fach 313-01 «Physik und Chemie der Atmosphäre"

Prof. Dr. Christoph Jacobi:
Mitglied im Vorstand der Meteorologischen Gesellschaft, Sektion Mitteldeutschland
Leiter der Division II „Aeronomic Phenomena“ der IAGA
Leiter der Arbeitsgruppe II-D der IAGA: „External Forcing of the Middle Atmosphere“
Vorsitzender der Mitgliederversammlung des TROPOS

Prof. Dr. Johannes Quaas:
Vorsitz, Sektion Mitteldeutschland, Deutsche Meteorologische Gesellschaft
Mitglied im Fakultätsrat, Fakultät für Physik und Geowissenschaften
Prodekan, Fakultät für Physik und Geowissenschaften
Mitglied im Wissenschaftlichen Beirat, Leibniz-Institut für Troposphärenforschung
Scientific Steering Committee, Aerosols-Clouds-Precipitation and Climate Initiative
Mitglied im Wissenschaftlichen Beirat, Deutsches Klimarechenzentrum
Stellvertretender Vorsitz, University Partnership for Atmospheric Sciences

Dr. Maximilian Maahn:
Member ESA WIVERN (wind velocity radar nephoscope) Mission Advisory Group

Mitgliedschaften in Redaktionskollegien, Herausgebergremien

Prof. Dr. Manfred Wendisch:

Seit 2008	Ko-Editor “Journal on Atmospheric Measurement Techniques”
Seit 2019	Mitglied im Editorial Board des *Bulletin of the American Meteorological Society* (*BAMS*) (Subject Matter Editor for Aerosol and Cloud Physics)

Prof. Dr. Christoph Jacobi:

Annales Geophysicae	Editor-in-Chief
Mitteilungen der DMG	Mitglied Redaktionsteam

Prof. Dr. Johannes Quaas:

Atmospheric Chemistry and Physics	Editor
Meteorologische Zeitschrift	(Special Issue)

PD Dr. Matthias Tesche:

Atmospheric Chemistry and Physics	Editor

Dr. Maximilian Maahn:

Atmospheric Measurement Techniques	Associate Editor

Mitarbeitende am LIM 2022

Name	E-Mail-Adresse
Alexandri, Fani	fani.alexandri@uni-leipzig.de
Becker, Sebastian	sebastian.becker@uni-leipzig.de
Brückner, Marlen	m.brueckner@uni-leipzig.de
Block, Karoline	karoline.block@uni-leipzig.de
Cherian, Ribu	ribu.cherian@uni-leipzig.de
Choudhury, Goutam	goutam.choudhury@uni-leipzig.de
Doktorowski, Sabine	sabine.hoernig@uni-leipzig.de
Ehrlich, André	a.ehrlich@uni-leipzig.de
Fortunato-Winter, Dominique	dominique.fortunato-winter@uni-leipzig.de
Foth, Andreas	andreas.foth@uni-leipzig.de
Gonzalez Villarreal, Jessenia	jessenia.gonzalesv@uni-leipzig.de
Goren, Tom	tom.goren@uni-leipzig.de
Haghighatnasab, Mahnoosh	mahnoosh.haghighatnasab@uni-leipzig.de
Haustein, Karsten	karsten.haustein@uni-leipzig.de
Henkes, Alice	alice.henkes@uni-leipzig.de
Jacobi, Christoph	jacobi@rz.uni-leipzig.de
Jäkel, Evelyn	evi.jaekel@uni-leipzig.de
Jha, Sudhanshu Shekhar	sudhanshu_shekhar.jha@uni-leipzig.de
Jia, Hailing	hailing.jia@uni-leipzig.de
Kaiser, Falk	fkaiser@rz.uni-leipzig.de
Kalesse-Los, Heike	heike.kalesse@uni-leipzig.de
Karami, Khalil	khalil.karami@uni-leipzig.de
Kandieva, Kanykei	Kanykei.Kandieva@uni-leipzig.de
Kirbus, Benjamin	benjamin.kirbus@uni-leipzig.de
Klingebiel, Marcus	marcus.klingebiel@uni-leipzig.de
Kötsche, Anton	anton.koetsche@uni-leipzig.de
Kretzschmar, Jan	jan.kretzschmar@uni-leipzig.de
Kuchar, Ales	ales.kuchar@uni-leipzig
Kwakye, Samuel	samuel.kwakye@uni-leipzig.de
Lange, Charlotte	charlotte.lange@uni-leipzig.de
Lenhardt, Julien	julien.lenhardt@uni-leipzig.de
Lindemann, Simone	simone.lindemann@uni-leipzig.de
Linke, Olivia	olivia.linke@uni-leipzig.de
Lochmann, Moritz	moritz.lochmann@uni-leipzig.de
Lonardi, Michael	michael.lonardi@uni-leipzig.de
Maahn, Maximilian	maximilian.maahn@uni-leipzig.de

Maherndl, Nina	nina.maherndl@uni-leipzig.de
Marjani, Sajedeh	sajedeh.Marjani@uni-leipzig.de
Mehrdad, Sina	sina.mehrdad@uni-leipzig.de
Metzner, Enrico	enrico.metzner@uni-leipzig.de
Müller, Felix	felix.mueller.2@uni-leipzig.de
Müller, Hanno	hanno.mueller@uni-leipzig.de
Papakonstantinou-Presvelou, Iris	i.presvelou@uni-leipzig.de
Quaas, Johannes	johannes.quaas@uni-leipzig.de
Röttenbacher, Johannes	johannes.roettenbacher@uni-leipzig.de
Rosenburg, Sophie	sophie.rosenburg@uni-leipzig.de
Ruiz-Donoso, Elena	elena.ruiz_donoso@uni-leipzig.de
Saavedra Garfias, Pablo	pablo.saavedra@uni-leipzig.de
Salzmann, Marc	marc.salzmann@uni-leipzig.de
Schäfer, Michael	michael.schaefer@uni-leipzig.de
Schandert, Katrin	schandrt@rz.uni-leipzig.de
Schimmel, Willi	willi.schimmel@uni-leipzig.de
Schmidt, Jörg	joerg.schmidt@uni-leipzig.de
Schwarz, Anja	anja.schwarz@uni-leipzig.de
Seelig, Torsten	torsten.seelig@uni-leipzig.de
Seydel, Birgit	birgit.seydel@uni-leipzig.de
Sperzel, Tim Robert	tim.sperzel@uni-leipzig.de
Steinke, Isabelle	Isabelle.steinke@uni-leipzig.de
Sudhakar, Dipu	dipu.sudhakar@uni-leipzig.de
Tesche, Matthias	matthias.tesche@uni-leipzig.de
Tesche-Achtert, Peggy	peggy.achtert@uni-leipzig.de
Vaishnav, Rajesh Ishwardas	rajesh_ishwardas.vaishnav@uni-leipzig.de
Wendisch, Manfred	m.wendisch@uni-leipzig.de
Witthuhn, Jonas	jonas.witthuhn@uni-leipzig.de
Wolter, Steffen	steffen.wolter@uni-leipzig,de

Anzahl der Studierenden am Institut für Meteorologie

Bachelor of Science Meteorologie

Datum	Semester	1.FS	2.FS	3.FS	4.FS	5.FS	6.FS	7.FS	8.FS	9.FS	10.FS	>10.FS	gesamt
15.10.22	WS 22/23	55		25		23		16	2	5		2	128
15.10.21	WS 21/22	40		27		24	4	12		4	1		112
15.10.20	WS 20/21	34	1	32	7	21		9	2	2		1	109
15.10.19	WS 19/20	58		17		12		9					96
15.10.18	WS 18/19	48		14		9		5					76
15.10.17	WS 17/18	37		17		7		5					66
15.10.16	WS 16/17	48		7		5		3					63
15.10.15	WS 15/16	35		5		9		3					52
15.10.14	WS 14/15	35		14		15		3		3		1	71
15.10.13	WS 13/14	39		23		21		13		4			100
15.10.12	WS 12/13	60		29	1	22	2	16	1	2			133
15.10.11	WS 11/12	60		27		26	1	19		1			134
15.10.10	WS 10/11	64		34		20							118
15.10.09	WS 09/10	67		21		20							108
15.10.08	WS 08/09	71		28		12							111
15.10.07	WS 07/08	98		15									113
13.12.06	WS 06/07	31											31

Master of Science Meteorologie / Meteorology

Datum	Semester	1.FS	2.FS	3.FS	4.FS	5.FS	6. FS	7. FS	>7. FS	gesamt
15.10.22	WS22/23	11		8		11	4	5	2	41
15.10.21	WS21/22	8		13						21
15.10.20	WS20/21	14	4	6	1	3	1			29
15.10.19	WS 19/20	9		5		5				19
15.10.18	WS18/19	5		5		9				19
15.10.17	WS 17/18	5		9		10				24
15.10.16	WS 16/17	9		13		17				39
15.10.15	WS 15/16	13		19		18				50
15.10.14	WS 14/15	19		18		16				53
15.10.13	WS 13/14	18		16		20				54
15.10.12	WS 12/13	18		20	1	15				54
15.10.11	WS 11/12	21		17		10				48
15.10.10	WS 10/11	20		9		5				34
15.10.09	WS 09/10	11								11

Diplom Meteorologie (bis 2013)

Datum	Semester	1.FS	2.FS	3.FS	4.FS	5.FS	6.FS	7.FS	8.FS	9.FS	10.FS	>10.FS	Meteo. Dipl.
15.10.2013	WS 13/14											2	2
17.10.2012	WS 12/13											3	3
16.10.2011	WS 11/12											3	3
15.10.2010	WS 10/11											14	14
15.10.2009	WS 09/10									14		7	21
15.10.2008	WS 08/09							14		23	1	25	63
15.10.2007	WS 07/08					22		26	1	18	2	19	88
13.12.2006	WS 06/07			40		36		24	2	14	1	17	175
15.10.2005	WS 05/06	109		49		30	2	16	1	17	1	13	237
08.12.2004	WS 04/05	97		35	1	20		19		12	1	15	200
03.12.2003	WS 03/04	68	1	25		20	1	13	1	12	1	13	155
14.10.2002	WS 02/03	45		19		16		15	1	12	1	9	118
06.12.2001	WS 01/02	43		21		16		13		7		5	105
07.12.2000	WS 00/01	41	1	27		22		8		6	1	6	112
01.12.1999	WS 99/00	40		24		9		9		6	1	6	95
16.12.1998	WS 98/99	36		11		17	1	9	1	5		8	88
10.11.1997	WS 97/98	29		17		10	1	8		7		4	76

Abschlussarbeiten Institut für Meteorologie 2022

Bachelorarbeiten 2022

Eckermann, Oliver: Schneefall im nordostdeutschen Tiefland an ausgewählten Messstationen und in globalen sowie regionalen Klimamodellen

Heckmann, Valentin: Ableitung von Oberflächenparametern aus dem Grenzschichtwindprofil über Leipzig

Schmidt, Judith: Bestimmung von Bedeckungsgrad und Wolkentyp mit Himmelskamerabeobachtungen und Vergleich mit schiffsgebundenen synoptischen Beobachtungen

Walper, Nils: Characterization of tradeclouds by remote sensing methods

Berghald, Sebastian: Evaluierung des Abgleichs von Klimaprojektionsdaten für sächsische Gemeinden mit dem heutigen Klima von Städten in Südeuropa

Pomnitz, Nelly: Einfluss der subgitterkaligen Vertikalgeschwindigkeit auf den effektiven Strahlungsantrieb durch Aerosol-Strahlungs- und Aerosol-Wolken-Wechselwirkungen im ICON-HAM Aerosol-Atmosphärenmodell

Öhlert, Maurice: On the reliability of large ensembles simulating the stratospheric polar vortex

David, Johannes: Zeitabhängige Größenverteilung von Wolkentröpfchen aus geostationären Satellitenbeobachtungen

Bruder, Sina: Gibt es einen messbaren Rückgang im Auftreten tiefer Wolken?

Baumer, Finja: Comparison of radiosonde data from Leipzig to meteorological profiles of two atmospheric models

Gundlach, Josephiene: Temperaturempfindlichkeit biogener und arktischer Eiskeime

Monrad-Krohn, Lukas: Analysing the variability of dropsonde profiles of four Arctic airborne campaigns in the vicinity of Svalbard

Trosits, Anna: A statistical analysis of the hydrometeor classification by the Thies Laser Precipitation Monitor

Wieltsch, Julia: Analysis of atmospheric rivers during the DACAPO-PESO field campaign in Punta Arenas, Chile

Kunze, Pascal: Klimatische Einordnung der meteorologischen Bedingungen ausgewählter Flüge während der CIRRUS-HL Kampagne

Masterarbeiten 2022

Ritter, Oscar: Characterisation of the properties of trade wind cumulus clouds with Sentinel-2 observations, including cloud cover, cloud height, cloud size distribution and their radiative effects

Kötsche, Anton: Investigating precipitation evaporation in the trade wind zone using EUREC4A data

Engelhardt, Richard: Precipitation-based methods for absolute cloud radar calibration

Seidel, Clara: Analysis of water vapour mixing ratio profiles in the Arctic from Raman lidar measurements during the MOSAiC-campaign

Müller, Jason: Global adjustments and circulation responses to smoke aerosol forcing from Australian wildfires

Rosenburg, Sophie: Melt pond depth retrieval applying airborne hyperspectral imagery and the potential of a new RGB band approach

Schaefer, Jonas: Investigation of stratospheric ice nucleating particle concentrations for background conditions and in a biomass burning plume

Kraulich, Florian: Role of atmospheric and oceanic processes in Arctic amplification: Sensitivity to climate engineering

Adler, Anja: Ableitung von Profilen der Schneekorngröße einer Schneewand aus Messungen mit einem abbildenden Spektrometer

Dissertationen 2022

Hannes Jascha Griesche: Arctic low-level mixed-phase clouds and their complex interactions with aerosol and radiation - Remote sensing of the Arctic troposphere with the shipborne supersite OCEANET-Atmosphere

Martin Radenz: Hemispheric contrasts of ice formation in stratiform supercooled liquid clouds: Long-term observations with the ground-based remote-sensing supersite LACROS

Johannes Stapf: Influence of surface and atmospheric thermodynamic properties on the cloud radiative forcing and radiative energy budget in the Arctic

Jonas Witthuhn: Aerosol - remote sensing, characterization and aerosol-radiation interaction

Honey Dawn C. Alas: Mobile measurements of black carbon and PM: optimization of techniques and data analysis for pedestrian exposure

Athina Avgousta Floutsi: Development and application of an automatic lidar-based aerosol typing algorithm

Carola Barrientos Velasco: Radiative effects of clouds in the Arctic

Sebastian Düsing: Investigation of physio-optical aerosol properties with in-situ and remote-sensing techniques

Daniel Hertel: Optimierung von urbanen Hitzeanpassungsmaßnahmen

Willi Schimmel: Identifying cloud droplets beyond Lidar attenuation from vertically pointing cloud radar observations using artificial neural networks

Wissenschaftliche Mitteilungen aus dem Institut für Meteorologie der Universität Leipzig

Band 1	*A. Raabe, G. Tetzlaff* und *W. Metz* (Edn.), 1995: Meteorologische Arbeiten aus Leipzig I
Band 2	*R. Devantier*, 1995: Wolkenbildungsprozesse über der südwestlichen Ostsee - Anwendungen eines neuen Wolkenschemas in einem mesoskaligen Modell
Band 3	*J. Laubach*, 1996: Charakterisierung des turbulenten Austausches von Wärme, Wasserdampf und Kohlendioxid über niedriger Vegetation anhand von Eddy-Korrelations-Messungen
Band 4	*A. Raabe* und *J. Heintzenberg* (Edn.), 1996: Meteorologische Arbeiten aus Leipzig II
Band 5	Wind- und Seegangsatlas für das Gebiet um Darß und Zingst *D. Hinneburg, A. Raabe* und *G. Tetzlaff*, 1997: Teil I: Windatlas
Band 6	*W. von Hoyningen-Huene* und *G. Tetzlaff* (Edn.), 1997: Sediment and Aerosol Teil I: Beiträge zur Alfred-Wegener-Konferenz, Leipzig 1997 Teil II: Aktuelle Beiträge aus dem Institut für Meteorologie
Band 7	*B.-R. Beckmann*, 1997: Veränderungen in der Windklimatologie und in der Häufigkeit von Sturmhochwassern an der Ostseeküste Mecklenburg-Vorpommerns
Band 8	*P. Posse*, 1997: Bestimmung klimarelevanter Parameter des maritimen Aerosols unter besonderer Berücksichtigung der Nichtkugelform realer Aerosolteilchen
Band 9	*A. Raabe, K. Arnold* und *J. Heintzenberg* (Edn.),1998: Meteorologische Arbeiten aus Leipzig III
Band 10	Wind- und Seegangsatlas für das Gebiet um Darß und Zingst, Teil II, 1998: *D. Hinneburg, A. Raabe* und *G. Tetzlaff*: Vergleich Windatlas –Beobachtungsdaten; *M. Börngen, H.-J. Schönfeldt, F. Riechmann, G. Panin* und *G. Tetzlaff:* Seegangsatlas; *M. Stephan* und *H.-J. Schönfeldt*: Sedimenttransportatlas
Band 11	*J. Rissmann, 1998*: Der Einfluss langwelliger Strahlungsprozesse auf das bodennahe Temperaturprofil
Band 12	*A. Raabe, K. Arnold* und *J. Heintzenberg* (Edn.), 1999*:*Meteorologische Arbeiten aus Leipzig IV
Band 13	*U. Müller, W. Kuttler und G. Tetzlaff (Edn.)*, 1999: Workshop Stadtklima 17. / 18. 02. 1999 in Leipzig
Band 14	*R. Surkow, 1999*: Optimierung der Leistungsverfügbarkeit von Windenergie durch ihre Integration in Wind-Biogas-Hybridanlagen
Band 15	*N. Mölders,* 1999: Einfache und akkumulierte Landnutzungsänderungen und ihre Auswirkungen auf Evapotranspiration, Wolken- und Niederschlagsbildung
Band 16	*G. Tetzlaff und U. Grünewald* (Edn.), 1999:2. Tagung des Fachausschusses Hydrometeorologie 15./16. 11. 1999 in Leipzig
Band 17	*A. Raabe und K. Arnold* (Edn.), 2000: Meteorologische Arbeiten aus Leipzig V
Band 18	*K. Arnold*, 2000: Ein experimentelles Verfahren zur Akustischen Tomographie im Bereich der atmosphärischen Grenzschicht
Band 19	*A. Ziemann*, 2000: Eine theoretische Studie zur akustischen Tomographie in der atmosphärischen Grenzschicht
Band 20	*Ch. Jacobi*, 2000: Midlatitude mesopause region dynamics and its coupling with lower and middle atmospheric processes
Band 21	*M. Klingspohn*, 2000: Interdekadische Klimavariabilität über dem Nordatlantik – Statistische Analysen und Modellstudien –
Band 22	*A. Raabe* und *K. Arnold* (Edn.), 2001: Meteorologische Arbeiten aus Leipzig VI
Band 23	*K. Arnold, A. Ziemann, G. Tetzlaff, V. Mellert* und *A. Raabe* (Edn.), 2001: International Workshop Tomography and Acoustics: Recent developments and methods 06. - 07.03.2001 in Leipzig
Band 24	*O. Fanenbruck*, 2001: Ein thermophysiologisches Bewertungsmodell mit Anwendung auf das Leipziger Stadtgebiet
Band 25	*M. Lange*, 2001: Modellstudien zum CO_2-Anstieg und O_3-Abbau in der mittleren Atmosphäre und Einfluss des Polarwirbels auf die zonale Symmetrie des Windfeldes in der Mesopausenregion
Band 26	*A. Raabe* und *K. Arnold* (Edn.), 2002: Meteorologische Arbeiten aus Leipzig VII
Band 27	*M. Simmel*, 2002: Ein Modul zur spektralen Beschreibung von Wolken und Niederschlag in einem Mesoskalenmodell zur Verwendung auf Parallelrechnern
Band 28	*H. Siebert*, 2002: Tethered-Balloon Borne Turbulence Measurements in the Cloudy Boundary Layer
Sonderband	*G. Tetzlaff* (Hrsg.), 2002:- Atmosphäre - Aktuelle Beiträge zu Luft, Ozon, Sturm, Starkregen und Klima
Band 29	*U. Harlander*, 2003: On Rossby wave propagation in atmosphere and ocean
Band 30	*A. Raabe* und *K. Arnold* (Edn.), 2003: Meteorologische Arbeiten aus Leipzig VIII
Band 31	*M. Wendisch*, 2003: Absorption of Solar Radiation in the Cloudless and Cloudy Atmosphere
Band 32	*U. Schlink*, 2003: Longitudinal Models in Biometeorology: Effect Assessment and Forecasting of Ground-level Ozone
Band 33	*H. Heinrich*, 2004: Finite barotrope Instabilität unter synoptischem Antrieb
Band 34	*A. Raabe* und *K. Arnold* (Edn.), 2004: Meteorologische Arbeiten aus Leipzig IX
Band 35	*C. Stolle*, 2004: Three-dimensional imaging of ionospheric electron density fields using GPS observations at the ground and on board the CHAMP satellite
Band 36	*A. Raabe* und *K. Arnold* (Edn.), 2005: Meteorologische Arbeiten (X) und Jahresbericht 2004 des Institutes für Meteorologie der Universität Leipzig
Band 37	*A. Raabe* und *K. Arnold* (Edn.), 2006: Meteorologische Arbeiten (XI) und Jahresbericht 2005 des Institutes für Meteorologie der Universität Leipzig
Band 38	*K. Fröhlich*, 2006: The Quasi Two-Day Wave – its impact on zonal mean circulation and wave-wave interactions in the middle atmosphere
Band 39	*K. Radtke, 2006: Zur Sensitivität von Starkwindfeldern gegenüber verschiedenen meteorologischen Parametern im Mesoskalenmodell LM*

Wissenschaftliche Mitteilungen aus dem Institut für Meteorologie der Universität Leipzig

Band 61 (2023):

Meteorologische Arbeiten XXVIII
Jahresbericht 2022

ISBN 978-3-9823985-1-8

Die einzelnen Beiträge dieses Heftes wurden in einem internen Verfahren begutachtet

Abbildung auf Umschlag

Institutsgebäude – Leipziger Institut f. Meteorologie (LIM)
© Foto: Cornelia Ködderitzsch, Staatsbetrieb Sächsisches Immobilien- und Baumanagement

Herausgegeben im Selbstverlag:
Institut für Meteorologie, Universität Leipzig

Herausgeber:
M. Wendisch

Bestellungen richten Sie bitte an:

Institut für Meteorologie, Universität Leipzig
Stephanstr. 3
D-04103 Leipzig

Tel: 0341 - 9732850
Fax: 0341 - 9732899
E-Mail: birgit.seydel@uni-leipzig.de
Preis pro Band: 20,– €